GEMS & GEMOLOGY

FALL 2014
VOLUME L

THE QUARTERLY JOURNAL OF THE GEMOLOGICAL INSTITUTE OF AMERICA

Sri Lanka: Where Tradition and Technology Meet

Characteristics of Pen Pearls

An Introduction to Pleochroism in Colored Gems

GEMS & GEMOLOGY

Fall 2014
VOLUME 50, No. 3


pg. 175


pg. 203

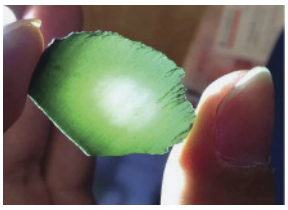
pg. 229


pg. 243

Editorial

Feature Articles

Notes and New Techniques

Regular Features

GEMS & GEMOLOGY®

gia.edu/gems-gemology

Subscriptions
Copies of the current issue may be purchased for $29.95 plus shipping. Subscriptions are $79.99 for one year (4 issues) in the U.S. and $99.99 elsewhere. Canadian subscribers should add GST. Discounts are available for group subscriptions, GIA alumni, and current GIA students. To purchase print subscriptions, visit store.gia.edu or contact Customer Service. For institutional rates, contact Customer Service.

Database Coverage
Gems & Gemology's impact factor is 0.778, according to the 2013 Thomson Reuters Journal Citation Reports (issued July 2014). *G&G* is abstracted in Thomson Reuters products (Current Contents: Physical, Chemical & Earth Sciences and Science Citation Index—Expanded, including the Web of Knowledge) and other databases. For a complete list of sources abstracting *G&G*, go to gia.edu/gems-gemology, and click on "Publication Information."

Manuscript Submissions
Gems & Gemology, a peer-reviewed journal, welcomes the submission of articles on all aspects of the field. Please see the Guidelines for Authors at gia.edu/gandg or contact the Managing Editor. Letters on articles published in *G&G* are also welcome. Please note that Field Reports, Lab Notes, and Gem News International entries are not peer-reviewed sections, but do undergo technical and editorial review.

Gems & Gemology is published quarterly by the Gemological Institute of America, a nonprofit educational organization for the gem and jewelry industry.

Postmaster: Return undeliverable copies of *Gems & Gemology* to GIA, The Robert Mouawad Campus, 5345 Armada Drive, Carlsbad, CA 92008.

Our Canadian goods and service registration number is 126142892RT.

About the Cover

The lead article in this issue examines the revitalization of Sri Lanka's gem and jewelry industry, achieved by combining modern manufacturing methods with traditional artisanal practices handed down over generations. The cover photo, taken in Ratnapura during a GIA field expedition, shows Master Simon heating a star ruby to remove its purplish tint using a centuries-old blowpipe method. Photo by Vincent Pardieu/GIA.

Printing is by L+L Printers, Carlsbad, CA.
GIA World Headquarters The Robert Mouawad Campus 5345 Armada Drive Carlsbad, CA 92008 USA

ISSN 0016-626X

Supporting the **Researchers of Tomorrow**

In our recent print issues, you've likely noticed an ad on the journal's inside cover promoting postdoctoral research opportunities. This is part of a GIA initiative to attract new research scientists. We recognize that supporting future research is fundamental to all of GIA's core gemological laboratory and education services that support the industry and our mission to safeguard consumers.

As part of this effort, we're delighted to announce that GIA will be the principal sponsor of the International Diamond School (IDS), to be held January 27–31 in Brixen, Italy. The school will be led by three leading diamond geoscientists: Fabrizio Nestola of the University of Padova, Italy; Steven Shirey of the Carnegie Institution in Washington, DC; and Graham Pearson of the University of Alberta, Canada. The school brings together leading academics and practicing members of the diamond geoscience community—including our own Dr. Wuyi Wang—with the next generation of postdoctoral and masters-level researchers. It's a fantastic opportunity for attendees to network with the leaders in diamond exploration, advanced research-level analysis, diamond morphology, inclusion chemistry, and geologic occurrences in a way that will inspire their future studies. GIA's contribution will directly benefit these up-and-coming research scientists by reducing the attendance fees for the conference. The IDS website is at http://www.indimedea.eu/diamond_school_2015.htm

"Supporting future research is fundamental to all GIA's core gemological activities..."

Our lead article in this edition, a collaboration between GIA and Sri Lankan authors, presents an illuminating survey of Sri Lanka's gem and jewelry industry based on firsthand visits to mining, cutting, jewelry manufacturing, and retail centers. They document a revitalized industry that's blending hard-won traditional skills with innovative strategies and technologies to gain a stronger presence in global markets.

Our second paper, by Nicholas Sturman and his colleagues from GIA's Bangkok laboratory, provides a gemological characterization of 22 non-nacreous pen pearls. This study reveals not only the porcelaneous nature of these pearls, but also the unusual beauty of their surface textures and inner structures.

Next, noted author and corundum expert Richard Hughes delves into a basic gemological property: pleochroism. His intriguing paper—aimed at practicing gemologists as much as researchers—examines this property's impact on the appearance of faceted gems and looks to demonstrate that pleochroism is always visible to some degree, even when viewing a gem along an optic axis.

In the final article, Dr. Zuowei Yin from the China University of Geosciences in Wuhan heads a study of pale-colored nephrite jade from a new deposit in Guangxi Province with interesting banded or dendritic patterns.

In addition to the four feature articles, you'll find our regular Lab Notes and Gem News International sections, along with the winners of the 2014 *G&G* Challenge.

For all our print subscribers: You'll notice that your copy of journal was delivered inside a new recyclable (polyhydroxyalkanoate, or PLA) wrapper. We'd like to thank Dr. George Rossman of *G&G*'s editorial review board for this suggestion.

Please enjoy the Fall 2014 edition!

Duncan Pay | Editor-in-Chief | dpay@gia.edu

Sri Lanka: Expedition to the Island of Jewels

Andrew Lucas, Armil Sammoon, A. P. Jayarajah, Tao Hsu, and Pedro Padua

In February 2014, the authors explored Sri Lanka's entire mine-to-market gemstone and jewelry industry. The team visited numerous mining, cutting, trading, jewelry manufacturing, and retail centers representing each sector and witnessed a dynamic blend of traditional and increasingly modern practices. Centuries of tradition as a colored gemstone mining, trading, and cutting source now converge with the technologies, skill sets, and strategies of today's global market.

Sri Lanka is one of the meccas of gemology. Few sources, especially among active localities, can match its rich history as a gem producer and trade center. As Sri Lanka takes its place in today's gem and jewelry industry, the gemologist can observe a combination of traditional methods and modern technologies as well as new business strategies for a highly competitive market.

What appear to be primitive practices are often highly efficient and well suited to the task. While most of the mining enterprises are small operations using simple hand tools, these allow for continuous mining, employ a large workforce, and are less damaging to the environment (figure 1). Cutting is another sector where traditional techniques still prevail, providing excellent initial orientation of the rough crystal for maximum face-up color and weight retention. At the same time, highly skilled recutting in Sri Lanka is achieving international market standards of proportions, symmetry, and brightness (figure 2). Fine precision cutting to tight tolerances on modern lapidary equipment is being applied to calibrated goods that meet the strictest requirements, including those of the watch industry.

While the small shops rely on jewelry manufacturing techniques such as hand-blown soldering, modern factories use lost-wax and casting as well as die-striking. Gem trading has evolved, partly due to more trade-friendly import and export regulations, making Sri Lankan buyers more competitive globally. The retail industry continues to find a large domestic market for traditional 22K gold jewelry while expanding to meet the diverse tastes of younger Sri Lankans and tourists.

SRI LANKA

Sri Lanka is a large island in the Indian Ocean, just off the southern tip of India. It measures 65,610 square kilometers (40,768 square miles), with 1,340 kilometers (832 miles) of coastline. In the southwest, where most of the gemstone mining takes place, the monsoon season lasts from June to October. Sri Lanka is located in the path of major trade routes in the Indian Ocean, an advantage that helped establish it as one of the world's most important gem sources.

In addition to gemstones, Sri Lanka has natural resources of limestone, graphite, mineral sands, phosphates, clay, and hydroelectric power. The country is also known for its tea, spices, rubber, and textiles. Of the total workforce, 42.4% are employed in the service sector, 31.8% in agriculture, and 25.8% in industry, which includes mining and manufacturing (CIA World Fact Book, 2014). The tourist industry is expected to see strong growth, although the existing infrastructure may struggle to accommodate a large influx of visitors to such attractions as the ruins at Sigiriya, a UNESCO World Heritage site (figure 3).

Sri Lanka's economy has experienced strong growth since 2009, which marked the end of a 26-year

See end of article for About the Authors and Acknowledgments.
Gems & Gemology, Vol. 50, No. 3, pp. 174–201,
http://dx.doi.org/10.5741/GEMS.50.3.174.

Figure 1. As Sri Lanka develops its colored stone mining industry, traditional practices still prove effective. Photo by Andrew Lucas.

civil war that long plagued economic development. The country's population of nearly 22 million encompasses different ethnicities and religions that are reflected in the styles of jewelry manufactured and sold domestically. The population is 73.8% Sinhalese, 7.2% Sri Lankan Moor, 4.6% Indian Tamil, and 3.9% Sri Lankan Tamil (with 10% unspecified). Buddhists account for 69.1% of the population, Muslims 7.6%,

Figure 2. Sri Lankan lapidaries incorporate traditional techniques, modern precision cutting, and highly skilled recutting. This worker has decades of experience cutting and recutting corundum and chrysoberyl. Photo by Andrew Lucas.

Figure 3. Sigiriya, a massive rock standing more than 200 meters high, was transformed into a royal fortress during the reign of King Kashyapa (477–495 AD), with palaces, gardens, swimming pools, and frescos. It is a major tourist attraction in Sri Lanka. Photo by Andrew Lucas.

Figure 4. While Sri Lanka produces a variety of prized gemstones, sapphire is the most important commercially. Photo by Robert Weldon.

Hindus 7.1%, and Christians 6.2% (CIA World Fact Book, 2014). While Muslims and Hindus represent a distinct minority, they have a rich jewelry tradition, and the authors witnessed the importance of their buying power in the retail industry.

GEM TRADE HISTORY

Gemstone use in Sri Lanka dates back at least 2,000 years. The gem-laden island was referred to in Sanskrit as Ratna Dweepa, meaning "Island of Jewels" (Hughes, 2014). Early Arab traders called it Serendib, which is the origin of the word "serendipity." Known until 1972 as Ceylon, it has a rich history as a source of economically important gemstones, particularly sapphire (figure 4) and cat's-eye chrysoberyl.

James Emerson Tennent, an administrator of British Ceylon from 1846 to 1850, noted that the *Mahavamsa* (*The Great Chronicle of Ceylon*) mentions a gem-encrusted throne owned by a Naga king in 543 BC, when the earliest accounts of the island were written (Hughes, 1997). The Roman naturalist Pliny the Elder wrote that ambassadors from Taprobane, as Sri Lanka was known at the time, boasted of its fine gemstones during the reign of Emperor Claudius from 41 to 54 AD (Hughes, 1997). The Greek astronomer Ptolemy referred to the island's beryl, sapphire, and gold in the second century AD (Hughes, 1997). Marco Polo traveled there in 1293 and noted the abundance of gems, including ruby, sapphire, topaz, amethyst, and garnet (Ariyaratna, 2013). The famous Arab explorer Ibn Battuta, visiting in the 14th century, wrote of the variety of precious stones he saw (Ariyaratna, 2013).

Between 500 and 1500 AD, during the rule of ancient and medieval Sinhala kings, the mining, possession, and commerce of precious stones was controlled by the monarch. Arab and Persian merchants purchased many fine gemstones. During the periods of European colonization—Portuguese (1505–1656), Dutch (1656–1796), and British (1796–1948)—gem commerce expanded beyond the royal family, as the Europeans were solely interested in trading and profit (Mahroof, 1997). European traders brought more of these goods to the West and furthered the island's reputation as a source of gemstones and trade expertise.

In Brief

- Due to its geological makeup and location along major trade routes, Sri Lanka has long been an important source and trading center for gems, including sapphire and cat's-eye chrysoberyl.
- Traditional methods of mining, cutting, and treatment have been combined with modern techniques to keep Sri Lanka competitive in the world's gemstone market.
- Jewelry manufacturing is a major growth area, as the industry meets the traditional needs of consumers along with the emerging youth market and tourist demand.

During the 20th century, Sri Lanka's standing as a premier gem trade center diminished. This was due to numerous factors: the emergence of other sources, a failure to adapt and master technology such as heat treatment and modern cutting, and government regulations that hindered the rapid growth enjoyed by Thailand and other countries. In the last two decades, Sri Lanka has overcome those setbacks and now has a dynamic, rapidly growing gem and jewelry industry.

Sri Lanka is best known for its large, exceptional sapphire and star corundum. Important stones re-

Figure 5. The 423 ct Logan sapphire is one of many famous stones from Sri Lanka. Photo by Chip Clark; courtesy of the Smithsonian Institution.

ported to be from Sri Lanka include (Ariyaratna, 2013):

- the 466 ct Blue Giant of the Orient, supposedly mined from the Ratnapura area in 1907
- the 423 ct Logan blue sapphire (figure 5) and the 138 ct Rosser Reeves star ruby, both housed in the Smithsonian Institution's National Museum of Natural History
- the 400 ct Blue Belle of Asia, said to have been found in a paddy field in the Ratnapura district in 1926, and described as having the highly desirable "cornflower" blue color
- the 363 ct Star of Lanka, owned by the National Gem and Jewellery Authority
- the 850 ct Pride of Sri Lanka blue sapphire, found in Ratnapura in June 1998
- the 563 ct grayish blue Star of India, which was actually discovered in Sri Lanka and donated to the American Museum of Natural History in 1900 by J.P. Morgan
- the 12 ct blue sapphire in the engagement ring of Diana, Princess of Wales, which is now worn by the Duchess of Cambridge, Kate Middleton

THE EXPEDITION

The goal of this study was to document the entire Sri Lankan colored gemstone industry from mine to market. While many past articles have focused on geology and mining, we decided to cover the entire spectrum, including gem mining, import and export, cutting, treatment, jewelry manufacturing, and retail. We wanted to rely heavily on our own observations for all of the sectors. We sought direct communications with industry leaders and trade members. Through extensive travel and numerous visits to different operations and businesses, we assembled the whole picture. Hundreds of hours of video footage and interviews and more than 7,000 photos documented all aspects of the industry in Sri Lanka.

Our first stop was at the offices of Sapphire Capital Group, where we saw Sri Lankan dealers serving as expert consultants for foreign buyers. For an entire day, we watched a buyer from New Zealand purchase parcel after parcel of sapphire and other gemstones from dealers his local contact had arranged (figure 6). As he chose his sapphires, the foreign buyer would consult the Sri Lankans on how the stones would recut. There we also captured the highly skilled recutting of sapphire and cat's-eye chrysoberyl.

Over the next few days, we paid visits to wholesalers, retailers, and cutting facilities in Colombo. At Precision Lapidaries, we caught a glimpse of the modern Sri Lankan gemstone cutting industry,

Figure 6. Foreign buyers often rely on a trusted local dealer to bring in other dealers to showcase their goods. The local contacts advise their foreign clients on buying decisions and recutting. Photo by Andrew Lucas.

Figure 7. The street scene in Beruwala was full of trading activity. Photo by Andrew Lucas.

which emphasizes precision and quality. Our first trip outside of Colombo was to the weekend market at Beruwala, which was particularly busy (figure 7). We were able to see the art of street dealing in Sri Lanka, along with trading activity in the offices. We also interviewed traditional cutters and a specialist in the heat treatment of sapphire.

Our next stop was the famous gemstone market near Ratnapura, where the trading in the streets was even heavier than at Beruwala. We were allowed to visit numerous offices and traditional cutting and treatment facilities. After spending several hours at the market in Ratnapura, we explored pit-mining operations in the area.

At Balangoda we saw three mechanized mining operations and interviewed several miners. We were also able to watch a river mining operation. By this point in our trip, we had observed the three main types of gem recovery in Sri Lanka: (1) pit mining, including simple narrow pits with galleries and small open-cast operations, both worked by hand; (2) mechanized mining in open pits, incorporating backhoes or bulldozers for digging and sluices for washing; and (3) traditional river mining. In Elahera, another famous locality on our itinerary, we observed a mechanized operation and traditional pit mining.

Back in Colombo, we had three days to explore other cutting facilities, wholesalers and retailers, modern and traditional jewelry manufacturers, and the famous gem and jewelry hub of Sea Street.

GEM DEPOSITS

The classification of Sri Lanka's gem deposits is summarized in figure 8. Most of the gem deposits are of sedimentary nature, though there are some primary deposits related to metamorphic and magmatic rock. Regional and/or contact metamorphism favored the formation of corundum and spinel by removing silica and water, transforming aluminum- and magnesium-

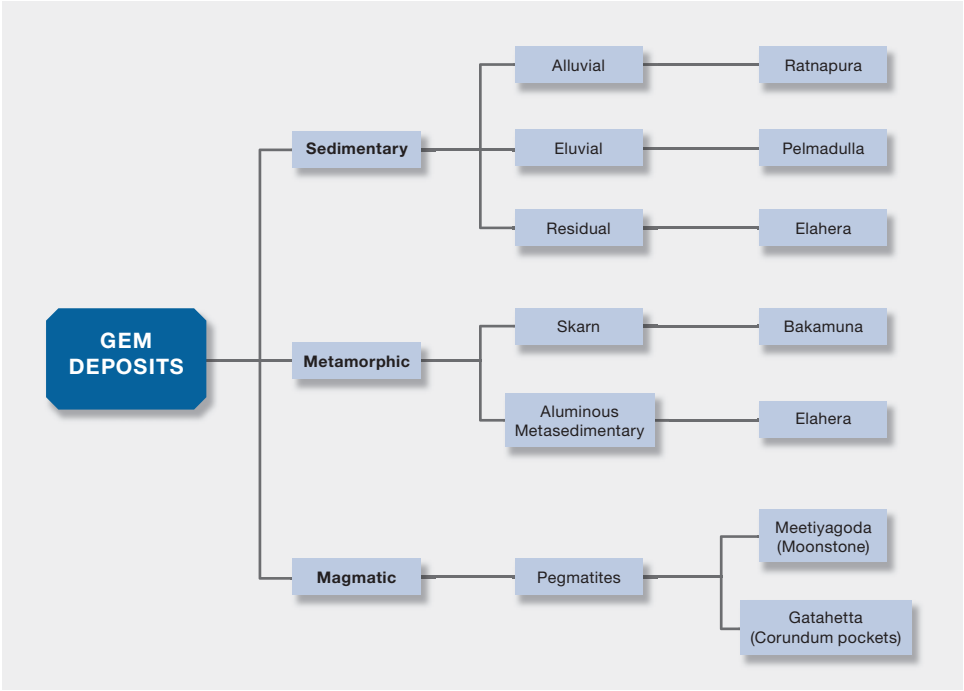

Figure 8. Main gem deposit categories in Sri Lanka and the corresponding mining areas. From Dissanayake and Chandrajith (2003).

BOX A: RELATED EARTH HISTORY

The island of Sri Lanka has been blessed with some of the richest gem deposits on the planet. Metamorphism generated by a series of mountain-building events resulted in the gem wealth we see today. Before the well-known Pangaea, there were several supercontinents in Earth's early history. The assembly and breakup cycles of these supercontinents are the engines that formed most of the world's gem deposits (figure A-1), and some of these events are closely related to gem formation in Sri Lanka.

Nearly nine-tenths of Sri Lanka is underlain by high-grade metamorphic rocks of Precambrian age. Neodymium and rubidium-strontium dating (see Milisenda et al., 1988; Kröner and Williams, 1993) indicate an age between 1,000 and 3,000 million years (Ma). The supercontinent Rodinia, the predecessor of Pangaea, assembled between 1300 and 900 Ma (Li et al., 2008), so the protolith of these high-grade metamorphic rocks must have been inherited from previous supercontinent cycles. McMenamin and McMenamin (1990) considered Rodinia the "mother" of all subsequent continents. More than 75% of the planet's landmass at that time had clustered to form Rodinia, but gigantic size did not translate to stability for the supercontinent. Due to the thermal insulation caused by the giant landmass, the first breakup of Rodinia happened at about 750 Ma along the western margin of Laurentia. Rifting between Amazonia and the southeast margin of Laurentia started at about the same time (Li et al., 2008). While Rodinia was breaking up, the individual continents of Gondwanaland started to join together.

Gondwanaland was assembled between 950 and 550 Ma (Kröner, 1991). Detrital zircon age distributions indicate that the global-scale Pan-African orogeny reached its peak between 800 and 600 Ma (Rino et al., 2008). This orogeny formed one of the longest mountain chains in Earth's history: the Mozambique belt that extends from modern-day Mozambique to Ethiopia and Sudan and also covers most of Madagascar, the southern tip of India, Sri Lanka, and the eastern coast of Antarctica. This belt, a thrust-and-fold zone that marks the junction between East and West Gondwanaland, is also a mineral belt. Modern-day Sri Lanka occupied a central position in this belt. Uranium-lead geochronology shows that the zircons from Sri Lanka's high-grade metamorphic rocks experienced significant Pb loss at 550 Ma, and new growth of zircon, monazite, rutile, and garnet occurred between 539 and 608 Ma (Kröner and Williams, 1993). These are the dates of the near-peak metamorphism that created the gemstones in this country.

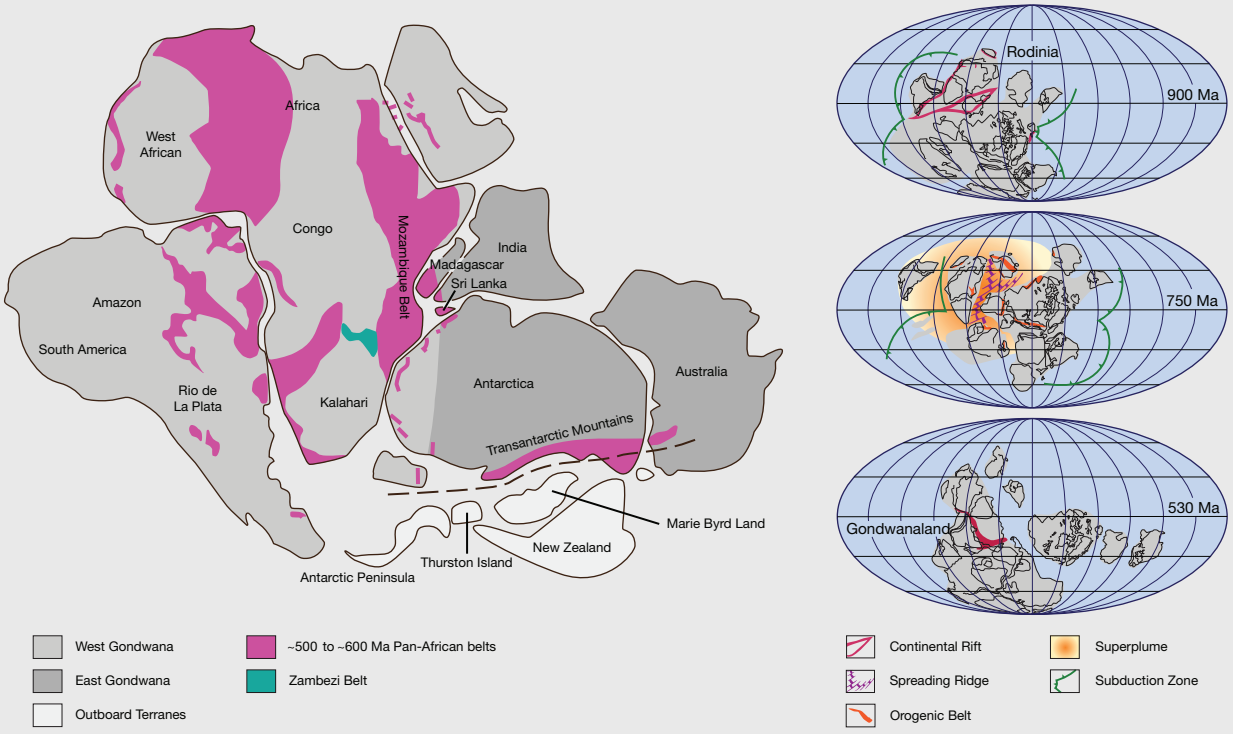

Figure A-1. The supercontinent Rodinia was formed 900 million years ago and started to break apart about 150 million years later. Some of its fragments reassembled to form Gondwanaland, which later became part of the supercontinent Pangaea. South America, Africa, Madagascar, India, Sri Lanka, Antarctica, and Australia were once connected in Gondwanaland. Adapted from Li et al. (2008) and Dissanayake and Chandrajith (1999).

Figure 9. Most Sri Lankan gemstones are from gem-bearing gravel known as illam. The gravels are washed with the hope of revealing a treasure within the heavier material left behind in the miner's hand. Photo by Andrew Lucas.

bearing silicates into oxides. Pegmatites are the most important magmatic source of Sri Lankan gems, hosting beryl, tourmaline, corundum, and moonstone, among others. The most famous pegmatite is the moonstone deposit at Meetiyagoda, in southern Sri Lanka (Dissanayake and Chandrajith, 2003). Mendis et al. (1993) noted that many deposits are distributed along structural features such as faults, folds, and shear zones. Although these structures can influence the distribution of gem deposits, it remains unclear whether they are genetically related.

Almost all of Sri Lanka's sources are alluvial, containing rich concentrations of gem-bearing gravels called *illam* (figure 9). In addition to sapphires, a variety of other gems are recovered from the illam, including spinel, cat's-eye chrysoberyl, and moonstone. Very few important primary deposits have been found. One was discovered by accident during road construction in 2012 near the town of Kataragama (Dharmaratne et al., 2012; Pardieu et al., 2012). The sapphire find was highly valuable, estimated at US$100 million or higher, so the government auctioned off surrounding plots of land for mining. Although these small plots sold for the highest price ever recorded for gem mining licenses in Sri Lanka, no commercially valuable deposits were subsequently found. But a full geological study of the deposit has yet to be conducted, so the true potential of Kataragama is still unknown (V. Pardieu, pers. comm., 2014). Approximately 10 to 15 primary deposits of sapphire have been discovered over the last 20 years, all by accident (P.G.R. Dharmaratne, pers. comm., 2014).

Most alluvial mining is done in areas with a history of gem production. There are many such areas in the central to southern part of the island. Due to the nature of alluvial mining deposits, concentrated gem-bearing gravels may be left behind. The alluvial gravels of Ratnapura and Elahera may contain samples from several types of primary deposits (Groat and Giuliani, 2014). Crystals found at or near the original source rocks can be beautifully shaped, such as those at Kataragama (figure 10). Crystals that have been transported longer distances, like specimens found in Ratnapura, are usually rounded pebbles (Zwaan, 1986).

Prospecting in Sri Lanka is rarely scientific. When evaluating an area, the traditional method is to drive a long steel rod into the ground (figure 11). The prospectors examine the end of the rod for scratches and marks from contact with quartz and corundum, and for gravel stuck to it. Some can even distinguish the sound it makes. This method may also help in determining the depth, composition, size, character, and color of the illam (Ariyaratna, 2013).

With more than 103 natural river basins covering 90% of the country's landmass (Dissanayake and Chandrajith, 2003), there are numerous places for gemstones to be concentrated in gravels. Deposits of corundum and other gems are known to occur in the southern two-thirds of the island (Hughes, 1997). We visited the mining areas around Ratnapura, Balangoda, and Elahera. Although these are but a small

Figure 10. This sapphire crystal is from the primary deposit at Kataragama. Photo by Vincent Pardieu.

BOX B: LOCAL GEOLOGY

Consistent with the nomenclature suggested by Cooray (1994), the Precambrian basement of Sri Lanka can be divided into four units: the Highland Complex (HC), the Vijayan Complex (VC), the Wanni Complex (WC), and the Kadugannawa Complex (KC). Most of the gem deposits are located in the HC, which extends northeast to southwest (figure B-1). Found within the VC are klippes (island-like, isolated fragments of an overthrust rock layer) from the HC. One of Sri Lanka's few primary sapphire mines was accidentally discovered in the Kataragama klippe (Pannipitiye et al., 2012). The Highland Complex contains high-grade metamorphic rocks such as pelitic gneisses, metaquartzite, marble, and charnockite gneiss (Cooray, 1994). Rocks in the HC have the highest grade of metamorphism (granulite facies), and the complex is younger than the VC to the east and south. The contact between these two complexes is a thrust fault dipping west and northwest, with the HC on top. This thrust fault is also a major tectonic boundary interpreted as a suture zone that marks the final junction between West and East Gondwanaland at approximately 550 Ma (Kröner, 1991). The VC is comprised of migmatites, granitic gneisses, granitoids, and scattered metasediments (Cooray, 1994). Lying west of the HC, the WC contains migmatites, gneisses, metasediments, and granitoids. The nature and exact position of the contact between the WC and HC is still not well defined (Cooray, 1994). The smaller KC is within the elongate synformal basins around Kandy. Hornblende and biotite-hornblende gneiss are the main rocks in the KC (Cooray, 1994). Other than these Precambrian basement units, the northern and northwestern coasts of the island are covered by Miocene limestone, Quaternary red beds and clastic sediments, and recent sediments (Dissanayake, 1986).

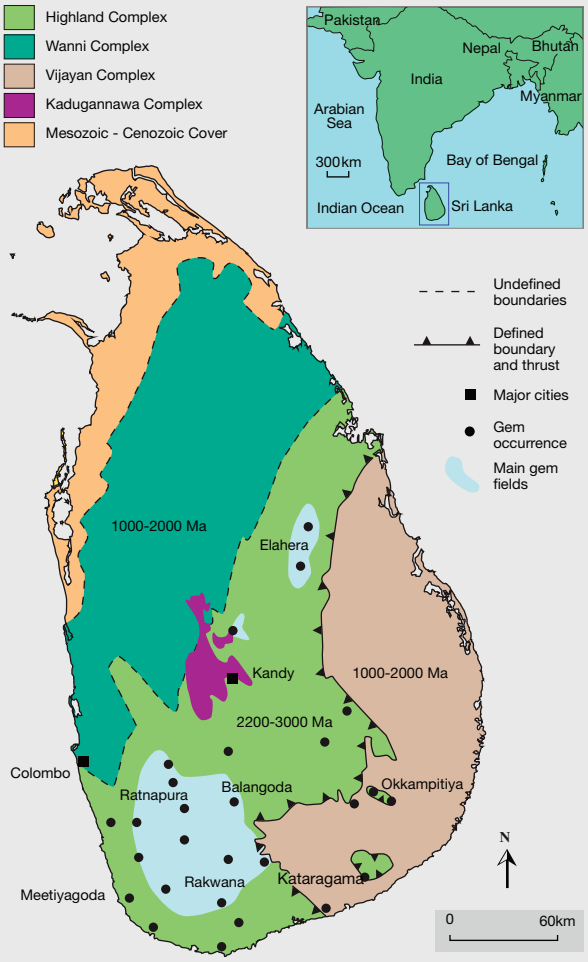

Figure B-1. Simplified geological map of Sri Lanka showing the main basement units and major gem deposits. Adapted from Sajeev and Osanai (2004) and Dissanayake and Chandrajith (1999).

percentage of Sri Lanka's gem deposits, they gave a representative overview of mining operations throughout the country. All of these are secondary gravel deposits—we could not find any primary deposits being mined.

MINING

While the modern mining industry promotes recovery by the fastest means possible, Sri Lanka embraces almost the opposite philosophy. Mining is done primarily by manual labor. The National Gem and Jewellery Authority (NGJA), the regulatory body that issues mining licenses, is very strict in its requirements for mechanized mining. This strategy keeps approximately 60,000 to 70,000 gem miners continuously employed (P.G.R. Dharmaratne, pers. comm., 2014). The predecessor to the NGJA was the State Gem Corporation, which established regional offices and took control of mining licenses and guidelines in 1972. Its regulations for the gem industry supported legal mining operations (Dharmaratne, 2002).

Sri Lanka issued 6,565 gem mining licenses in 2013. Mining licenses must be renewed every year, and the number has steadily increased since 2009,

Figure 11. The traditional method of prospecting in Sri Lanka involves driving a steel rod into the ground and examining it for scratches and marks from quartz and corundum. Photo courtesy of Janka Hemachandra.

when the NGJA granted about 4,000 of them. Many of these licenses are for small areas, half an acre to two acres. Each can accommodate two to four traditional pits, with about 7 to 10 miners per pit; deeper pits may accommodate 10 to 15 miners. This system has maintained a fairly constant number of active mines over the years.

Once a mining area is finished, the shaft or open pit must be filled in according to regulations enforced by the NGJA. These environmental measures pertain to loose gravel contaminating the surrounding water, damage to the landscape, and holes filled with stagnant water, a breeding ground for malaria-bearing mosquitos.

Pit Mining. In Sri Lanka, pit mining is the traditional mining method and by far the most widespread. More than 6,000 of the current licenses are for pit mines, compared to approximately 100 licenses for river mining and 10 for mechanized mining (P.G.R. Dharmaratne, pers. comm., 2014). We witnessed numerous pit mining operations, all excellent demonstrations of the processes described to us by industry leaders. Miners are actually shareholders in such operations, receiving a small stipend and a percentage of the rough stone sales. As shareholders, they need little or no supervision. Several other people are involved in such a venture, including the landowner, the holder of the mining rights, and the person who supplies the pump to dewater the pit; they typically receive 20%, 10%, and 10% of the sales, respectively. The rest of the revenue is split among the financial stakeholders and the miners (P.G.R. Dharmaratne, pers. comm., 2014).

To give an idea of scale, a standard pit mine in Sri Lanka consists of a two by four meter opening at the surface (figure 12). If the pits are deep and located in harder ground, the miners may choose smaller dimensions. The vertical shafts generally range from 5 to 25 meters deep.

Figure 12. The classic two by four meter pits are seen throughout the mining areas of Sri Lanka. These pits are near Balangoda. Photo by Andrew Lucas.

Figure 13. These miners are pumping out rainwater and removing gravel with baskets. Foliage in the wooden structure keeps the pit walls from collapsing during heavy rains. Photo by Andrew Lucas.

The pits are created by first digging the opening to about a meter deep. The next step is making a wooden frame of timbers slightly taller than the depth of the pit. The miners place the first set of four timbers into the pit wall, which is grooved for a secure fit. Vertical struts of timber are wedged between the crossbeams. Branches and foliage help shore up the pit walls from water erosion, and timber braces are used in the center (figure 13). This process continues down the depth of the pit about every meter, until the miners reach the gem-bearing gravel. At this point they create horizontal crawl tunnels about 1.5 meters in height, called galleries, from the pit into the gem-bearing gravel. The length of these tunnels varies depending on the extent of the illam, but often reaches 5 to 10 meters.

The galleries extending from the pit are interconnected with other tunnels. This leaves some areas of illam that cannot be mined because they are needed for structural support. Buckets of gravel are either passed to the surface or hauled up by rope on a manual winch. Some pits have a wood and branch rooftop to shield the miners from the intense sunlight.

A pit with an opening wider than the traditional two by four meters is more like a very small open pit (also called an open cast), but it is still worked by manual labor. We witnessed some of these operations in Ratnapura and Elahera. Usually there were a half dozen people working in each pit. At least one miner at the bottom would shovel the illam into a woven bamboo basket held by another miner. That person would toss the basket to another miner, slightly higher up in the pit, who simultaneously tossed back an empty basket, like a perfectly harmonized juggling act. This process continued through several miners until the illam-filled basket reached the top, where it was dumped into a pile for washing. The accumulated mound of gem-bearing gravel could be covered with leafy branches, similar to those used to shore up the pit walls, to prevent rainwater from washing it away.

Pit mines with a standard two by four meter shaft opening follow a similar process for removing the illam, but often using a manually operated winch for hauling buckets to the surface (figure 14). In both examples, the illam is either washed in a nearby reser-

Figure 14. At this pit in Ratnapura, miners haul the overburden and gravel to the surface in buckets by a hand-powered winch. Photo by Andrew Lucas.

voir by simple panning or removed to a more sophisticated washing facility featuring a sluice. The sluices are often modified from Australian designs, as they are in other parts of the world. The washed gem-bearing gravel is called *dullam* (Zwaan, 1982), which is also the term for the smaller, lower-quality gems picked from washing baskets and usually given to miners to sell.

While rain caused the erosion that created the amazingly rich gem gravels of Sri Lanka, it also poses a significant obstacle to the mining process. Pits quickly fill up with rainwater that must be removed. This is often done by a pump, which is much faster than old-fashioned methods. Substantial rains can also cause erosion damage to the pits. We saw this at several locations, having arrived after fairly heavy rains.

With around 6,500 mining licenses issued annually and around four or five pits in each mine, at any given time there could be 20,000–25,000 active pits in Sri Lanka. With extensive mining over the past 50 years, more than a million pits may have been dug altogether. Compared to many African mining countries, very few abandoned pits are left unfilled. This is because the NGJA collects a cash deposit upon issuing a mining license. If the mine owner fails to rehabilitate the land, the NGJA keeps the deposit for that purpose (P.G.R. Dharmaratne, pers. comm., 2014).

Mechanized Mining. Only a limited number of mechanized mining licenses are issued in Sri Lanka each year. They may be granted if the concentration of gemstones is not high enough to make pit mining viable, or if there is a serious threat of illicit mining. To avoid large rushes of illicit miners to a rich discovery, the government may block access to the area or issue a mechanized mining license so the deposit can be mined quickly and legally (P.G.R. Dharmaratne, pers. comm., 2014).

Mechanized mining speeds the removal of overburden soil and the recovery of gem-bearing gravel for washing. Most mechanized mines in Sri Lanka are relatively small open-pit operations. Overburden soil sometimes contains dispersed gemstones, and it too may be washed. At mechanized operations, the illam is washed by sluices to keep up with the production (figure 15). Mechanized operations in Sri Lanka must also pay a deposit for the rehabilitation of the land.

While mechanized mining operations may use bulldozers, backhoes, excavators, front-loaders, trucks, and sluices for washing, they are still small-scale compared to those in other countries. The mechanized mining licenses are often issued by auction from the NGJA in blocks measuring 30 square meters.

We witnessed three mechanized mining operations near Balangoda. The largest was an open-pit operation about 60 meters deep on a property covering 50 acres (figure 16). It had four excavators, two washing sluices, and a few trucks. The excavators at the bottom of the pit loaded the trucks with gem-bearing gravel. The trucks climbed the roads on the pit

Figure 15. Mechanized mining in Sri Lanka usually includes washing the illam. Trucks move the gravel, which backhoes load into a sluice for washing. Photo by Andrew Lucas.

benches back to the top to the washing operations. The four excavators worked in tandem to move the gravel up the pit until the highest one loaded the trucks.

With global weather changes, Sri Lankan miners are finding that the rainy seasons are no longer as predictable. This interferes with mining operations, whether traditional or mechanized. At the time of our trip, rainwater had filled many of the pits and needed to be pumped out before mining could resume. The pit at the largest mechanized operation we visited took more than a week to dewater.

River Mining. Although nowhere near as prevalent, river mining is also conducted in Sri Lanka. These areas may contain alluvial gem deposits where the river bends or otherwise slows down. The miners choose shallow waters and build a dam made of wood or rock where the stream slows, allowing the water to escape from one side of the dam but trapping the gravels.

Using metal blades attached to long wooden poles called *mammoties*, the miners dredge the gravel until they reach the illam (figure 17). Long pointed steel rods are used to loosen the illam, which is dragged up and washed by the rushing water. Once any visible gemstones are removed, the remaining gravel may be further washed.

We observed a river mining operation in Balangoda next to a tea plantation. There were four miners using mammoties to remove the illam, two miners washing gravels with baskets, and another removing larger rocks and building dams. Another miner would wade into the water to remove gravels and larger rocks. We did not see the use of mechanized or powered dredgers at any river mines.

Figure 16. This open-pit sapphire mine near Balangoda, a large one by Sri Lankan standards, had partially filled with water from rains the week before. Photo by Andrew Lucas.

CUTTING

Gemstone cutting is another area where the traditional meets the modern in Sri Lanka. Centuries of experience in cutting corundum and other colored

Figure 17. River mining near Balangoda involves constant dragging with mammoties to scoop out the illam for washing. Photo by Andrew Lucas.

gemstones continue alongside new technologies and business models. The time-honored art of reading rough and orienting stones is integrated with the global market's growing demand for exact calibration, well-balanced proportions, and high-quality polish.

Our team observed several examples of traditional and modern cutting, as well as some of the highest-precision cutting of colored gemstones we have ever witnessed. Numerous interviews with members of the Sri Lankan cutting industry revealed the interwoven nuances of blending the past, present, and future. There is still a relevant place for old-style cutters and their expertise, even as innovative companies are thriving.

While Sri Lanka has seen some growth in diamond cutting, with 20 companies active in 2013—including De Beers sightholder Rosy Blue—most of the activity is focused on colored stones, particularly sapphire. The number of licensed cutting businesses has increased only slightly over the last five years, from 174 to 192, though today there are larger, more modern lapidary companies.

Traditional Cutting. While the West and Japan sometimes view traditional cutting in Sri Lanka as outdated and not up to modern global proportion and symmetry standards, one can still appreciate the craft. These cutters use a bow to power a vertical lap, often holding the stone by hand or with a handheld dop as they cut and polish (figure 18). They have a high degree of skill in orienting rough gemstones to achieve the best face-up color while retaining weight. Decades and even centuries of knowledge have been passed down on orienting sapphires and other gemstones such as cat's-eye chrysoberyl. Of all the cutting steps for colored stones, orienting the rough to display the best color through the table requires the highest skill, especially with valuable rough where weight retention is foremost. For high-quality sapphires, this method is still preferred by Sri Lanka cutters, especially for preforming.

While blue sapphire often displays its best color through the c-axis, a skilled cutter can make slight angle adjustments to the table and still achieve a fine color with higher weight yield. If this is not done at the initial orientation, multiple recuts may be needed to get the right orientation of the table. With the orientation properly set, the recut produces a beautiful stone with minimum weight loss. For example, a 22 ct blue sapphire that is properly oriented for face-up color can be recut to close windows and optimize proportions and symmetry, while keeping the stone above 20 ct.

Figure 18. While their equipment appears primitive, Sri Lankan cutters' knowledge of orienting rough sapphire transcends technology and generations. Careful orientation to optimize color is a critical skill. Photo by Andrew Lucas.

If the orientation or proportions of a blue sapphire cause a reduction of color, the stone's value suffers accordingly. This is especially true for light- to medium-tone blue sapphires, where even a 5% to 10% reduction of color diminishes the value more than a 5% to 10% weight reduction.

Precision Cutting and Free Size Cutting. For Sri Lanka to become a leader in the colored stone trade, its cutting industry must meet the specific needs of the global market, where customers from different countries require a wide variety of cutting specifications and tolerances. In Sri Lanka, many fine-quality sapphires over one carat are cut as free sizes. The cutting is performed to minimize windowing and yield pleasing proportions and symmetry rather than exact calibrated measurements. This allows weight retention on more valuable material while creating

a beautiful stone with high brilliance. This is essentially a cost decision. It is less expensive to adjust mountings from the standard 12 × 10, 10 × 8, and 9 × 7 mm sizes than to lose weight from valuable gem material. With larger fine-quality material, sizing considerations always give way to beauty and weight retention.

Even customers of calibrated sapphires have a range of tolerances. Some can accept a tolerance range as wide as 0.5 mm. For instance, sapphires cut to 7 × 5 mm sizes can vary up to 7.5 × 5.5 mm for some clients. Others have stricter tolerances, such as 0.2 mm, based on their jewelry manufacturing and mounting requirements. Some cutting companies offer tolerances of 0.1 mm or less (figure 19).

In Colombo, our team visited Precision Lapidaries and interviewed managing director Faiq Rehan. We also spoke with Saman K. Amarasena, vice chairman of the lapidary committee of the Sri Lanka Gem and Jewellery Association and owner of Swiss Cut Lapidary. On both occasions, we gained insights on the state of precision cutting in Sri Lanka.

Despite being a fifth-generation member of the gem industry, Rehan started Precision Lapidaries in 1990 with a business model that was unconventional for Sri Lanka. Rather than cutting only large stones and selling them individually, he specialized in bulk quantities of calibrated cuts, applying the precision standards he had learned years earlier while cutting diamonds. The new company soon received large orders for calibrated sapphires in 2 to 4 mm princess cuts from Japanese clients who constantly pushed for tighter precision and higher quality. In expanding his business, Rehan preferred to hire young people directly out of school and train them to cut sapphire to his exacting standards. This philosophy was unusual in Sri Lanka, where cutters often come from a long line of cutters with deeply ingrained procedures and standards.

As he entered the American market, Rehan found buyers wanting much larger quantities of stones cut at a much faster rate. They did not share the Japanese appreciation for precision measurements and higher quality of symmetry and polish. Rehan did not want to abandon his standards of precision and quality, however. He found that serving a high-quality niche market, rather than having a large inventory full of product similar to what was already available, allowed for constant inventory turnover.

Rehan believes that the high-end and commercial markets in the United States and elsewhere are moving toward stricter precision and cut quality, and he has expanded his business to fill this demand. Many others are doing the same, and this is changing how the world views the Sri Lankan cutting industry. China now requires very bright stones with no windows or dark areas, as well as excellent proportions and symmetry. Chinese demand for its massive jewelry manufacturing industry has helped fuel the growth of precision cutting in Sri Lanka.

Figure 19. The girdle outline of this sapphire is being cut to precise calibrated measurements for jewelry manufacture. Photo by Andrew Lucas; courtesy of Precision Lapidaries.

The actual production model at Precision Lapidaries is also very different from many other cutting operations. Each cutter assumes full responsibility for a given stone instead of handing it off at different stages as in an assembly line. Some large-scale diamond cutting factories in India have also switched to this model to achieve higher quality standards through personal accountability (D. Pay, pers. comm., 2014). Using this model, Rehan treats his cutters more like partners, basing their compensation on both production and quality.

Each cutter has an individual glass-walled workstation to eliminate distractions. A cutter's typical output, using an already preformed and calibrated 8 × 6 mm oval as a benchmark, is 140 to 180 stones per eight-hour workday. The stones are tracked throughout the process and entered into a database. There are several quality control checks at the calibration stage (which requires tolerances of 0.1 mm or less), the faceting stages, and the finished product stage. The company's production manager noted that if any quality factors are not up to standards for calibration

Figure 20. At Swiss Cut Lapidary, Saman Amarasena conducts quality control for the fitting of gemstones in a watch bezel. Photo by Andrew Lucas; courtesy of Swiss Cut Lapidary.

tolerance, facet symmetry, proportion variations, or polish, the stone is returned to the cutter with a repair order.

Another nontraditional practice at Precision Lapidaries is its use of detailed inventory and grading reports, the kind favored by large diamond cutting companies. While there was initial resistance, over time customers became comfortable with the information contained in these reports. Each one itemizes a parcel by shape, weight, cutting style, color, and other quality factors. Established customers can review the reports to make buying decisions and place orders, even through the Internet.

Swiss Cut Lapidary, which supplies the watch industry with colored gemstones, also stakes its reputation on precision and accuracy. The luxury watch industry requires very small stones cut with a high degree of precision, including very tight proportion tolerances for crown height, pavilion depth, and crown angle. Swiss Cut Lapidary cuts round faceted stones below 1 mm, and even down to 0.35 mm for ladies' watches. At these sub-millimeter sizes, each faceted stone has eight crown facets and eight pavilion facets. By achieving zero tolerances to the hundredth of a millimeter, the company is able to meet the stringent demands of watch manufacturers. In finished rounds below one millimeter, the size difference between the starting rough and the faceted stone is very slight—for Amarasena, only 0.20 mm. In other words, for a round faceted stone of 0.50 mm, the rough can be as small as 0.70 mm.

To achieve this level of precision, Mr. Amarasena first learned traditional cutting by hand before working with mechanical lapidary equipment for Japanese clients. To further his skills, he traveled to Germany and Spain, where he cut a variety of colored gemstones using modern machines and techniques. Upon returning to Sri Lanka with high-precision Swiss-made equipment, Amarasena purchased mine-cut sapphires and recut them to global market standards. In Europe he had seen many Sri Lankan sapphires being recut, so he knew the exact requirements.

Amarasena also decided to shift his focus from recutting to unique designer cuts. At the annual Basel jewelry show, he noticed watches with small faceted gemstones set in the bezels. Back in Sri Lanka, he looked for small rough to use for cutting these stones. Rough chips were practically given to him because they were abundant and there was no real market for them. Amarasena faceted tiny precision stones from these chips in a wide variety of colors and tones, providing many options to watchmakers (figure 20). Although the rough costs slightly more today, its cost is minimal compared to the finished cut product. Micro-pave settings are another growing market for these precision-cut gemstones.

Recutting. In Sri Lanka, some sapphires are initially cut with what has been termed a mine cut or native cut (figure 21). While the proportions and symmetry are not up to modern gem industry standards, the cutters execute a high degree of skill in orienting the rough primarily for weight retention. These stones are considered advanced preforms that can be recut to market-friendly proportions and symmetry without substantial weight loss. The ideal color orientation has already been applied, so many Sri Lankan dealers simply have them recut to close windows and remove excess depth from the pavilions while making the shapes less bulky and more appealing.

The same holds true for gemstones sold decades ago that are reentering the global market. Special care must be taken with stones that have deep pavilions. While the market prefers pavilions that are not overly deep, any reduction of color will lower the value considerably (figure 22). If the recut involves more substantial weight loss, then the calculations become more complicated, and every case is unique.

Figure 21. This 6.76 ct "mine cut" sapphire has been oriented by a Sri Lankan cutter primarily for weight retention. It can be recut to meet global standards of proportion and symmetry. Photo by Robert Weldon.

If a 2.08 ct stone is to be recut to 1.80 ct, the buyer must decide if too much of the premium would be lost below the 2 ct size.

These mine cuts from Sri Lanka were once exported to Thailand, the United States, and other countries to be recut to modern global standards. Eventually, Sri Lankan dealers realized they were missing out on a significant value-added service for their customers. Since the 1990s, they have provided that service, selling stones directly that meet the highest international cutting standards.

Besides facet-grade sapphire, our team witnessed the recutting of cat's-eye chrysoberyl and star sapphire. The original mine cuts strongly favored weight retention over symmetry and placement of the cat's-eye or the star. Recutting was needed to reposition these effects to the center of the cabochon and add symmetry. The recutting also made for a straighter cat's-eye that moved more smoothly across the stone. While this involved some weight loss, it was often limited to a few points, and the final product would have significantly higher value on the global market. Japan was once the main market for cat's-eye chrysoberyl from Sri Lanka, but that distinction now belongs to China.

TRADING

Much of Sri Lanka's gemstone trading industry is centered on sapphire. Traditionally this was limited to goods of domestic origin, but today sapphires from around the world are brought to Sri Lanka for enhancement and cutting. Most import and export businesses are family-owned and go back several generations. For example, the fifth-generation Sapphire Capital Group has more than 100 family members involved in the industry. In 2013 there were 4,429 gem dealing companies in Sri Lanka, only a slight in-

Figure 22. The recutting of sapphire (left) requires great skill to close windows and improve symmetry, all while minimizing weight loss and retaining depth of color. Cat's-eye chrysoberyl and star sapphire (right) are recut for better positioning of the effect. Photo by Andrew Lucas.

TABLE 1. Sri Lankan gem exports, 2009–2013.[a]

	2009		2010		2011		2012		2013	
	Weight (carats)	Value (US$)	Weight (carats)	Value (US$)	Weight (carats)	Value (US$)	Weight (carats)	Value (US$)	Weight (carats)	Value (US$)
Cut colored stones	7,134,824	55,429,200	7,380,126	57,444,800	9,154,359	76,921,800	9,176,836	109,016,000	14,349,723	109,273,000
Diamond re-exports[b]	596,528	275,895,000	537,205	276,387,000	573,032	348,119,000	478,668	405,746,000	510,929	290,618,000
Rough imported, exported with added value[c]	6,376,567	1,426,400	7,192,354	1,336,130	7,834,954	1,469,970	12,696,789	2,647,230	14,931,781	3,016,540
TOTAL	14,107,919	332,751,000	15,109,685	335,168,000	17,562,345	426,510,000	22,352,293	517,409,000	29,792,433	402,907,000
Rough gemstone exports	572,958	13,341,378	76,192	2,095,076	275,821	5,278,503	378,624	8,553,650	376,053	24,008,303

[a] *Source: National Gem and Jewellery Authority.*
[b] *Imported as rough diamonds and re-exported as polished diamonds.*
[c] *Cutting performed in Sri Lanka for companies abroad.*
[d] *Rough geuda sapphire exported to Thailand under an existing agreement.*

crease since 2009. Yet the quantity and value of exports has risen sharply over those five years (table 1).

During the 1970s and 1980s, Thailand emerged as the undisputed leader in corundum trading. Its facilities began mastering the art of heat treatment, purchasing corundum rough from around the world. This included Sri Lankan *geuda* sapphire, which is translucent and has a desaturated, often grayish color. As the Thais discovered, heating this material gives it a transparent, highly saturated blue color. Sri Lankan buyers considered the geuda rough virtually worthless and were slow to capitalize on the use of heat treatment to turn it into a very valuable gemstone (Kuriyan, 1994).

Unlike their Thai counterparts, Sri Lankan buyers dealt primarily in domestically mined rough. Part of this had to do with the idea of preserving a national brand identity, but what really hindered them was a cumbersome import policy for rough. This changed in the mid-1990s when the government lifted import duties that had inhibited the purchase of corundum rough from other sources. Sri Lankan buyers have, in turn, established a strong presence in the marketplace, especially at global gem sources such as Madagascar and Mozambique. While the country's industry still capitalizes on the brand identity of domestic gems, the trade is much more open to gems mined elsewhere.

The improvements in the Sri Lankan industry are timed perfectly to take advantage of the increased global demand for sapphire, particularly the Chinese colored stone market ("China becoming Sri Lanka's top gem buyer...," 2011). As an example of the rise in sapphire prices over the last few decades, untreated top-quality blue sapphires sold in Sri Lanka can reach US$15,000 to $20,000 per carat. Those are dealer to dealer prices. In 1969 similar stones would have sold for US$400 to $1,000 per carat—approximately $2,600 to $6,500 per carat, adjusted for inflation (N. Sammoon, pers. comm., 2014).

Local Mining Area and Street Markets. The first major street market we toured was in Beruwala, 60 km south of Colombo. The gem trading area of Beruwala is also known as China Fort, named for the Chinese merchants who arrived about 300 years ago. Most of the dealing occurs within a single block, where there is constant activity of dealers on the street. This market is open on Saturday from 6:00 a.m. to 2:30 p.m., or later if there is strong activity. During our visit, the market was also busy on Sunday. At any given time, over 5,000 dealers may be active on the street and in the hundred or so offices—the major dealers in Colombo have offices in Beruwala—offering rough sapphire from the mines of Sri Lanka, as well as Africa and other global sources. We witnessed a flurry of trad-

Figure 23. Rough sapphire trading on the street in Beruwala sometimes had a modern twist, with dealers negotiating on motorbikes. Photo by Andrew Lucas.

Figure 24. The streets in Ratnapura were crowded with local dealers and dealers from Colombo and other Sri Lankan trading areas. Photo by Andrew Lucas.

ing activity. Sri Lankan dealers often traded rough among themselves on the street (figure 23). Once word got out of a foreign buyer in a dealer's office, other dealers would come by with their stones. There were also traditional Sri Lankan cutters and heat treatment facilities in Beruwala.

Just off the street was Emteem Gem Laboratory, where dealers could bring in stones for testing and identification. The demand for lab services has grown tremendously with the influx of foreign customers, especially Chinese buyers. One of the most sought-after services is the detection of heat treatment in corundum. This is also one of the most challenging identifications, especially if relatively low temperatures are used in the treatment. For corundum that has been subjected to very high temperatures, clients were advised to submit the stone to a foreign laboratory with more sophisticated instrumentation that could conclusively identify beryllium diffusion. About half of the stones submitted to the Emteem lab are believed to be of African origin (M.T.M. Haris, pers. comm., 2014).

We also stopped at the gem market in Ratnapura on the way to several nearby gem-mining operations. This market is active daily from 6:00 a.m. to 4:00 p.m. Like Beruwala, this market was bustling on the streets and in dealer offices (figure 24). While the streets were crowded with dealers, the market was spread out over several streets, as opposed to the single block in Beruwala.

Ratnapura had numerous small traditional cutting operations. Like Beruwala, transactions were happening all over the street, particularly between Sri Lankan dealers. The market at Ratnapura is centered in one of the country's major gem sources and offered plentiful rough from the nearby mines and other areas (figure 25). There was also an abundance of cut stones for sale. Some foreign buyers on the street dealt directly with local miners, but most transactions were between Sri Lankan miners and dealers. We saw the same dealers attending different markets.

Figure 25. Numerous parcels of rough corundum were offered in the Ratnapura street market. Most of the rough had the rounded, waterworn appearance typical of stones from an alluvial deposit. Photo by Andrew Lucas.

Figure 26. Local dealers with decades of experience provide invaluable consultation to foreign buyers on recutting stones and purchasing rough material. Photo by Andrew Lucas.

Consulting for Foreign Buyers. One growing trend is for foreign buyers to work with Sri Lankan dealers to develop long-term supply chain management. The foreign dealers can arrange to have a variety of goods brought to their local contact's office, allowing them to see much more inventory during a trip. The local dealer puts the word out to suppliers for the type of material required. Dealers bring their goods to the office for inspection by the foreign buyer. Prospective sellers are screened, making the transaction process more organized and less of a selling frenzy. Once the price is negotiated, the rest of the logistics—payment for the stones, export requirements, and shipping if required—are handled by the local contact, who receives a set commission from the seller.

Besides convenience, this arrangement offers several other benefits. The local contact can give expert advice on recutting, including the difference in carat weight and price per carat. They can also recommend an acceptable counteroffer and give an expert opinion on the nature of the material (figure 26). This system minimizes risk, as the local contact stands behind the goods they have brought to the foreign buyer. For extra assurance, they can have the stones checked by a gemologist before the buyer leaves the country. Colombo is a hub for such services, and this same expertise and assurance is sought by foreign buyers in Sri Lankan mining areas and street markets.

Imports and Exports. Sri Lanka's import policies have been greatly simplified, making the process much easier and more cost-effective. For a US$200 charge, rough, preformed, and cut stones can be imported for cutting, recutting, and heat treatment. The flat rate charge is assessed regardless of quantity and value. As of 2013, foreign customers buying gemstones parcels valued at over US$200,000 are expedited through customs so they can board their flight with minimum processing. The export fee for these parcels is a flat rate of $1,500. Parcels valued below US$200,000 require about two hours to be processed by the NGJA for export (A. Iqbal, pers. comm., 2014).

Buying on the Secondary Market. Because Sri Lanka has been supplying sapphire, cat's-eye chrysoberyl, and other gemstones to the global market for so long, many dealers have decades of experience and an international clientele. Having maintained relationships with their customers, they know where to find important stones that were sold years before. They can contact their clients and act as brokers to resell the gemstones, making a substantial profit for both parties. As global wealth shifts toward China, previous customers in Japan and the West have become sources of fine-quality gemstones for this secondary market. These stones may be recut to more contemporary proportion and symmetry standards, and sapphires that were heated 30 years ago can be retreated using modern technology. A couple of decades ago, Sri Lankan dealers would attend exhibitions and trade shows in Japan and the United States to sell gemstones. Now some of them go to buy gemstones for recutting, heat treatment, and resale in the Chinese market.

HEAT TREATMENT

Sri Lanka is highly regarded for its heat treatment expertise (figure 27). Those who perform heat treatment, called burners, are known for their ability to get the finest blue color out of a sapphire. They typically use a two-part process, a combination of gas and electric furnaces. The second burn, in the electric furnace, refines the blue color, often achieving a much more valuable color. Some other countries that treat sapphire send their heated material to Sri Lanka for the second burn (A. Iqbal, pers. comm., 2014).

We visited one burner in Beruwala who heated blue sapphire from Sri Lanka and Madagascar in a gas furnace. The stones were heated to approximately 1600°C to 1700°C for four hours in an aluminum oxide crucible with a reducing atmosphere. For yellow Sri Lankan sapphires, the burner used an oxidizing atmosphere at approximately 1600°C for six hours. No compounds or fluxes were used in the crucible. The gas furnace is typically a Lakmini furnace, which has an alumina chamber covered in insulation and a stainless steel exterior, a water cooling system, two gas flow meters, two thermocouples and temperature indicators (digital or analog), a view hole, and an inlet top feed for an additional gas such as nitrogen or hydrogen (M. Hussain, pers. comm., 2014). An atmosphere rich in carbon dioxide is reported to work best for geuda sapphires, turning them transparent and blue (Kuriyan, 1994).

Clients typically bring mixed parcels of sapphires in different colors. The burner will divide the lot by color and type of sapphire and the desired result, and then advise the client of the different heating processes and what can be expected after treatment. Most stones brought to the burner are in the preform stage, so most of the inclusions that could cause damage are already cut away. Treatment in the gas furnace is almost always followed by heating in an electric oven to further improve the color (M. Hussain, pers. comm., 2014).

Expertise in heat treatment has also made Sri Lankans more competitive in buying rough from Africa and other sources. Some African blue sapphire, especially from Madagascar, is similar to Sri Lankan geuda material (F. Rehan, pers. comm., 2014). In value terms, the effect of modern heat treatment is tremendous. One Sri Lankan burner can reportedly take light blue sapphire with silk inclusions causing a foggy appearance, valued at US$300 per carat for a 10 ct stone, and heat it to a transparent fine blue color valued at US$2,000 per carat. This burner asks for one-third the value of the heated stone rather than a flat fee (N. Sammoon, pers. comm., 2014).

Figure 27. Rough sold in mine-area markets can be dramatically improved through heat treatment. It takes considerable experience to predict the change in value. Photo by Andrew Lucas.

JEWELRY MANUFACTURING

As with gemstone cutting, there are both traditional and modern methods for jewelry manufacture. Both approaches are used in Sri Lanka, though some metals and styles are more suited to modern manufacturing. Mass-production techniques give some companies a competitive advantage by lowering costs. Jewelry made in Sri Lanka is targeted to the domestic retail market and to Sri Lankans living abroad. Manufacturing for export and for the emerging tourist industry is expected to grow.

Traditional 22K Gold Jewelry Manufacturing. The 22K gold jewelry manufactured in Sri Lanka is alloyed to have a slightly more reddish yellow color than similar goods from India, Singapore, Dubai, and Turkey. This is accomplished by using a slightly higher percentage of copper and a lower percentage of silver in the alloy.

In countless small workshops in Colombo and other areas of Sri Lanka, 22K gold jewelry is manufactured using time-honored and modern methods. We witnessed many of these shops in Colombo and during an extensive tour of the Sujitha Jewellery workshop on the famous hub of Sea Street. While small by global standards, this was one of the larger facilities we observed. They worked primarily with 22K gold and created traditional styles.

About a dozen jewelers were working in small rooms that made very efficient use of space. The jewelers sat on the floor as they fabricated by hand. Many of them were shirtless due to the heat. They bent and formed metal with pliers, filed, sawed, polished with flex shafts and traditional leather strips embedded with polishing compounds, and soldered. Most used jeweler's torches, but one still preferred a blowpipe for soldering (figure 28). Equipment such as a hand-powered rolling mill and draw plate was used to make gold sheet and wire.

Figure 28. This jeweler preferred the traditional blowpipe for soldering 22K gold jewelry. His ability to control the direction and intensity of the flame was remarkable. Photos by Andrew Lucas.

Modern Jewelry Manufacturing. In contrast to these traditional shops are modern facilities where technology has been embraced by the Sri Lankan jewelry manufacturing industry. Large-capacity vacuum casters imported from Italy can handle numerous waxes for mass production of both 22K gold jewelry and more contemporary pieces in 18K gold, white gold, platinum, or even silver. Other technologies such as casting diamonds in place, laser welding (instead of soldering), stamping or die striking, machining, and CAD/CAM—the methods used in manufacturing centers such as Italy, China, and India—have been adopted by progressive Sri Lankan jewelry manufacturers (figure 29).

We visited the modern factory of Wellawatta Nithyakalyani Jewellery in Colombo. The company manufactures jewelry primarily for its retail store and online business, which also serves overseas clients. The spacious facility handled all types of gold alloys, silver, and platinum, but a large part of the production consisted of 22K gold jewelry. While the factory incorporated methods such as lost-wax casting and die striking, there were also jewelers working on hand fabrication using traditional forming techniques, albeit at modern jeweler's benches.

Besides traditional 22K gold jewelry for the domestic market, modern jewelry manufacturing is also being adopted by colored stone cutting and trading companies who are moving into finished jewelry. Customers from the United States and other developed markets are increasingly purchasing Sri Lankan jewelry with mounted colored stones (S. Ramesh Khanth, N. Seenivasagam, and N.S. Vasu, pers. comms., 2014). Jewelry that can be designed and custom-made to specifications is also manufactured in Sri Lanka.

One of Sri Lanka's leading retailers and jewelry exporters, Wellawatta Nithyakalyani Jewellery is also one of its most progressive manufacturers. Along with mass-market 22K gold jewelry, they manufacture a full range of styles, including gemstone, synthetic gemstone, white gold, and platinum jewelry (figure 30). To safeguard against cross-contamination, tools such as files, polishing wheels, and

Figure 29. CAD/CAM is used for all styles of Sri Lankan jewelry design, even traditional 22K gold jewelry. Photo by Andrew Lucas; courtesy of Wellawatta Nithyakalyani Jewellery.

burs are dedicated solely to platinum manufacturing.

In 1990, Wellawatta Nithyakalyani invested in a vacuum casting machine from Italy. The few other casting operations in existence used centrifugal casting. This machine gave the company an advantage in capacity, speed, and cost of producing jewelry for its retail store. In terms of consistency, vacuum casting lowered the weight variation of pieces from about 10% with hand fabrication to less than 1%. Today, the factory incorporates hand fabrication, wax carving, casting, stamping, and various settings such as prong, bead, pavé, and channel.

Wellawatta Nithyakalyani's manufacturing methods are becoming more modernized and cost-effective. Even though hand fabrication costs remain relatively low in Sri Lanka, the competitive market and low margins for 22K jewelry have led to the widespread use of casting (figure 31) and stamping. Companies that manufacture and sell directly to retail customers have a distinct advantage, as they can eliminate distribution costs for this low-markup jewelry.

The company focuses its retail efforts on women and middle- to upper-class consumers in Colombo and its suburbs, where the country's strongest jewelry market exists. The precious metal weight of its jewelry ranges from one gram to over 100 grams in a single piece, catering to a broad span of income. Wellawatta Nithyakalyani also manufactures and retails jewelry set with diamonds, colored gemstones, cubic zirconia, and crystal glass. This includes white precious metals, 18K gold, and traditional 22K gold used for weddings and as financial assets. The 22K gold wedding necklaces generally range from US$450 to $4,500.

Between its manufacturing and retail operations, the company staffs about 115 employees, representing a cross-section of Sri Lanka's ethnic and religious groups. Its two full-time designers have degrees in architecture and are trained in jewelry design using CAD/CAM.

Most of Wellawatta Nithyakalyani's export business is for mass-produced lines of jewelry sold in high volume. These are shipped to retailers in Canada, UK, Switzerland, Australia, and Dubai, where they are usually purchased by Sri Lankans living abroad. These expatriates also buy jewelry, especially diamond and gemstone merchandise, when they return to Sri Lanka for holidays. In addition, the company's website offers an extensive line of jewelry directly to retail customers worldwide.

Another company that encompasses the manufacturing-to-retail value chain can be found on Sea Street, home of Ravi Jewellers. The company, founded in the 1960s by Ravi Samaranayake as a small traditional 22K gold jewelry retailer, has operated continuously for almost 50 years. Today, the firm is involved in jewelry manufacturing, creating jewelry of all styles sold directly to retail customers (figure 32).

With its modern manufacturing capability, Ravi Jewellers also sells wholesale to other retailers throughout Sri Lanka. This demonstrates another

Figure 30. While 22K gold jewelry represents the mainstream in Sri Lanka, contemporary jewelers also sell white metal and gem-set jewelry, such as the earrings and ring worn by this model. Photo by Andrew Lucas; courtesy of Wellawatta Nithyakalyani Jewellery.

Figure 31. These wax carvings are being fine-tuned to make master models from which tens of thousands of pieces can be reproduced. Photo by Andrew Lucas; courtesy of Wellawatta Nithyakalyani Jewellery.

emerging trend where companies that cover the manufacturing-to-retail value chain sell wholesale to smaller domestic retailers. Their manufacturing division also allows them to provide an extensive custom design service to their retail clients and on the wholesale level to other retailers, a business model that creates a competitive advantage. In addition to being the Sri Lankan agent for Swarovski synthetic cubic zirconia, the company markets Italian alloys and serves as an official currency exchange to accommodate tourists. It has even ventured into selling gold bullion purchased in Dubai. For all its modernization and expansion of services, Ravi Jewellers remains a family business, typical of the Sri Lankan industry.

JEWELRY RETAIL

Sri Lanka has a thriving domestic retail jewelry industry. Its dynamics are different from those of Western jewelry markets and even elsewhere in Asia. Its retail industry is strongly influenced by jewelry's role in Sri Lanka as an investment and hedge against economic uncertainty, the tradition of gold wedding jewelry, the preferences of religious groups, the tourist trade, the Western tendencies of younger consumers, and the lack of emphasis on gemstones in jewelry.

Jewelry as a Financial Asset. The use of gold jewelry for financial security is a tradition among many Sri Lankans. As one European gem dealer noted, they are more practical than Western jewelry buyers, who purchase luxury branded products as status symbols that lose most of their value immediately. When there is ample income, Sri Lankans typically buy gold jewelry that can be converted to cash during difficult economic times.

The pawn industry is a major component of the Sri Lankan economy, and most major banks issue loans with jewelry as collateral. The loans are based almost entirely on the commodity value of the gold, with

Figure 32. Sri Lankan retailers needed a large inventory for their customers to choose from. Box after box of 22K gold and other types of jewelry would be brought out for customers. Photo by Andrew Lucas; courtesy of Ravi Jewellers.

heavier 22K pieces receiving the highest loan value. Some of the country's major banks have anywhere from 17% to 40% of their lending portfolios concentrated in gold jewelry as collateral (A.P. Jayarajah, pers. comm., 2014). Many lower- to middle-class Sri Lankans use pawn shops for 22K gold jewelry loans, receiving instant cash for 75% to 80% of the gold value. Most of these pieces are heavy, from about 80 to 160 grams. Clients generally redeem their items within six months to a year and pay a slight interest charge. Men tend to pawn jewelry more than women (V. Rishanthan, pers. comm., 2014).

During the height of the gold market, when prices soared to more than US$1,700 an ounce, the lending industry became very competitive and pawn shops were offering around 90% of the gold value of jewelry. Many consumers did not redeem their jewelry at these loan values, and when the price of gold fell, the pawn shops lost substantial collateral value.

Wedding Jewelry. For most jewelers in Sri Lanka, the wedding business is arguably the most important. Although jewelry trends inevitably change, gold is an essential component of a Sri Lankan wedding. Jewelry is given to the bride and the groom, as well as the bridal party. Around 80% of this wedding jewelry is for the bride, though jewelry purchases for the groom are on the rise (V. Rishanthan, pers. comms., 2014). Traditional 22K gold jewelry remains the wedding jewelry of choice, and it is still used as a dowry in Sri Lanka.

Sri Lankans comprise many of the major religions: Buddhism, Hinduism, Islam, and Christianity. Each religion has its own style of jewelry, especially for weddings, with differences both subtle and obvious (A.P. Jayarajah and V. Rishanthan, pers. comms., 2014). Hindus tend to wear larger, heavier jewelry of a more Indian style, and designs are often based on what is popular in India (V. Rishanthan, pers. comm., 2014). In Hindu weddings, the bride is given substantial amounts of 22K gold jewelry, including a thick Thali necklace (often weighing between 80 and 250 grams) and longer chains, as well as bangle bracelets. The groom usually receives one simple ring. The bridesmaids and the groom's mother and sisters also receive 22K gold jewelry, making Hindu weddings a major jewelry purchasing event in Sri Lanka.

Buddhists use both rings and necklaces for weddings, often with more floral and classic Sinhalese designs. Sinhalese Buddhists tend to choose lighter, more delicate designs than Hindus for weddings. Brides are presented with a ring, necklace, bangle, and matching earrings in their wedding sets, and the groom receives a gold ring. Still, most Buddhist weddings do not involve as much gold jewelry as Hindu weddings.

In addition to the Thali, Sri Lanka's Christian community uses rings for the bride and groom. Whereas Hindu Thali necklaces often incorporate a square shape with a symbol of Vishnu inside, Christian Thali designs feature the Bible or a heart shape with a dove. Muslims tend to buy larger and heavier bangle bracelets than the Hindus, Buddhists, or Christians.

Sri Lankan retailers immediately know the ethnicity and religion of their customers by observing the jewelry they wear into the store. Of the more than 3,500 bangle bracelets in Wellawatta Nithyakalyani's product lines, around 95% of these are 22K gold. This is the bracelet of choice in the Muslim community, whose women display their bangles stacked on the arm. Muslim brides also receive a Thali and a large chain, matching earrings, and engagement necklace. Grooms often prefer a white metal for their ring.

Expatriate and Tourist Trade. The strong tie between Sri Lankans and their jewelry is not confined to the island. Sri Lankans living abroad, many of whom left during the civil war, purchase traditional jewelry when returning to their native land. The month of August is especially busy for Sri Lankan retailers, as many expatriates living in Europe return for vacation (V. Rishanthan, pers. comm., 2014). They will plan out and purchase all the jewelry gifts needed for the entire year, such as weddings, birthdays, and other occasions. Again, most of them choose traditional 22K gold jewelry based on ethnic or religious heritage.

Since the end of the civil war in 2009, tourism has been growing. With over one million tourists in 2013 and an expected doubling of that figure in 2014, retailers noted a dramatic impact on sales. Many of these tourists are Sri Lankans living abroad, but retailers are seeing more European, Australian, American, and especially Chinese visitors. The country's jewelry industry is working to brand Ceylon sapphires, which are sold in boutiques of major hotels (A. Iqbal, pers. comm., 2014). Retailers are reporting the positive effects of tourism on sapphire jewelry sales. Global awareness of Sri Lankan sapphires was also heightened in October 2010, when Great Britain's Prince William gave Kate Middleton a Sri Lankan blue sapphire engagement ring—the same ring worn by his mother, Diana, Princess of Wales. According to officials from the NGJA and the Inter-

national Colored Gemstone Association (ICA), demand for Sri Lankan blue sapphires in engagement rings rose sharply in the West and in China.

Sea Street. One of the most important areas for Colombo's jewelry trade is near the harbor on Sea Street. The Sea Street jewelry trade was started in the early 1900s by the Chettiar community, a Hindu caste originating in southern India. They are known as a mercantile class of businesspeople and bankers. The Chettiar merchants were involved in money lending, largely with jewelry as collateral. Over time, this led to the development of jewelry retail, wholesale, and manufacturing businesses on Sea Street. By the 1950s, the district had become the major jewelry hub of Sri Lanka, focusing on 22K gold. There are still Chettiar temples on Sea Street today, though much of the community has returned to India (V. Rishanthan, pers. comm., 2014).

While Sea Street remains the country's jewelry hub, the rest of the country has seen significant retail and wholesale growth since the end of the civil war. Sea Street often supplies these new retailers with wholesale jewelry and manufacturing, or with specialized services such as stone setting, laser welding, and plating. In return, small local manufacturers throughout Sri Lanka supply finished jewelry to Sea Street retailers (V. Rishanthan, pers. comm., 2014).

Walking down the few blocks of Sea Street, you see hundreds of jewelry stores and pawn shops (figure 33). Closer examination reveals that some of the storefronts lead to complexes divided into 50 to 100 very small shops, some just 10 by 10 meters. Within these shops, jewelry is crafted using traditional methods. Much of the manufacturing on Sea Street consists of family businesses that continue from one generation to the next.

Gemstone Jewelry Market. While Sri Lanka is known all over the world as an abundant supplier of sapphire and other colored gemstones, the local market for gemstone jewelry is surprisingly weak. Much of the domestic demand is for 22K gold jewelry without gemstones.

Even more interesting is the Sri Lankan preference for synthetic cubic zirconia and crystal glass in jewelry. This is directly related to the custom of buying jewelry as much for financial security as for personal adornment. Sri Lankans can always go to a pawn shop or bank and receive a high percentage of the gold value in their jewelry as a loan. Once gemstones are added to the jewelry, it becomes more difficult to receive a loan value close to the cost of the piece. The gemstone value is not as liquid and cannot be assigned a market value for a loan.

Figure 33. Sea Street is a concentrated center of retailers, pawn shops, and jewelry manufacturers. Photo by Andrew Lucas.

As a low-cost alternative to add color and sparkle to their jewelry, many Sri Lankans opt for cubic zirconia and crystal glass (figure 34). For instance, a 22K gold bracelet set with CZ might cost US$500 at Wellawatta Nithyakalyani, compared to US$5,000 for a comparable bracelet set with good-quality natural diamonds. Unlike consumers in the West or Japan and China, Sri Lankans see little reason to spend the difference. For mass-market 22K gold jewelry, most consumers only allow the addition of gemstones up to 25% above the price of the gold. After that, there is price resistance. Sri Lankans are often willing to spend more on gemstones in 18K gold jewelry—approximately 40% above the gold value—and even more for platinum jewelry. But this custom is slowly changing, and the market for natural colored gemstones and diamonds set in jewelry is growing, especially among upper-income and young consumers.

Younger Consumers. V. Rishanthan, director of Ravi Jewellers, compared the buying preferences of his mother's generation and his wife's generation. His mother's generation, composed of women in their sixties, prefers large sets of 22K gold jewelry and substantial pieces weighing 40 to 80 grams. These impressive sets are reserved for special occasions such as weddings, birthdays, and visits to the temple. The rest of the time, such jewelry is kept in a safe or other

secure location. This generation also views jewelry as a commodity that can be readily pawned for cash.

Rishanthan's wife, representing the younger generation of women in their twenties and thirties, prefers lighter jewelry, such as necklaces weighing around 8 to 10 grams. His wife may own ten lighter pendants while his mother may have only two much heavier pendants. Younger women are very aware of jewelry's financial uses but want to wear it every day, in a variety of fashionable styles.

Another trend among younger Sri Lankans is to resell their jewelry back to a store within six months to a year to trade it in for a new style. So while younger consumers may be buying lighter jewelry, they are buying more pieces and constantly exchanging them for new styles, creating more opportunities for the Sri Lankan retail industry. These younger consumers pay close attention to design trends and up-and-coming designers (V. Rishanthan, R. Samaranayake, J. Sasikumaran, and Y.P. Sivakumar, pers. comms., 2014).

The younger generation is also far more open to other gold alloys such as 18K, and they are especially fond of white metals such as platinum, white gold, and silver. Still, the sentimental and investment aspects of 22K yellow gold jewelry are not lost on the new generation of Sri Lankan consumers. Younger men are buying more jewelry for themselves, and these still tend to be heavier pieces.

With their preference for modern designs, younger consumers also buy more jewelry with diamonds (especially smaller ones) and colored gemstones, usually set in white metal. Blue sapphire is quite popular. Synthetic cubic zirconia or crystal glass can also be used to achieve the desired color. As with yellow gold jewelry, these white metal pieces tend to be lightweight.

Figure 34. Many retail stores offer gold jewelry with less-expensive Swarovski crystal and cubic zirconia to add color and sparkle. Photo by Andrew Lucas.

CONCLUSION

Our expedition to Sri Lanka took us through all sectors of the colored gemstone and jewelry industry. While other reports have tended to focus on mining or treatment, very few have tackled the entire scope of the Sri Lankan industry. Over the course of two weeks, we witnessed mining operations, traditional and modern cutting, trading, treatment, and retail. The resulting documentation revealed a very vibrant industry across all sectors and allowed us to construct a complete picture.

The changes over the last decade have been significant. Modernized cutting has allowed Sri Lanka to produce precision cuts of the highest caliber. Meanwhile, traditional cutting continues to incorporate centuries of experience orienting sapphire, cat's-eye chrysoberyl, and other colored stones for color and weight retention. Mining is still aggressively pursued but mostly by small-scale operations, helping to preserve the environment and gem resources so more Sri Lankans have more opportunities to strike it rich.

A wealth of trade expertise gives Sri Lanka a competitive advantage as it looks to expand its share of the global gem market. Many foreign buyers consult with local dealers on purchasing decisions and the potential benefits of recutting and heat treatment. Rough stones imported from other global sources fuel the value-added industries of cutting and treatment. With decades of trading experience and a global client list, Sri Lankan dealers know where to find important stones for the growing secondary market, particularly in China. Meanwhile, trade organizations such as the National Gem and Jewellery Association and the National Gem and Jewellery Authority are working on a bilateral trade agreement that could eliminate import tariffs on colored gemstones entering China from Sri Lanka (R. Kamil, pers. comm., 2014).

Jewelry manufacturing is another sector that incorporates both traditional and modern techniques. Most of the manufacturing is to satisfy consumer demand for 22K gold jewelry, as a wedding gift and as a financial asset, at home and in Sri Lankan communities around the world. Younger consumers are demanding contemporary styles, new metals and alloys, and a greater use of gemstones. A growing tourist industry is also influencing Sri Lankan jewelry manufacture.

Figure 35. The Sri Lankan retail industry hopes to maintain the traditional market in 22K gold jewelry while developing new products to meet the tastes of future generations. Photo by Andrew Lucas.

With rapid economic development since the end of the civil war in 2009, the Sri Lankan gem and jewelry industry could see dramatic growth, albeit at a much smaller scale than in neighboring India. Some of this growth is already happening in the diamond jewelry market, which has long been hindered by consumers' limited purchasing power and the tradition of pawning jewelry for the commodity value of the precious metals. It remains to be seen whether Sri Lankan demand for contemporary jewelry featuring diamonds, colored stones, and alternative precious metals will match the popularity of 22K gold jewelry (figure 35).

The island's gem and jewelry industry displays remarkable vitality and ambition for growth. With the ICA Congress coming to Colombo in 2015, the influx of foreign buyers to the annual Facets Sri Lanka show, and a stronger presence at trade shows in China, the Sri Lankan industry is striving for greater international recognition.

For More on Sri Lanka

Explore Sri Lanka's mine-to-market industry through *G&G*'s exclusive multimedia content. Our online collection provides direct links to videos, field reports, and additional resources that reveal this island nation's impact on the global gem and jewelry trade.

Visit www.gia.edu/gia-news-research-sri-lanka-mining-part1, or scan the QR code on the right.

ABOUT THE AUTHORS

Mr. Lucas is manager of field gemology, Dr. Hsu is technical editor of Gems & Gemology, *and Mr. Padua is video producer, at GIA in Carlsbad, California. Mr. Sammoon is a member of the board of directors of the National Gem and Jewellery Authority, chairman of the Sapphire Capital Group, chairman of foreign promotions and deputy chairman of Facets Sri Lanka of the Sri Lanka Gem and Jewellery Association. Mr. Jayarajah is CEO of Wellawatta Nithyakalyani Jewellery and chairman of the Sri Lanka Gem and Jewellery Association.*

ACKNOWLEDGMENTS

The authors would like to thank the following members of the Sri Lankan gemstone and jewelry industry for all their support and sharing their experience and knowledge: Shamil Sammoon (Sapphire Capital Group); Naji Sammoon (Sapphire Cutters Ltd.); Faiq Rehan (Precision Lapidaries); Sujitha Traditional Jewellery; Ravi Samaranayake and V. Rishanthan (Ravi Jewellers); Y.P. Sivakumar and J. Sasikumaran (Wellawatta Nithyakalyani Jewellery); Prof. P.G.R. Dharmaratne (former chairman, National Gem and Jewellery Authority); Ajith Siriwardena (deputy superintendent of Customs); Saman K. Amarasena (Swiss Cut Lapidary); A.H.M Imtizam (Gem Paradise); H.C.J. Bandara; N. Seenivasagam and N.S. Vasu (Devi Jewellers); S. Ramesh Khanth (Devi Gold Cast); M.S.M Fazli (Saleems Limited); Juzar Adamaly and Roshen Weeeratne (Facets Sri Lanka); Aly Farook; Ruzwan Kamil (MSM Kamil Exporter of Fine Gemstones); W.D. Nandasari (Sapphire Gems); Nabeel Salie (FJC The Fine Jewellery Company); Altaf Iqbal (Regal Gems); M. Hussain; M.T.M Haris (Emteem Gem Laboratory); and M.L.M. Sanoon (San Gems). The National Gem and Jewellery Authority of Sri Lanka, the Sri Lanka Gem and Jewellery Association, and the International Colored Gemstone Association provided access to and understanding of the country's industry.

REFERENCES

Ariyaratna D.H. (2013) *Gems of Sri Lanka*, 7th ed. A&B Graphics Nawinna, Maharagama, Sri Lanka.

China becoming Sri Lanka's top gem buyer from emerging markets (2011) Xinhua News Agency, http://news.xinhuanet.com/english2010/china/2011-09/15/c_131141158.htm [date accessed: Oct. 10, 2014].

CIA World Fact Book (2014) South Asia: Sri Lanka, https://www.cia.gov/library/publications/the-world-factbook/geos/ce.html.

Cooray P.G. (1994) The Precambrian of Sri Lanka: A historical review. *Precambrian Research*, Vol. 66, No. 1–4, pp. 3–18, http://dx.doi.org/10.1016/0301-9268(94)90041-8.

Dharmaratne P.G.R. (2002) Gem mining and sustainable environmental management in Sri Lanka. *Journal of Gemmology*, Vol. 28, No. 3, pp. 153–161.

Dharmaratne P.G.R., Ranjith Premasiri H.M., Dillimuni D. (2012) Sapphires from Thammannawa, Kataragama area, Sri Lanka. *G&G*, Vol. 48, No. 2, pp. 98–107, http://dx.doi.org/10.5741/GEMS.48.2.98.

Dissanayake C.B. (1986) *Preliminary Assessment of the Gem Potential of Sri Lanka*. Economic Development Board (EDB), Colombo, Sri Lanka, p. 160.

Dissanayake C.B., Chandrajith R. (2003) *Gem-Bearing Stream Sediments of Sri Lanka Geology and Geochemistry*. Gem and Jewellery Research and Training Institute and the National Gem and Jewellery Authority, Colombo, Sri Lanka.

Groat L.A., Giuliani G. (2014) *Geology of Gem Deposits*, Second Edition, Short Course Series Volume 44, Chapter 2: The Geology and Genesis of Corundum Deposits, Mineralogical Association of Canada, p. 95.

Grunow A., Hanson R., Wilson T. (1996) Were aspects of Pan-African deformation linked to Iapetus opening? *Geology*, Vol. 24, No. 12, pp. 1063–1066, http://dx.doi.org/10.1130/0091-7613(1996)024<1063:WAOPAD>2.3.CO;2.

Hughes R.W. (1997) *Ruby & Sapphire*. RWH Publishing, Boulder, CO.

Hughes R.W. (2014) *Ruby & Sapphire: A Collector's Guide*. Gem and Jewelry Institute of Thailand, Bangkok.

Kröner A. (1991) African linkage of Precambrian Sri Lanka. *Geologische Rundschau*, Vol. 80, No. 2, pp. 429–440, http://dx.doi.org/10.1007/BF01829375.

Kröner A., Williams I.S. (1993) Age of metamorphism in the high-grade rocks of Sri Lanka. *Journal of Geology*, Vol. 101, No. 4, pp. 513–521, http://dx.doi.org/10.1086/648243.

Kuriyan V. (1994) Sri Lanka's growing heat treatment expertise. *ICA Gazette*, April, pp. 8–9.

Li Z.X., Bogdanova S.V., Collins A.S., Davidson A., De Waele B., Ernst R.E., Fitzsimons I.C.W., Fuck R.A., Gladkochub D.P., Jacobs J., Karlstrom K.E., Lu S., Natapov L.M., Peace V., Pisarevsky S.A., Thrane K., Vernikovsky V. (2008) Assembly, configuration, and break-up history of Rodinia: A synthesis. *Precambrian Research*, Vol. 160, No. 1–2, pp. 179–210, http://dx.doi.org/10.1016/j.precamres.2007.04.021.

McMenamin M.A.S., McMenamin D.L.S. (1990) *The Emergence of Animals: The Cambrian Breakthrough*. Columbia University Press, New York.

Mahroof M.M.M. (1997) Corundum in Sri Lanka: Its historical and social role. Part 1. *The Canadian Gemmologist*, Vol. 18, No. 4, pp. 111–116.

Mendis D.P.J., Rupasinghe M.S., Dissanayake C.B. (1993) Application of structural geology in the exploration for residual gem deposits of Sri Lanka. *Bulletin of the Geological Society of Finland*, Vol. 65, pp. 31–40.

Milisenda C.C., Liew T.C., Hofmann A.W., Kröner A. (1988) Isotopic mapping of age provinces in Precambrian high-grade terranes: Sri Lanka. *Journal of Geology*, Vol. 96, No. 5, pp. 608–615, http://dx.doi.org/10.1086/629256.

Pardieu V. (2012) Sapphire rush near Kataragama, Sri Lanka. *GIA News from Research*, www.giathai.net/pdf/Kataragama.pdf.

Rino S., Kon T., Sato W., Maruyama S., Santosh M., Zhao D. (2008). The Grenvillian and Pan-African orogens: World's largest orogenies through geologic time, and their implications on the origin of superplume. *Gondwana Research*, Vol. 14, No. 1–2, pp. 51–72, http://dx.doi.org/10.1016/j.gr.2008.01.001.

Sajeev K., Osanai Y. (2004) Ultrahigh-temperature metamorphism (1150°C, 12 kbar) and multistage evolution of Mg-, Al-rich granulites from the Central Highland Complex, Sri Lanka. *Journal of Petrology*, Vol. 45, No. 9, pp. 1821–1844, http://dx.doi.org/10.1093/petrology/egh035.

Zwaan P.C. (1982) Sri Lanka: The gem island. *G&G*, Vol. 18, No. 2, pp. 62–71, http://dx.doi.org/10.5741/GEMS.18.2.62.

Zwaan P.C. (1986) Gem minerals from the Embilipitiya and Kataragama areas in Sri Lanka. *The Australian Gemmologist*, Vol. 16, No. 2, pp. 35–40.

Observations on Pearls Reportedly From the Pinnidae Family (Pen Pearls)

Nicholas Sturman, Artitaya Homkrajae, Areeya Manustrong, and Nanthaporn Somsa-ard

Pearls of all kinds have been used for decorative purposes throughout history. The majority of these have been nacreous, yet certain non-nacreous pearls have also been sought by connoisseurs. *Pinna* (pen) pearls fall into the latter group. The nature of their non-nacreous structure often results in cracking, and because of stability concerns they are very rarely used in jewelry. Nineteen of the 22 samples from this study, reportedly from Pinnidae family mollusks, show similarities in color as well as external and internal structure. Raman, photoluminescence, and UV-Vis-NIR spectroscopic results are discussed, along with the internal characteristics of pearls likely produced by this mollusk.

Mollusks of the Pinnidae family include the *Atrina* species and the more familiar *Pinna* species such as *Pinna nobilis*, as well as the rarely encountered *Streptopinna* species. Like many mollusks, this bivalve contains several members, including *Atrina vexillum*, *Atrina fragilis*, *Atrina pectinata*, *Atrina maura*, *Pinna bicolor*, *Pinna muricata*, *Pinna rudis*, and *Pinna rugosa* (Wentzell, 2003; Wentzell and Elen, 2005). The 22 pearls discussed herein (see figure 1) were submitted for examination by William Larson (Pala International, Fallbrook, California). They were all referred to as "pen pearls," without any details concerning their recovery or provenance. Pen pearls have seldom been covered in the gemological literature, so the results presented here are intended as a reference for those interested in pearls from this important ocean dweller.

THE MOLLUSK

Bivalve shells from the Pinnidae family share a very characteristic outline, tapering from a broad curved end to a pointed tip (figure 2). This unique form, reminiscent of the quill pens once used as writing tools, gives the shell its name. Sometimes referred to as "fan clams," they average 100 to 600 mm in length, though specimens approaching 800 mm (2.5 feet) have been recorded. Apart from size, another claim to fame for *Pinna nobilis* is that its byssal threads, which anchor the shell in the sand during the mollusk's life, were once woven together to make a fabric known as "sea silk."

The Pinnidae family is widely distributed among the oceans of the world, from the Mediterranean to the Red Sea, the Arabian Gulf, and the Indo-Pacific (from southeastern Africa to Melanesia and New Zealand, extending north to Japan and down to New South Wales). In the Western Hemisphere, these mollusks inhabit American waters around Florida, North Carolina, and Texas, as well as Mexico, the Caribbean, and as far south as Argentina (Strack, 2006). One of the authors' diving adventures in the Arabian Gulf off the coast of Bahrain (Sturman et al., 2010) revealed numerous specimens deeply embedded within the sandy floor, typical of the mollusk's behavior.

A quick glance at most Pinnidae shells shows a clear area of nacre at the pointed end and a less-lustrous portion extending across the curved opposite end. Closer examination reveals that the nacreous portions do not, as a whole, exhibit the obvious classic overlapping nacre structures encountered in other bivalves from the same order (Pterioida). Rather, they show a much finer form of nacre that is more difficult to resolve in most cases, even at high magnification (figure 3). This difference stems from the fact that the nacreous portion is not constructed of concentric layers, but

See end of article for About the Authors and Acknowledgments.
Gems & Gemology, Vol. 50, No. 3, pp. 202–215,
http://dx.doi.org/10.5741/GEMS.50.3.202.

Figure 1. These 20 completely non-nacreous pen pearls, from the group of 22 samples in this study, are set against a pen shell displaying both nacreous (left) and non-nacreous areas (right). Photo by Lhapsin Nillapat.

of numerous small prisms arranged around the center (Taburiaux, 1985). Since the family comes from the same order as other nacreous species such as those of *Pinctada* and *Pteria*, it is not surprising that nacre should feature somewhere within the shells' composition. But it is intriguing to see the different degree of coverage, given that the *Pinctada* and *Pteria* species are completely nacreous on their inner shells and clearly display overlapping platelet ridges.

The non-nacreous structure that characterizes the bulk of the shell also shows a wonderful mosaic or cellular pattern (figure 4, left) found in most of the pearls produced by this mollusk. These cells often vary from shell to shell in form, transparency, and internal features. Their appearance relative to location within the shell also appears to vary. In the sample from Thailand, the cells near the lip of the shell contained small pinpoint features, while those toward the center lacked these features (figure 4, center).

The cellular structure is visible because each cell is actually a long thin crystal composed of calcite, as noted in previous studies (Gauthier et al., 1997). This acicular structure is clearly evident in shells where some of the crystals on the edge have been damaged and broken away (figure 4, right). The crystals' transparency often permits strong light to pass along their length, making areas of both shell and pearl semi-translucent to translucent (Sturman, 2007). This columnar structure also leads to frequent crazing or cracking between the cell and the column walls. This is likely exacerbated by the loss of any water content in the materials.

THE PEARLS

Pen pearls occur in various shapes and sizes, and their color usually ranges from black or dark brown to a more yellowish brown or yellowish orange (Strack,

Figure 2. The 22 pearls from this study are shown together with two shells from GIA's Bangkok laboratory reference collection. The lighter-colored Pinna *shell and the darker* Atrina *shell display the distinctive external appearances of mollusks from the Pinnidae family. The more lustrous nacreous structure is seen at the tapered ends. Photo by Lhapsin Nillapat.*

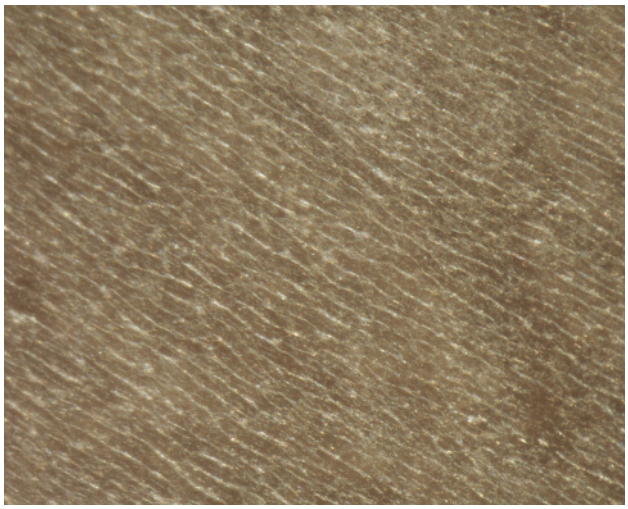

Figure 3. The nacreous structure visible at the pointed end of each pen shell half is not as clearly defined as the nacre in other Pterioida mollusks. Pen shells display a more "linear"-looking nacre. Photo by Artitaya Homkrajae; reflected light, magnified 112.5×.

2006). This range of color was apparent in the samples we studied, where one of the drops stood out from the darker, more typical pearls. Most pearls form as cyst or whole pearls, but some—again in keeping with other mollusks—occur as blister pearls or blisters (figure 5; CIBJO, 2013). Blister pearls and blisters are particularly useful when trying to compare the structure of pearls to their hosts, as they occur together and provide a direct means of comparison. One of the greatest drawbacks of pen pearls, though, is their tendency to crack or craze, a characteristic that significantly hinders their market value. This cracking appears to occur only in the non-nacreous pearls, but unfortunately these specimens are the norm.

Nacreous pen pearls (mainly *Atrina* species) are sometimes encountered in jewelry, though far less often than other types of pearls with more marketable color and greater durability. In recent years, however, pen pearls have become much more sought after as farmers, particularly in Indonesia, have learned to use them as nuclei for a new kind of atypical cultured pearl (Hainschwang, 2010). These atypical bead-cultured pearls can be quite challenging for laboratories to identify, though most present no real issues at the moment.

In Brief

- Like their host mollusks, pen pearls may be wholly nacreous or wholly non-nacreous, depending on the species. Partially nacreous examples may also be encountered.
- The surface structures of the non-nacreous areas show a beautiful cellular structure.
- While microradiography and X-ray computed microtomography (μ-CT) techniques are not required for identification, such examination does reveal the wonderful, often radial and concentric internal structures present within the pearls.

MATERIALS AND METHODS

Twenty loose undrilled pearls, weighing between 2.74 and 20.70 ct and ranging in color from dark

Figure 4. Left: This section of Pinnidae shell from Thailand shows a graduated cellular structure, with finer cells near the lip of the shell and larger cells toward the middle. Center: The structure within the center of each cell also varies. The cells toward the outer part of the shell exhibit minute impurities in their center, while the cells closer to the middle have empty centers. Right: The cause of the cellular pattern is clearly seen in this broken shell segment, which shows the acicular nature of the individual calcite crystals that form the non-nacreous areas. Photos by Nick Sturman; magnified 32× (left and right) and 176× (center).

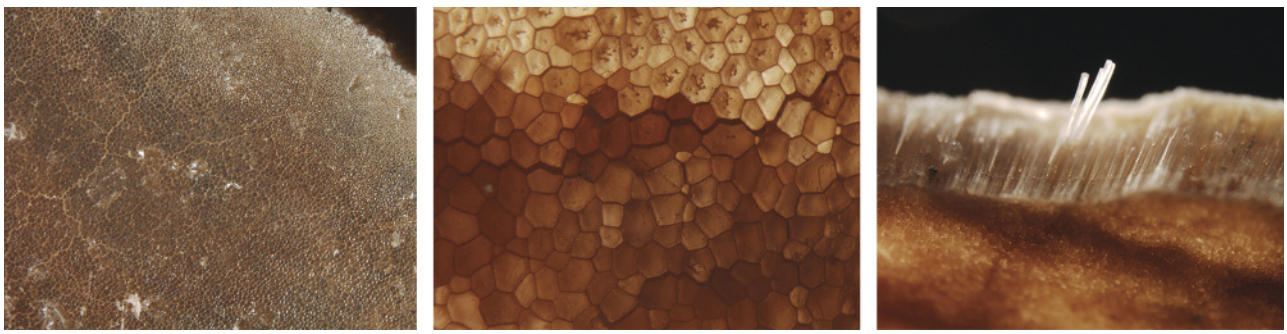

*Figure 5. This irregularly shaped blister pearl, attached to the interior of a Pinnidae family (*Atrina *species) shell, measures approximately 21.50 × 17.60 mm. Photo by Nicholas Sturman; shell courtesy of Kenneth Scarratt.*

brown to yellow-brown, were analyzed. Two additional samples weighing 2.78 and 5.81 ct (see pearls 19 and 20 in table 1), exhibiting both silver nacreous and brown non-nacreous areas, were also examined. The properties of all 22 samples are listed in table 1.

The pearls' internal structures were examined using a Faxitron CS-100 2D real-time (RTX) microradiography unit (90 kV and 100 mA excitation), and a Procon CT-Mini model X-ray computed microtomography (µ-CT) unit fitted with a Thermo Fisher 8W/90 kV X-ray tube and a Hamamatsu flat-panel sensor detector.

Their composition was analyzed with an inVia Raman microscope equipped with a 514 nm argon-ion laser (Ar^+), which was used to obtain Raman and photoluminescence spectra. The laser was set at 100% power, and spectra were collected using 10 accumulations, with an accumulation time of 10 seconds per scan.

The spectra required to characterize each sample's color were collected in the 200–2500 nm range with a Perkin-Elmer Lambda 950 ultraviolet/visible/near-infrared (UV-Vis-NIR) spectrophotometer using a reflectance accessory fitted with an integrating sphere. The 250–750 nm range is presented here, because this range contains most color-related reflectance features.

The pearls' chemical composition was analyzed using a Thermo X Series II laser ablation–inductively coupled plasma–mass spectrometry (LA-ICP-MS) system equipped with an attached New Wave Research UP-213 laser and an energy-dispersive X-ray fluorescence spectrometry (EDXRF) unit. Microanalytical carbonate standards MACS-1 and MACS-3 from the United States Geological Survey (USGS) were used as the standards for each method.

Photomicrographs of the surface structures were captured with a Nikon SMZ1500 system using various magnifications up to 176×. Other gemological microscopes with magnification ranges between 10× and 60× were also used during the examination of the shells and pearls. Shells from both *Pinna* and *Atrina* species in GIA Bangkok's reference collection were studied to compare their structural similarities with the sample pearls.

The pearls' fluorescence features were also observed under an 8-watt UV lamp with both long-wave (365 nm) and short-wave (254 nm) radiation, as well as a DiamondView unit.

OBSERVATIONS AND RESULTS

External Structure. The pearl samples showed characteristic non-nacreous structure consisting of a network of cells resembling those pictured in figure 4. The actual shape of the cells varied quite markedly, from a pseudo-hexagonal outline to an elongated curved form. Examples of the range of structures can be seen in figures 11–21. Diaphaneity ranged from opaque to semi-

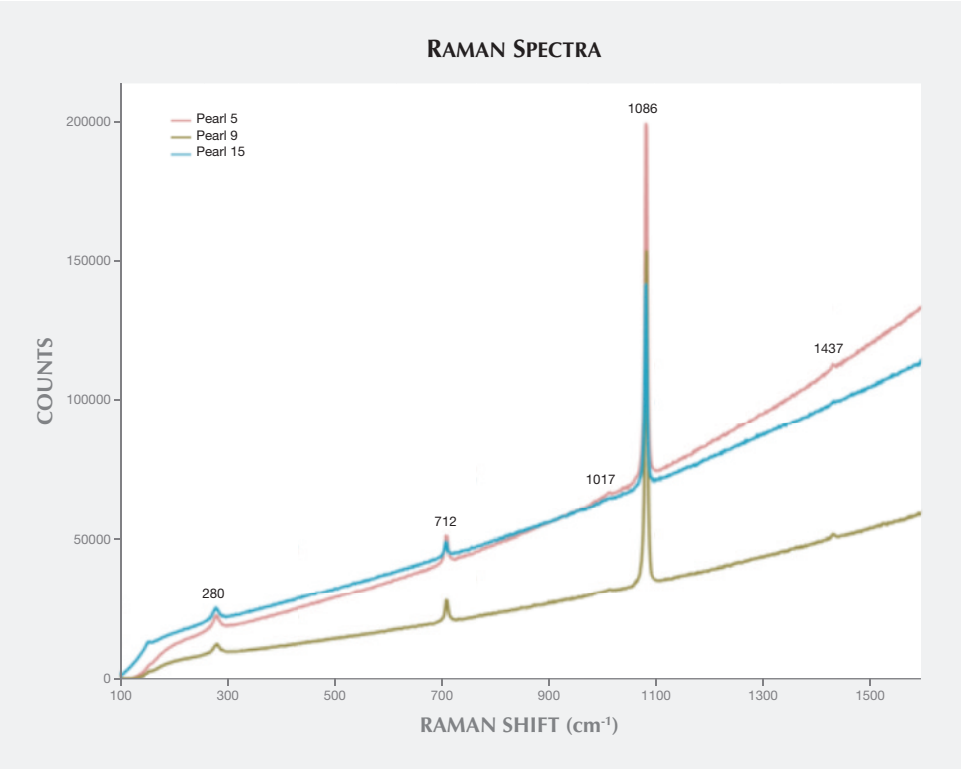

Figure 6. The Raman spectra of pen pearls 5, 9, and 15 show peaks at 280, 712, 1086, and 1437 cm^{-1} (the first two indicative of calcite) and a polyenic-related peak at 1017 cm^{-1}.

translucent, with the lighter-colored samples tending toward the latter (Gauthier et al., 1997; Karampelas et al., 2009). Cracking was very apparent in most of the samples, and some of the cracks were fairly wide and penetrated quite deeply. This is an accepted but undesirable trait encountered in most pen pearls. Using them as nuclei for atypical bead-cultured pearls solves this problem, since the nacre overgrowth hides not just the cracks but the whole pearl.

Samples 19 and 20 were considerably different from the rest of the group. Their shapes were baroque and quite flattened, while their colors were clearly uneven and more bicolored, with silver and brown areas mixed together. Their structure also varied, from a more nacreous type with silver portions to a non-nacreous cellular structure on the brown portions (consistent with the other samples). These two pearls differed in other ways that will be described later in this work.

External Composition. To identify the nature of the minerals forming the pearls, we examined the pearls using the Raman spectrometer with an attached microscope. This analysis showed that the non-nacreous areas consisted of calcite, as evidenced by the peaks at 280 and 712 cm^{-1}, with the associated band at 1086 cm^{-1} (figure 6). The only noticeable exceptions were the spectra for the two bicolored pearls, where the silver nacreous areas produced a slightly different spectrum. Here, the 280 cm^{-1} peak was very weak and accompanied by a series of peaks at 198, 206, 217, and 287 cm^{-1}, while the 712 cm^{-1} peak position shifted to a doublet feature at 701 and 705 cm^{-1}. These features are all characteristic of aragonite, the most common polymorph found in pearls and shells, so we were not surprised to detect it on the more nacreous portions. Previous studies on pearls from *Pinna nobilis* (Gauthier et al., 1997; Karampelas et al., 2009) attributed the cause of color to carotenoids. While we detected the 1017 cm^{-1} peak reported in their studies, the other peaks were not readily apparent, which is unusual. Such pigment peaks exhibit strong resonant phenomena. Their absence could be due to the particular mollusk that produced the pearls or the laser wavelengths used in collecting the spectra, as well as the parameters used to test the samples. No other lasers were used in this study.

Photoluminescence analysis was conducted for samples 5, 9, and 15 (figure 7). The spectra are not identical, as the maxima center is somewhat different on each curve. Yet the overall pattern is quite similar apart from sample 15, the yellow-brown pearl, which has a maximum at approximately 600 nm and is offset slightly to the left of the others. A subtle band at around 700 nm is quite consistent in the samples. Very weak peaks at 555 and 565 nm

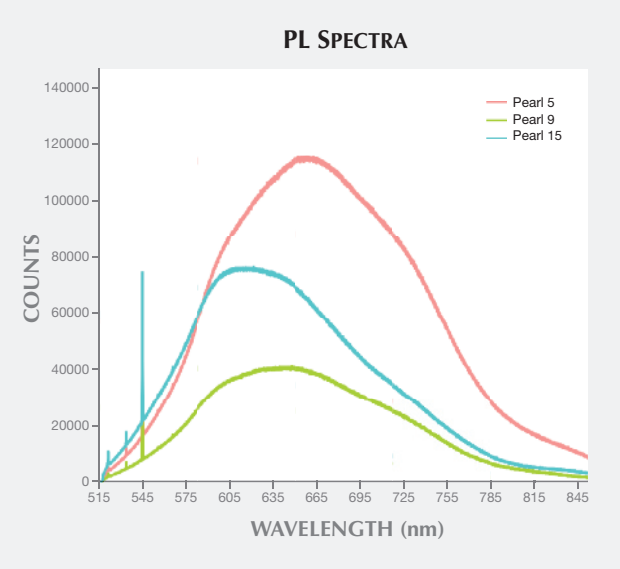

Figure 7. Photoluminescence (PL) spectra of samples 5, 9, and 15 showed different patterns, likely due to the variation in their relative intensities. While the weak feature at around 700 nm stayed consistent, the overall pattern of the peaks varied. The sharp features at 520 and 550 nm are due to the Raman effect.

were observed in the PL spectra. These do not appear to correlate with the polyenic pigment peaks seen around 546 and 558 nm in non-nacreous orange pearls such as Melo pearls, which exhibit polyenic peaks very similar to those stated for pen pearls. Therefore, we believe that polyenic compounds, which belong to the carotenoid family, were not observed in the PL spectra of the samples.

Fluorescence. Reactions to ultraviolet (UV) light were best seen under long-wave UV (LWUV) radiation, where 18 of the pearls exhibited a very weak to moderate chalky yellow fluorescence. Only sample 15 showed a strong chalky yellow of a brighter color. Sample 13 displayed an uneven moderate to strong yellow in the pearl's center, where the color was lighter. Samples 19 and 20 displayed strong chalky yellow reactions on the nacreous areas while the brown non-nacreous patches appeared relatively inert, but closer examination revealed a very weak yellow reaction, in keeping with most of the other pearls. Short-wave UV (SWUV) reactions showed the same colors as LWUV, but with weaker intensity. A few of the pearls that exhibited a very weak reaction to LWUV did not show any clear reaction under SWUV conditions.

To see whether these long- and short-wave reactions were in any way similar, all the samples were examined in the ultra-short UV wavelength (<230 nm) of the DiamondView. The results ranged from a clear bluish reaction to a rather inert reaction, with bluish boundaries between the cellular structure very prominent in most of the images (figures 8 and 9). The strong bluish reaction is a marked change from the yellow reactions the samples tended to ex-

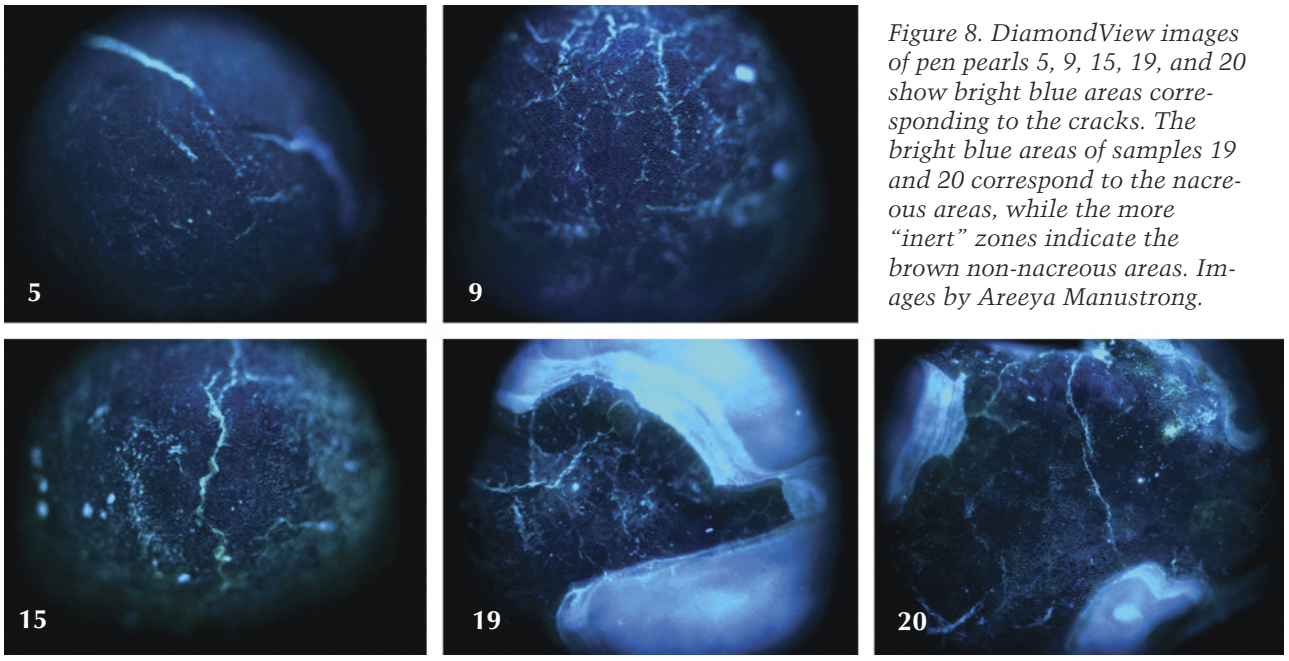

Figure 8. DiamondView images of pen pearls 5, 9, 15, 19, and 20 show bright blue areas corresponding to the cracks. The bright blue areas of samples 19 and 20 correspond to the nacreous areas, while the more "inert" zones indicate the brown non-nacreous areas. Images by Areeya Manustrong.

TABLE 1. Characteristics of the pen pearl samples.

	Pearl sample	Measurement (mm)	Carat weight	Shape	Color
1		8.67 x 8.50 x 8.44	3.65	Drop	Dark brown
2		10.83 x 8.80 x 8.75	4.75	Drop	Graduated brown
3		9.34 x 9.13 x 9.02	5.02	Button	Black
4		8.85 x 8.74 x 8.22	3.92	Button	Brown
5		9.34 x 8.62 x 8.59	4.22	Drop	Black
6		9.09 x 8.65 x 8.61	4.40	Drop	Dark brown
7		8.73 x 8.69 x 7.40	3.78	Button	Dark brown
8		7.49 x 7.46 x 7.27	2.74	Button	Dark brown
9		11.88 x 11.76 x 9.98	8.53	Button	Brown
10		9.16 x 7.51 x 7.48	3.17	Oval	Black
11		14.44 x 10.03 x 9.99	7.99	Drop	Dark brown
12		11.40 x 9.25 x 9.20	6.34	Oval	Dark brown
13		16.58 x 12.05 x 11.93	15.95	Drop	Brown and light brown
14		18.62 x 13.37 x 13.28	20.70	Drop	Black and brown
15		18.07 x 9.40 x 9.32	8.00	Drop	Yellow-brown
16		12.96 x 12.89 x 12.15	11.27	Drop/ Button	Black
17		17.75 x 9.05 x 9.00	9.52	Drop	Brown
18		11.44 x 11.35 x 8.75	7.80	Button	Dark brown
19		12.70 x 9.96 x 5.31	2.98	Baroque	Silver and dark brown
20		17.39 x 12.46 x 5.93	5.81	Baroque	Silver and brown
21		11.42 x 10.42 x 9.83	7.34	Baroque	Dark brown
22		10.38 x 10.27 x 9.69	6.68	Semi-baroque	Black

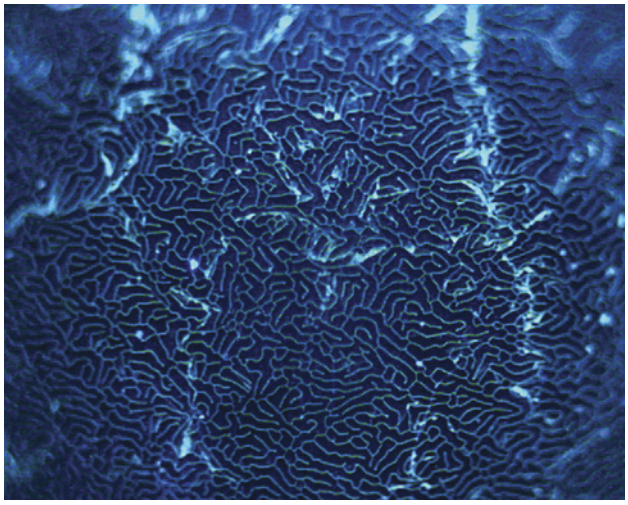

Figure 9. This magnified image of sample 9, as seen in the DiamondView, reveals the wonderful cellular structure in a whole new light. Image by Areeya Manustrong.

hibit under the standard gemological fluorescence unit found in most laboratories.

UV-Vis-NIR Spectrophotometry. While diffuse-reflectance spectra were obtained on all the pearls, only those for the three samples chosen for Raman analysis are shown in figure 10. Despite their differences in color, they showed little variation in the visible part of the electromagnetic spectrum (400–750 nm). Samples 9 and 15 displayed noise in the visible portion that was likely due to their structure and variable translucency, quite different from the more opaque pearls typically tested in the spectrophotometer. Sample 15 did exhibit higher diffuse reflectance than the darker samples, as would be expected for a lighter-colored pearl. All three spectra had a similar reflectance feature in the 320–630 nm range, yet sample 15 had a higher maximum reflectance in the UV region, centered at around 340 nm rather than 330 nm. The shift of this feature and the higher reflectance of the spectrum contributed to the pearl's lighter, more yellow coloration. Sample 5 in particular showed less reflectance and a slightly greater reflectance range. This, together with the approximately 330 nm point of maximum reflectance in the UV region, contributed to its darker appearance.

Chemical Composition. Two methods of chemical analysis were used in this study: EDXRF and LA-ICP-MS. EDXRF, a nondestructive technique, covers a greater sampling area and is more surface-specific. It is widely used by gemological laboratories and provides sufficient data to assist in most identification tasks. It does, however, have relatively high detection limits, and elements lighter than sodium cannot be detected. While the EDXRF results revealed low levels of Mn, consistent with pearls from a saltwater environment (Gutmannsbauer and Hänni, 1994), we wanted to gain a more accurate idea of the quantities of elements present.

We turned to LA-ICP-MS, which examines a smaller micron-sized area of the surface and the underlying material and offers better sensitivity and element coverage. The results confirmed the pearls' known saltwater origin on the basis of low manganese (Mn) levels and the expected results for boron (B), gallium (Ga), and barium (Ba). Strontium (Sr) levels were on average slightly lower than those usually recorded for saltwater mollusks, but still within the saltwater range. While they do not allow a direct comparison with pen pearl chemical composition, data collected from *Pinctada maxima* pearls show some similarities when each element is compared (Scarratt et al, 2012). Li and Fe were present in slightly higher concentrations in the pen pearls. The LA-ICP-MS results for the pen pearls are summarized in table 2.

Figure 10. Samples 5, 9, and 15 showed similar UV-Vis-NIR spectra despite their variation in color. The "noise" in the ultraviolet to visible region (250–750 nm) is likely due to the pearls' structure.

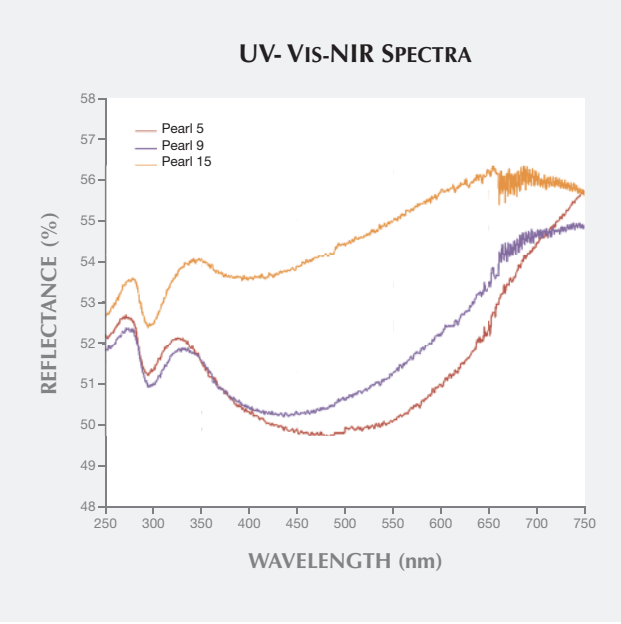

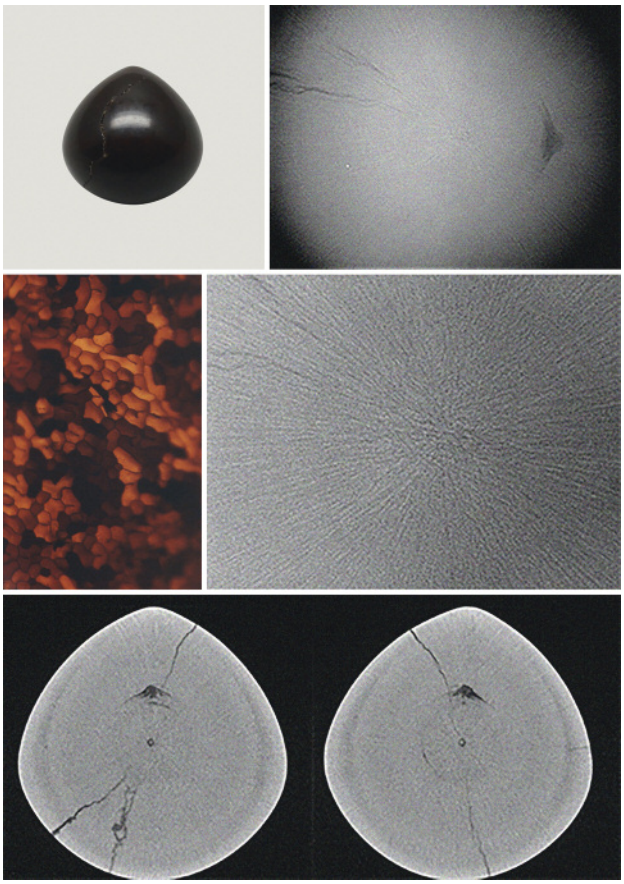

Figure 11. Pen pearl 1's external appearance (top left), microradiographic structure (top right and middle right), surface structure (middle left, magnified 60×), and µ-CT images of two slices (bottom). Photos by Artitaya Homkrajae.

The most significant differences observed between the nacreous and non-nacreous areas in samples 19 and 20 are highlighted by the bold numerals in the table. The most dramatic difference occurred with magnesium (Mg), which showed significantly lower concentrations in the nacreous areas than the non-nacreous areas of all the other pearls. The elemental concentrations in the non-nacreous areas of all 22 samples matched one another well, as would be expected for such similar-looking material. Many more samples of known pen pearls will need to be analyzed to determine whether any correlation exists, yet the detailed chemical analysis of pen pearls is not part of routine laboratory work.

Internal Structure. Viewed in cross-section, the internal structures of non-nacreous pen pearls appear to possess a distinct radial columnar structure. Not surprisingly, this radial structure often manifests itself clearly in microradiographic images, since the path length equals the entire thickness of the sample when exposed to the X-ray source. The clarity is usually not so obvious in the micron-thick slices of CT images. On the other hand, concentric ring structures are often more visible via CT than the RTX method. A selection of the thousands of RTX and CT slice images obtained by the authors appears in figures 11–21. These show that small, dark natural nuclei or cores sometimes exist at the center of the radial and concentric structures, while undesirable cracks also extend to various degrees throughout most of the samples.

Sample 15 exhibits the only atypical internal structure of the completely non-nacreous pearls in this study; it also differs in coloration and diaphaneity, as seen in figure 16. The structure consists of a series of connected voids and what are probably conchiolin-rich chambers that extend from the tapered

Figure 12. Sample 5's external appearance (top left), microradiographic structure (top right and middle right), surface structure (middle left, magnified 60×), and µ-CT images of two slices (bottom). Photos by Artitaya Homkrajae.

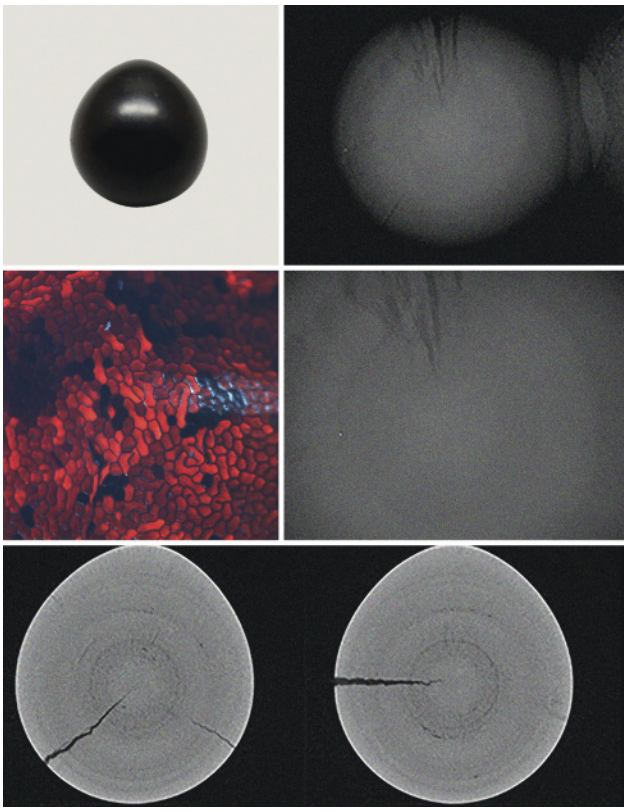

TABLE 2. Trace-element composition obtained by LA-ICP-MS of 22 pen pearls, in parts per million weight (ppmw).

Pearl sample	^{7}Li	^{11}B	^{23}Na	^{24}Mg	^{31}P	^{39}K	^{45}Mn	^{57}Fe	^{69}Ga	^{88}Sr	^{137}Ba
1	2.50	27.84	6222	4803	bdl	242	1.19	264	bdl	946	0.57
2	2.24	2.54	4312	2458	bdl	103	bdl	291	bdl	670	0.51
3	2.61	10.10	5560	3207	bdl	144	2.74	288	bdl	806	0.74
4	2.49	32.19	5924	3370	bdl	209	1.95	328	bdl	780	0.62
5	2.62	22.43	5674	2795	bdl	213	bdl	304	bdl	798	0.41
6	3.05	15.33	6127	3249	bdl	220	bdl	301	bdl	756	0.43
7	1.92	5.43	5297	3314	39.98	150	1.43	219	bdl	815	0.93
8	1.92	9.92	5016	3395	bdl	129	1.12	264	bdl	749	0.35
9	2.39	23.02	6352	3563	45.07	259	bdl	248	bdl	755	0.29
10	2.31	26.44	5787	4052	bdl	249	0.94	259	bdl	755	1.21
11	2.30	10.33	4902	2907	bdl	143	bdl	269	bdl	714	0.31
12	2.34	12.76	4600	4005	bdl	189	5.86	265	bdl	757	0.28
13	2.19	2.61	4838	3194	bdl	142	1.75	238	bdl	785	1.65
14	4.03	20.86	6792	2947	58.08	291	1.27	261	bdl	842	0.68
15	2.36	17.39	5958	5264	46.97	368	4.44	217	bdl	818	1.33
16	2.50	32.96	6217	3391	bdl	230	3.21	239	bdl	1044	1.09
17	3.04	30.09	6285	4096	40.57	158	1.04	220	bdl	836	0.41
18	2.25	37.72	5452	3412	bdl	114	1.72	271	bdl	529	0.73
19 - Brown	2.49	21.96	7129	3781	bdl	175	1.32	311	bdl	704	0.40
19 - Nacre	**0.96**	2.32	**9806**	**54**	**171**	110	bdl	218	bdl	1016	0.48
20 - Brown	2.52	9.90	6915	5250	bdl	213	1.23	321	bdl	813	0.34
20 - Nacre	**0.59**	9.01	**9170**	**51**	**151**	82	bdl	251	bdl	1030	0.23
21	2.32	17.79	5617	3837	bdl	262	2.80	217	bdl	789	1.45
22	2.37	14.34	6031	3983	bdl	225	0.90	255	bdl	776	0.63
Detection limits	0.25	2.13	11.92	0.70	36.17	5.42	0.80	31.33	0.12	0.11	0.12

Abbreviation: bdl = below detection limit

point toward the broader end. The central irregular nucleus consists of another void/conchiolin-rich area that possesses an internal structure. Given the specimen's size and the lack of commercial culturing of this mollusk, the pearl is almost certainly natural in origin.

Of the 22 pearls examined, samples 19 and 20 are the exceptions to the rule in nearly every way. Not only do they possess non-nacreous and nacreous structures within the same pearl, but the nature of their internal structure is also completely at odds with that of the other samples. Both show a very prominent void-

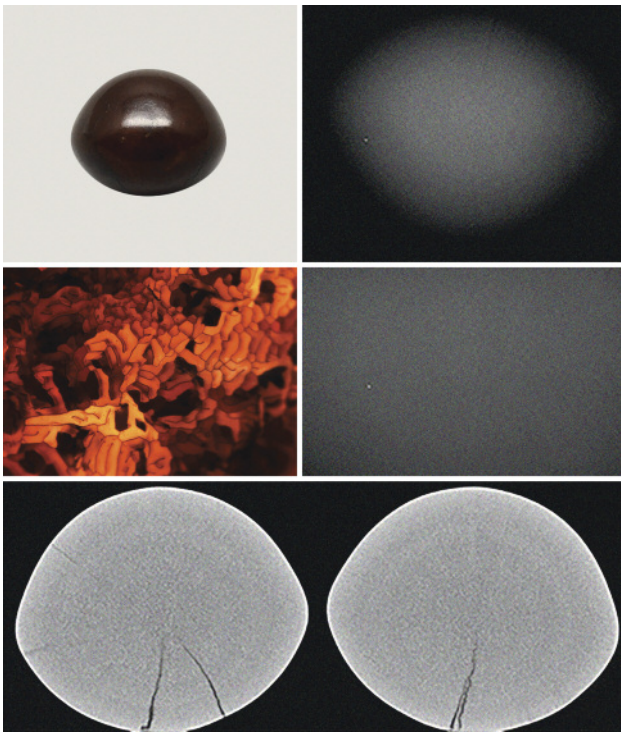

Figure 13. Sample 9's external appearance (top left), microradiographic structure (top right and middle right), surface structure (middle left, magnified 60×), and µ-CT images of two slices (bottom). Photos by Artitaya Homkrajae.

like feature (figures 17–20) in which a few "walls" of what is very likely conchiolin are associated with small white "seeds." These seeds appear to consist of material rich in calcium carbonate, given the similar radio-opacity of the features and their surrounding calcite and aragonite host, as well as the organic nature of the pearls themselves. It is interesting to note that the white seed features are similar to those observed in some non-bead-cultured pearls we have encountered during research on known samples from farms, though similar structures may also be encountered in natural pearls and are not conclusive proof of culture.

It is worth noting that we observed a direct correlation between the structure (solid or hollow) and the specific gravity in these 22 samples. All the solid pearls (samples 1–18, 21, and 22) gave SG values between 2.39 and 2.53; this variation was likely due to the size and depth of the cracks and any air trapped in them during hydrostatic measurements. Samples 19 and 20 again proved the exceptions, with SG values of 1.76 and 2.02, respectively. Given the large voids observed in their structures, this was not surprising.

Culturing and Treatments. While many different mollusks are known to produce cultured pearls, most are bivalves associated with species from the Pteriidae family or various freshwater mollusks from the *Hyriopsis* genus that are frequently used to produce non-bead-cultured, mantle-grown cultured pearls (Farn, 1991; Strack, 2006). Cultivation using mollusks from other families is usually the exception rather than the rule today. The only other mollusks known to produce cultured pearls to any commercial extent are from the *Haliotis* genus and, on rare occasion, the *Strombus gigas* (Queen conch) species. Cultured pearls from the Pinnidae family can be added to the list of those that have undergone trials but without commercial success so far (Landis, 2010).

As with all pearls, the subject of treatments was often at the forefront of our thoughts on these pen pearls. No treatments were detected in this group, nor are the authors aware of any treatment applied to the Pinnidae family. Waxing or some other method could

Figure 14. Sample 11's external appearance (top left), microradiographic structure (top right and middle right), surface structure (middle left, magnified 50×), and µ-CT images of two slices. Photos by Artitaya Homkrajae.

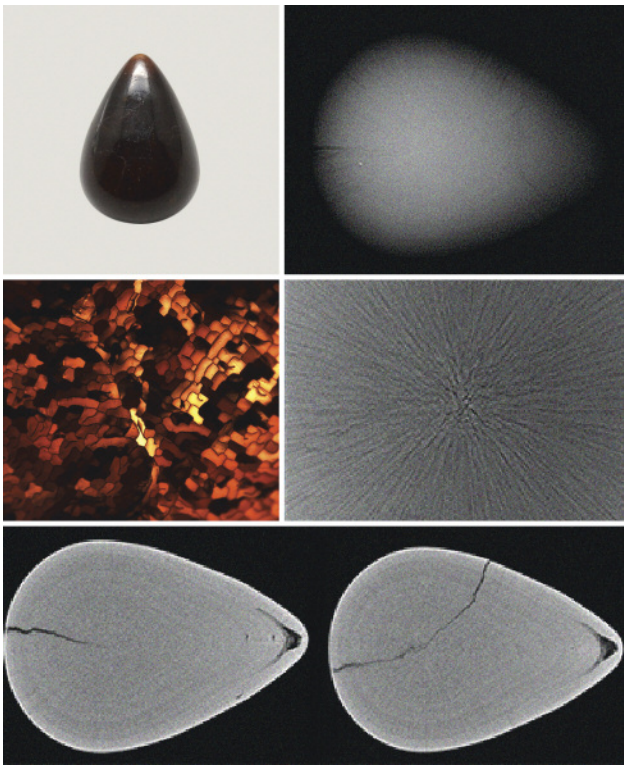

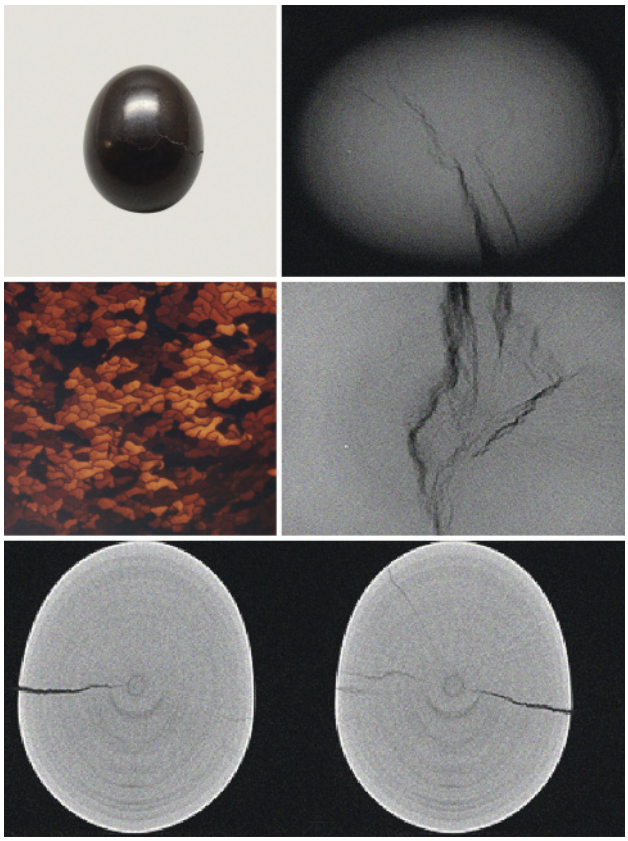

Figure 15. Sample 12's external appearance (top left), microradiographic structure (top right and middle right), surface structure (middle left, magnified 70×), and µ-CT images of two slices (bottom). Photos by Artitaya Homkrajae.

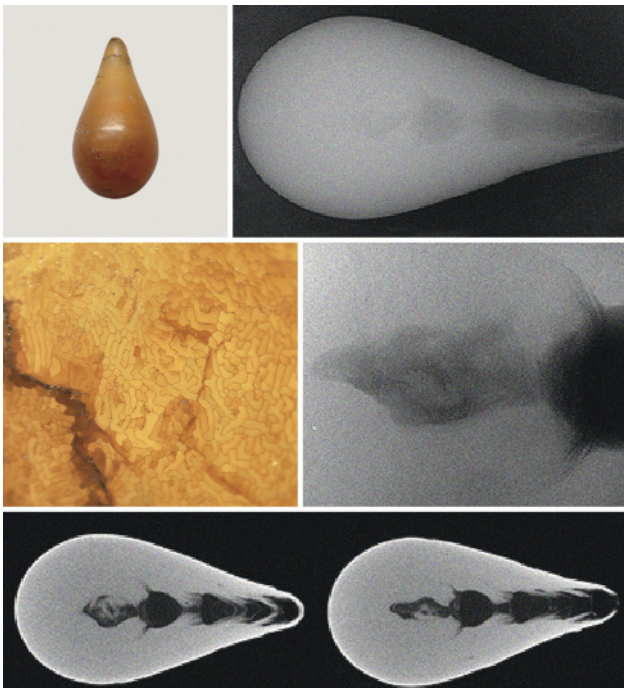

Figure 16. Sample 15's external appearance (top left), microradiographic structure (top right and middle right), surface structure (middle left, magnified 50×), and µ-CT images of two slices (bottom). Photos by Artitaya Homkrajae.

be used to hide cracks or prevent them from expanding and deepening, but no such procedure was observed in this study.

CONCLUSION

Pen pearls are among the least appreciated pearls due to durability issues and their rather plain appearance. Yet they possess one of the most wonderful internal structures of all mollusk creations, and the surface patterns revealed by magnification are truly remarkable works of nature that all pearl aficionados would do well to observe. The columnar structures in their radiating forms produce unique specimens that allow light to be transmitted along their length to varying degrees, causing some pen pearls to appear semi-translucent to the unaided eye. Not many pearls can lay claim to this characteristic.

These radiating concentric structures manifest themselves clearly during examination with direct microradiography and X-ray computed micro-tomography (µ-CT). These techniques also demonstrate that in the 22 samples studied here, the structures do not always conform to the norm. Pen pearls

Figure 17. Sample 19's external appearance (top left), microradiographic structure (top right), and surface structures (bottom, magnified 90× and 112×). Photos by Artitaya Homkrajae.

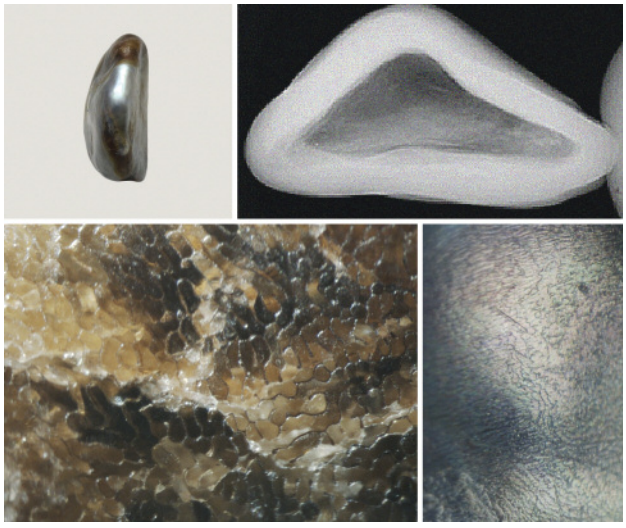

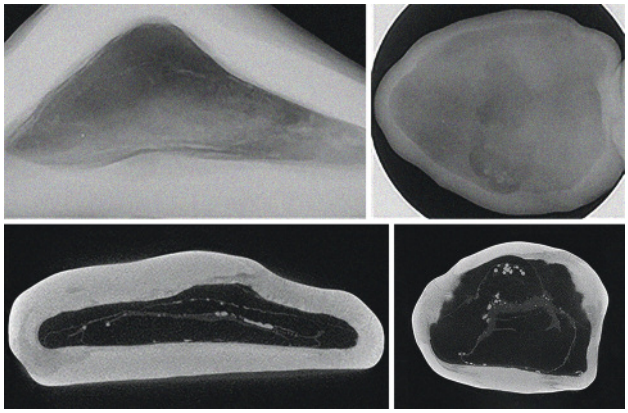

Figure 18. Additional microradiographic images of sample 19 (top) and µ-CT images of two slices (bottom) exhibit some interesting white "seeds" within the void area that are related to internal structural "walls."

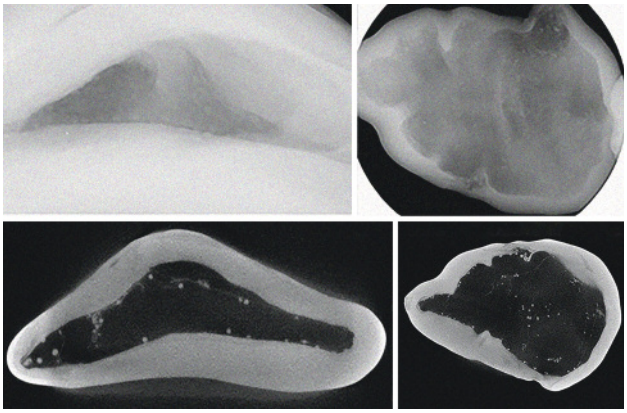

Figure 20. As with sample 19, microradiographic images of sample 20 (top) and µ-CT images of two slices (bottom) show white "seeds" within the void area.

15, 19, and 20 showed void-related features that clearly differed from the other samples examined. The latter two also differed in their external nacreous and non-nacreous appearances, which leads one to question if they are indeed pen pearls. While we cannot be certain, the surface structure seen on the pen shell in figure 4 does bear a close similarity with the features seen in these two examples and in other pearls of reported pen shell origin occasionally examined in the GIA laboratory, so the nature of the nacreous structure appears to support this conclusion. Additionally, the non-nacreous calcitic areas typical of pen pearls are present in both pearls, further supporting the identity. It is noteworthy that both of these pearls, though outwardly different

Figure 19. Sample 20's external appearance (top left), microradiographic structure (top right), and surface structures (lower images, magnified 60× and 112×). Photos by Artitaya Homkrajae.

Figure 21. Sample 21's external appearance (top left), microradiographic structure (top right and middle right), surface structure (middle left, magnified 50×), and µ-CT images of two slices (bottom). Photos by Artitaya Homkrajae.

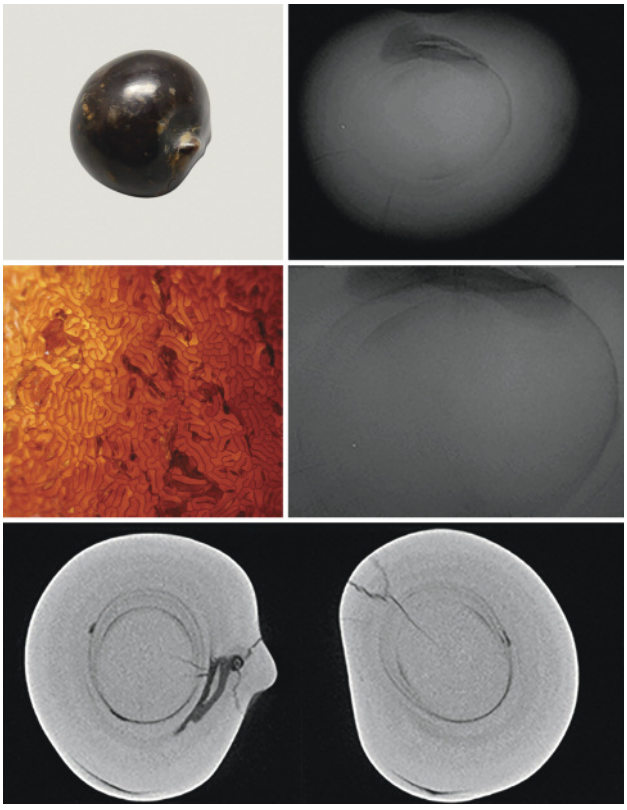

from the other 20 samples, share similar internal characteristics.

This work, along with those previously published by Gauthier et al. (1997) and Karampelas et al. (2009) appear to be the most comprehensive studies on pen pearls to date. Whereas the latter focused on pen pearls from a single known species of Pinnidae, the samples in this study are from unknown species and could come from several different members of the family.

The recent use of pen pearls as atypical nuclei to create natural-looking cores in cultured pearls has stimulated interest in these unusual specimens. The internal structures shown here will also serve as a reference for anyone studying the internal variations in pen pearls.

ABOUT THE AUTHORS

Mr. Sturman (nsturman@gia.edu) is senior manager of pearl identification, Ms. Homkrajae is supervisor of pearl identification, Ms. Manustrong is a staff gemologist, and Ms. Somsa-ard is an analyst, all at GIA's Bangkok laboratory.

ACKNOWLEDGMENTS

The authors would like to thank Mr. William Larson of Pala International in Pala, California, for allowing us to examine the pen pearls. We also thank our colleagues in Bangkok who assisted with this work and the reviewers for their helpful and constructive feedback.

REFERENCES

CIBJO (2013) CIBJO Pearl Blue Book. http://www.cibjo.org/download/13-10-27%20Official%20Pearl%20Book.pdf (date accessed: February 8, 2014).

Farn A. (1991) *Pearls: Natural, Cultured and Imitation*. Butterworth-Heinemann Ltd., Oxford, UK.

Gauthier J.-P., Caseiro J., Lasnier B. (1997) The red pearls of *Pinna nobilis*. *Australian Gemmologist*, Vol. 19, No. 10, pp. 422–426.

Gutmannsbauer W., Hänni H.A. (1994) Structural and chemical investigations on shells and pearls of nacre forming salt- and fresh-water bivalve molluscs. *Journal of Gemmology*, Vol. 24, No. 4, pp. 241–252.

Hainschwang T. (2010) A difficult new type of cultured pearl entering the market. *Gemnotes*, Vol. 1, No. 2, pp. 6–11.

Karampelas S., Gauthier J.-P., Fritsch E. (2009) Gem News International: Characterization of some pearls of the Pinnidae family. *G&G*, Vol. 45, No. 3, pp. 221–223.

Landis B.Y. (2010) Dreams of black pearls, http://younglandis.wordpress.com/2010/04/22/penshellpearls (date accessed: September 8, 2014).

Scarratt K., Bracher P., Bracher M., Attawi A., Safar A., Saeseaw S., Homkrajae A., Sturman N. (2012) Natural pearls from Australian *Pinctada maxima*. *G&G*, Vol. 48, No. 4, pp. 236–261, http://dx.doi.org/10.5741/GEMS.48.4.236.

Strack E. (2006) *Pearls*. Ruhle-Diebener Verlag, Stuttgart, Germany, 707 pp.

Sturman N. (2007) Gem News International: An unusually translucent non-nacreous pearl. *G&G*, Vol. 43, No. 3, pp. 259–260.

Sturman N., Karampelas S., Al-Attawi A., Abduriyim A. (2010) Gem News International: Natural pearl diving off the coast of Bahrain. *G&G*, Vol. 46, No. 4, pp. 318–319.

Taburiaux J. (1985) *Pearls: Their Origin, Treatment & Identification*. Chilton Book Co., Radnor, Pennsylvania.

Wentzell C. (2003) Gem News International: Some interesting pearls from the North American West Coast. *G&G*, Vol. 39, No. 4, pp. 332–334.

Wentzell C., Elen S. (2005) Gem News International: Pen shell pearls—nacreous and non-nacreous. *G&G*, Vol. 41, No. 3, p. 267.

PLEOCHROISM IN FACETED GEMS: AN INTRODUCTION

Richard W. Hughes

While virtually all gemological texts cover pleochroism, it is almost always related to viewing with a dichroscope. Exactly how pleochroism manifests itself in faceted gems is largely ignored. This article discusses this phenomenon in doubly refractive gemstones, specifically as it relates to overall color appearance in faceted gems. Contrary to popular belief, pleochroism can be visible in faceted gems even when they are cut with an optic axis parallel to the direction of view.

In describing colored gemstones, the major factors influencing color are hue (position of a color on a color wheel), lightness (tone), saturation (intensity), color zoning, metamerism (color-change), dispersion, and pleochroism. This article deals with the last of these properties. The term *pleochroism* (from the Greek "pleio," many, and "chros," color) describes a variation of color with direction in doubly refractive gems (figure 1). Virtually all gemological texts note this effect and describe it in detail. Yet many of these descriptions deal only with the identification of this property. When lapidary aspects are discussed, the focus is on orientation, generally omitting mention of exactly how pleochroism affects the appearance of faceted stones. The purpose of this article is to provide a detailed description of pleochroism as it relates to the appearance of faceted gems.

INTRODUCTION TO OPTICAL CRYSTALLOGRAPHY

For gemological purposes, crystals can be divided into three optical groups based on their lattice symmetry: isometric, dimetric (uniaxial), and trimetric (biaxial); see table 1.

See end of article for About the Author and Acknowledgments. This article is based on a piece the author originally published in *Gemological Digest* ("Pleochroism and Colored Stone Grading," Vol. 2, No. 3, pp. 16–24). This version is significantly revised and updated, with new illustrations.

GEMS & GEMOLOGY, Vol. 50, No. 3, pp. 216–226, http://dx.doi.org/10.5741/GEMS.50.3.216.

Imagine a perfect sphere. If you draw a line from the center to the surface in any direction, all possible lines will have the same length. This sphere represents how light behaves in isometric crystals. Now if we stretch or compress that perfect sphere in a single direction, it becomes dimetric: a perfect circle when viewed in one direction, but oval when viewed at right angles to the direction of distortion. In other words, two of the three dimensions are equidistant, but the third is either stretched (positive uniaxial) or compressed (negative uniaxial).

Finally, if we distort our perfect sphere in not just one direction but two, we end up with a trimetric crystal, where each of the three dimensions has a different length (see figure 2).

Within singly refractive gem materials, the spacing of lattice points is essentially identical in all three mutually perpendicular dimensions (top to bottom, side to side, back to front). As a result, these materials transmit light in a manner that is independent of crystal orientation—light therefore moves through these crystals in all directions at a single speed and is permitted to vibrate in any direction perpendicular to the direction of travel.

Figure 1. Pleochroism in a 15 ct tanzanite, as seen with the unaided eye through the crown and the pavilion sides and ends. Photo by Wimon Manorotkul.

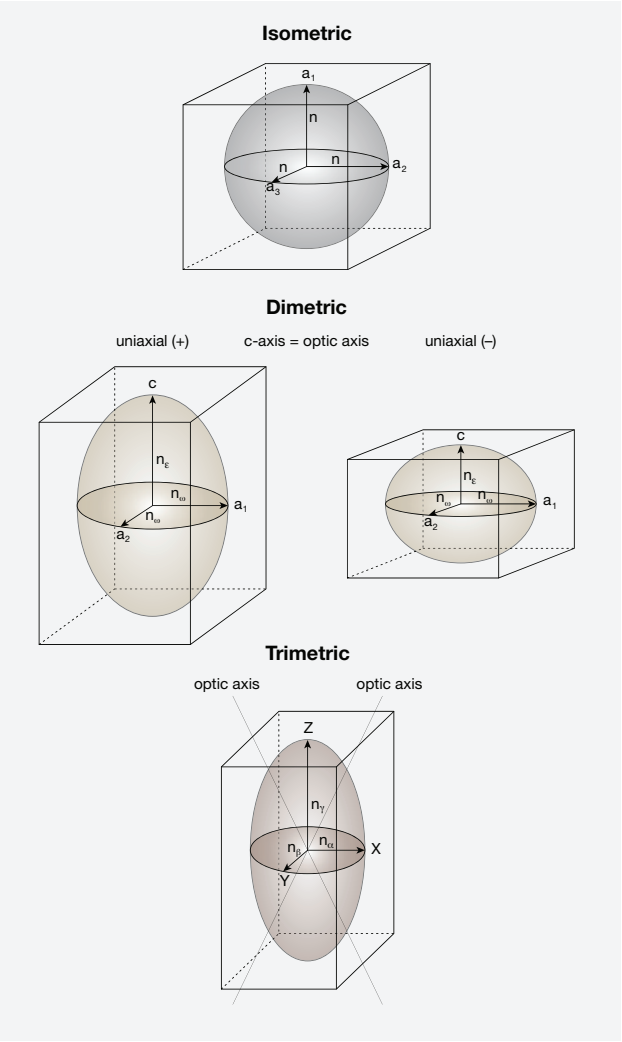

Figure 2. Vibration directions of light waves in crystals. Isometric crystals do not split light and therefore do not display pleochroism. Uniaxial crystals possess two vibration directions, allowing the possibility of two pleochroic colors (dichroism), while biaxial crystals have three vibration directions and thus the potential to display three pleochroic colors (trichroic). In both uniaxial and biaxial crystals, the major optical directions are always mutually perpendicular, which is not necessarily the case for the crystallographic axes in crystals (only cubic, tetragonal and orthorhombic crystals have exclusively mutually perpendicular crystallographic axes). Illustration by Richard W. Hughes.

This is not the case, however, in doubly refractive gems. All doubly refractive gems are anisotropic crystals, and the arrangement of their lattice points varies with direction. Uniaxial materials possess one unique optic axis (the c-axis) along which the orientation of lattice points differs from that of the other two crystal axes (the a-axes); with biaxial gems, the orientation differs along each of the three crystal axes (a-, b-, and c-axes). The result of this differing arrangement of lattice points in doubly refractive gems (as opposed to singly refractive gems) is that light traveling through these crystals is split into two separate paths or rays (with the exception of light waves traveling parallel to an optic axis), each traveling at a different speed and thus possessing a different refractive index (RI). For more on the behavior of light entering a crystal, see box A.

Uniaxial gems possess two rays—the ordinary (o) and extraordinary (e) rays—and two RI values—omega (ω) and epsilon (ε), respectively. The o-ray always vibrates perpendicular to the c-axis, while the e-ray vibrates in a plane containing the c-axis. The vibrations of each ray are mutually perpendicular, and they vibrate roughly perpendicular to the direction of travel.

In biaxial gems, there are three different rays and three different RIs: alpha (α), beta (β), and gamma (γ), although only two are ever found in any one direction. The vibrations of alpha, beta, and gamma are parallel to the optical directions X, Y, and Z, respectively. Although the three crystallographic axes of biaxial minerals are not always mutually perpendicular, X, Y, and Z are always mutually perpendicular.

In Brief

- Pleochroism, the variation of color with direction in doubly refractive gems, plays an important role in their overall appearance
- When viewing faceted gems that are strongly pleochroic, the pleochroism is always present, even along an optic axis.
- Pleochroism always varies in a symmetrical pattern, because the major optical directions of crystals are arranged symmetrically.
- Color variations in faceted gems are most often due to path length or color zoning rather than pleochroism.

Uniaxial gems contain one optic axis (the direction of single refraction), which is parallel to the c-axis; biaxial gems contain two optic axes (two directions of single refraction), which lie in the X-Z plane. The major vibration directions of both uniaxial and biaxial gems are shown in figure 2.

Because each polarized light ray in a doubly refractive gem is vibrating across a slightly different arrangement of lattice points, each ray is absorbed

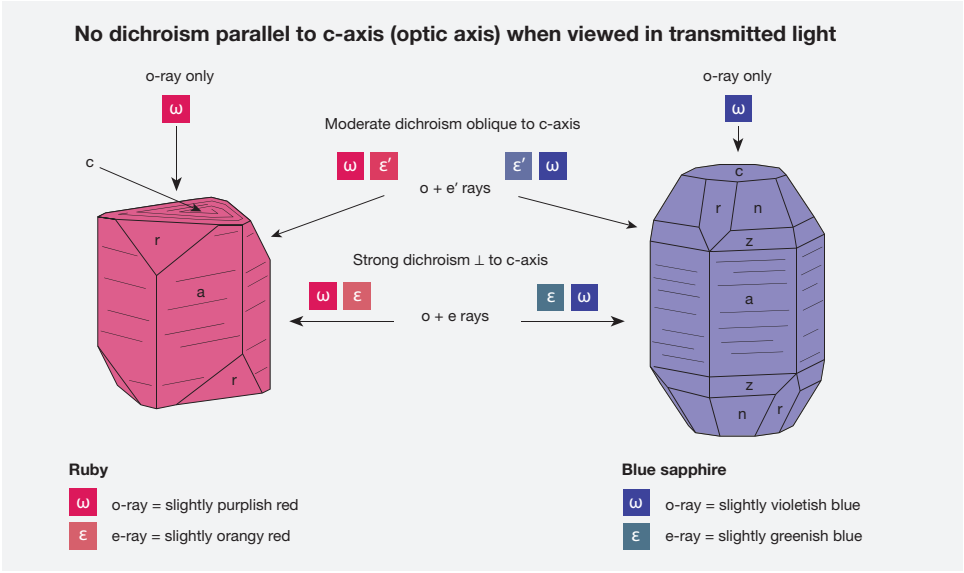

Figure 3. Pleochroism in uniaxial crystals, as viewed with the dichroscope, using ruby and sapphire as examples. Illustration by Richard W. Hughes.

differently. In many cases, the difference in absorption between one ray and another is too slight to detect with the eye, or even with a dichroscope. Where the differences are large enough, one observes a variation in color with viewing direction. Such variations are known as pleochroism, and they are most distinct in deeply colored specimens of the same gem species.

Uniaxial gems possess two different vibration directions—omega (ω) and epsilon (ε)—and may therefore exhibit two different colors (*dichroism*). Biaxial gems possess three different vibration directions—alpha (α), beta (β), and gamma (γ)—and so may show three different colors (*trichroism*), but only two in any single direction. Blue sapphire and tourmaline are strongly dichroic uniaxial gems, while tanzanite (again, see figure 1) provides an example of a strongly trichroic biaxial stone. Not all uniaxial gems display visible dichroism, however, and not all biaxial gems display visible trichroism. Some uniaxial gems show only one color, and biaxial gems may show only one or two colors.

When viewed in transmitted light with a dichroscope, pleochroism in uniaxial stones varies in the following ways, as shown in figure 3:

- Parallel to the c-axis, only the ordinary ray is seen. As a result, there is no pleochroism.
- At right angles to the c-axis, both the ordinary and extraordinary rays are seen; this position shows the strongest dichroism.
- At angles oblique to the c axis, the ordinary ray is seen; the second color (usually referred to as ε′) diverges from that of the o-ray as one moves away from the c-axis.

With biaxial stones, the situation is similar but slightly more complex. Light traveling along the Z direction will vibrate parallel to X and Y, so the two colors seen with a dichroscope will be those of alpha (X) and beta (Y). Light traveling along the X direction will vibrate across Y and Z, so the two colors seen will be those of beta (Y) and gamma (Z). When light travels parallel to Y, it vibrates along X and Z; the colors seen are those of alpha (X) and gamma (Z). Should light travel parallel to either of the two optic axes in a biaxial stone, only one color will be seen, that of beta (figure 4).

PLEOCHROISM IN FACETED UNIAXIAL GEMS

Let's examine how this applies to the appearance of faceted stones. Figure 5* shows a uniaxial gem cut with the c-axis perpendicular to the table facet (since the crown plays only a minor role in the pleochroism of a faceted stone, it will be eliminated from this discussion for simplicity's sake). Suppose the stone is a perfect square cut with only four pavilion facets (marked N, S, E, and W for north, south, east, and west). The a-axes are contained in the horizontal plane.

For light entering the stone parallel to the c-axis, only the o-ray would be obtained. When the light strikes facet W, however, the direction is changed. It then travels in the plane of the a-axes, giving an equal

*Author's note: RI variation (see Hurlbut, 1984) is a directly measurable manifestation of the more subjective differences we see with pleochroism. I have used RI variation to model pleochroism, based on the assumption that the two are identical in terms of their variation. If one assigns an RI value to each ray, it is no different than assigning a color value to each ray. It follows that as the RI varies, the color will also vary.

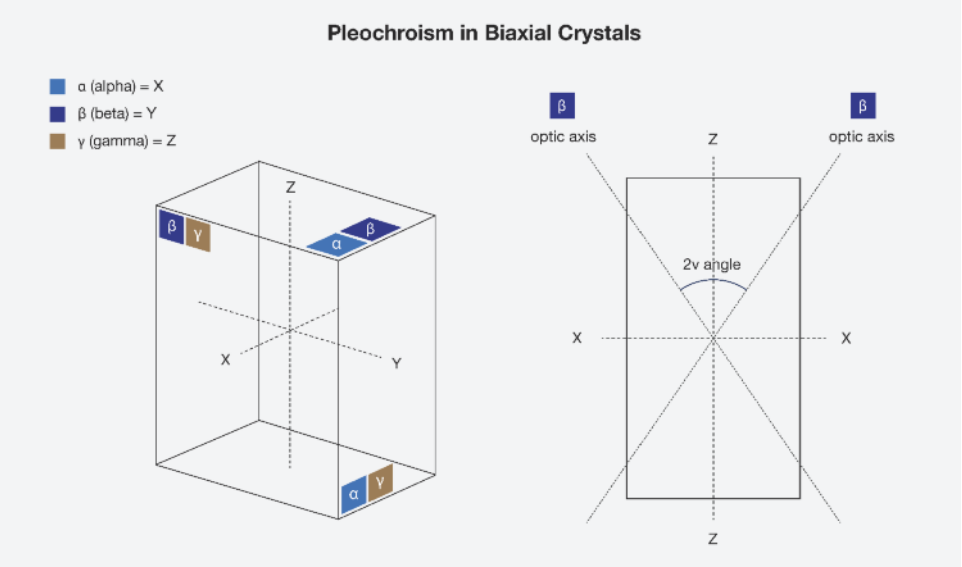

Figure 4. Pleochroism in biaxial crystals, as viewed with a dichroscope in each of the three major optical directions. When the crystal is viewed along either of the two optic axes (right), only the beta color will be seen. Illustration by Richard W. Hughes.

mixture of o- and e-rays. Upon striking facet E, the direction is again changed, causing the ray to exit the stone parallel to the c-axis. This again produces the o-ray only for this portion of its journey. Should the ray strike facets N or S instead, this still would not alter the above combinations.

At first it might seem that uniaxial stones cut with the c-axis perpendicular to the girdle plane would show one uniform color across their face. This is not the case, however, because the facet arrangement causes light to change direction during its journey through the gem. In uniaxial gems where the o-ray is more intensely colored than the e-ray, the color will appear slightly less intense near the girdle than near the culet, because the percentage of e-ray mixed into the color increases as light approaches the girdle.

In figure 5, the gem has a girdle diameter of 10 mm and a pavilion angle of 45°, and the c-axis is cut perpendicular to the table plane.

- Ray A enters near the girdle, traveling 4 mm parallel to the c-axis (o-ray only) and 6 mm parallel to the a-axis (3 mm of o-ray and 3 mm of e-ray). The color of Ray A therefore consists of 70% o-ray and 30% e-ray.

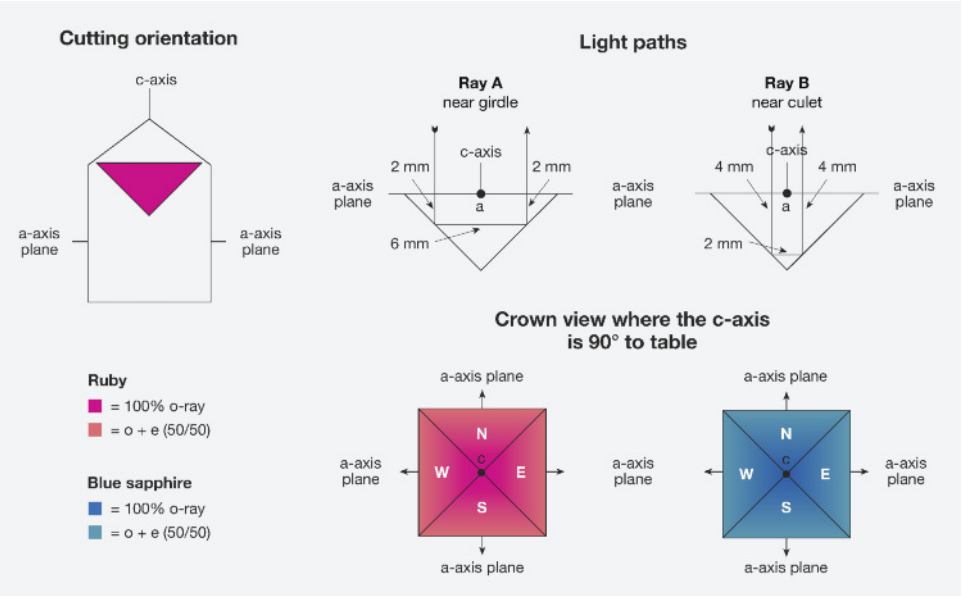

Figure 5. Pleochroism as seen through the face of ruby and sapphire cut with the table plane 90° to the c-axis. Illustration by Richard W. Hughes. Note that color variations in figures 5, 6, 8, and 12 are approximate only and designed to show general concepts. Refractive indices and pleochroism vary in logarithmic fashion, while the illustrations were generated showing linear variations. To validate these illustrations, the author compared his calculations and ray traces with photos and observations of actual gem samples.

TABLE 1. Optical crystallography simplified.

Structure	Structure type	Optic character	Pleochroism	Examples
Amorphous	No order No axes	Singly refractive	None	Amber, glass, opal
Isometric	One crystallographic axis length (cubic) a1 = a2 = a3	Singly refractive	None	Diamond, spinel, garnet
Dimetric (Uniaxial)	Two crystallographic axis lengths a1 = a2 ≠ c (tetragonal) a1 = a2 = a3 ≠ c (hexagonal)	Doubly refractive Uniaxial Two RIs (n_ω, n_ε), one optic axis	May be dichroic	Corundum, tourmaline, zircon
Trimetric (Biaxial)	Three crystallographic axis lengths a ≠ b ≠ c (orthorhombic, monoclinic, triclinic)	Doubly refractive Biaxial Three RIs (n_α, n_β, n_γ), two optic axes	May be trichroic	Andalusite, iolite, topaz, zoisite, chrysoberyl

- Ray B strikes the pavilion much closer to the culet. Ray A and Ray B have identical path length, each traveling 10 mm through the gem. But Ray B's light path consists of 8 mm parallel to the c-axis (8 mm of o-ray only) and just 2 mm parallel to the a-axis (1 mm of o-ray and 1 mm of e-ray). Thus, the color of Ray B is 90% o-ray and only 10% e-ray.

The conclusion is that when a uniaxial gem is cut with the c-axis perpendicular to the table facet, there can still be visible pleochroism. The o-ray color is stronger at the culet, gradually diminishing toward the girdle. To the best of the author's knowledge, this fact has not been described in the gemological literature.

In uniaxial gems such as blue zircon, ruby, blue sapphire, and tourmaline, where the e-ray is less saturated in color than the o-ray, the color near the girdle will appear slightly less saturated because it has a higher percentage of e-ray mixed into the color. With gems such as blue benitoite, where the e-ray is more intensely colored than the o-ray, the reverse would hold true. The color would be lightest at the culet, darkening toward the girdle. Since making this discovery, the author has found that such differences are subtle at best, and in many cases undetectable to the unaided eye. In large, strongly pleochroic stones, however, the effect can be striking.

Now let us consider a uniaxial gem cut with the c-axis parallel to the table rather than perpendicular (figure 6):

- Ray A has 6 mm of o-ray only, and 4 mm of equally mixed o- and e-rays, giving a total of 80% o-ray and 20% e-ray.
- Ray B consists of 2 mm of o-ray only, and 8 mm of equally mixed o- and e-rays, giving a total of 40% o-ray and 60% e-ray. As a result, the color on these facets will show more of the o-ray near the girdle and less at the culet.
- Rays C and D are equal mixtures of o- and e-rays because their entire journey takes place perpendicular to the c-axis. Those facets will display a uniform 50%–50% split.

In summary, when pleochroic gems are cut with the c-axis parallel to the table facet, a pleochroic "bow tie" can be seen, as shown at the bottom of figure 6. A striking example of these differences in color due to pleochroism is found in the first edition of Joel Arem's *Color Encyclopedia of Gemstones* (1977). Color plate 64 shows a round 15.6 ct Cambodian blue zircon (uniaxial) that has been cut with the c-axis parallel to the table facet (figure 7). In blue zircon, the o-ray is blue while the e-ray is colorless. This orientation has resulted in a large white "bow tie" that is obvious in the photo. Closer examination reveals that in the blue portion of the stone, the color is lightest at the culet and gradually deepens toward the girdle. This is because the percentage of o-ray in the color gradually increases from 50% at the culet to 100% at the girdle.

Pleochroism in Tourmaline. Tourmaline is one of the most strongly pleochroic gems. Indeed, its pleochroism is so distinct that it was once used to manufacture crude polariscopes ("tourmaline tongs"). Because of its strong pleochroism, the orientation of cut stones is extremely important (figure 8). In tourma-

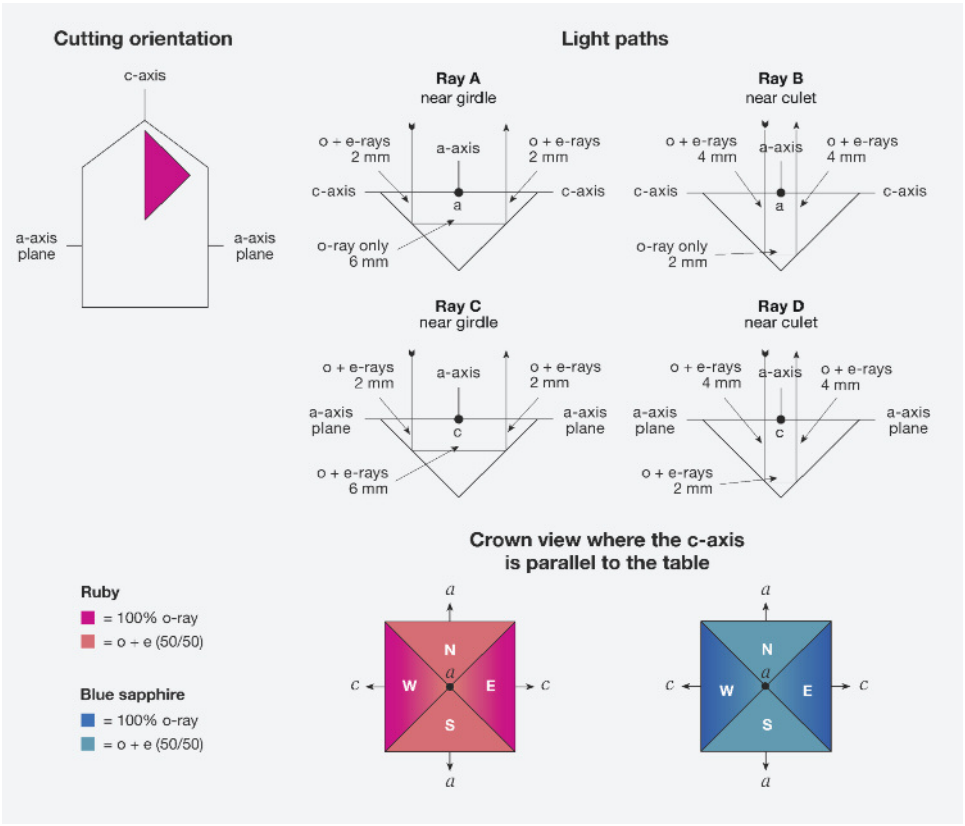

Figure 6. Pleochroism as seen through the crown in ruby and sapphire cut with the table parallel to the c-axis. Illustration by Richard W. Hughes.

line, the o-ray is always the darker of the two colors. Thus, light-colored specimens are oriented with the table perpendicular to the c-axis to achieve the richest color. In dark tourmalines the opposite orientation is used, with the c-axis parallel to the table facet. In these stones, the o-ray is so dark that the pavilion facets along the c-axis are typically cut very steep, to minimize the o-ray's effect on the face-up appearance (figure 9).

Pleochroic Differences in Natural and Verneuil Synthetic Corundum. Differences in the pleochroism of natural and Verneuil synthetic corundum often occur because of differences in their orientation. Natural corundum is generally oriented with the c-axis perpendicular to the table, which tends to provide the best color and weight retention. In the Verneuil product, the c-axis always lies within the plane along which the boule is split. Though not necessarily parallel to the boule's length, it is always parallel to the plane of the split. As most cutters of this synthetic are only concerned with weight retention—the price is the same regardless of orientation—they will normally place the table facet parallel to the split, so that the c-axis lies parallel to the table. The result is that Verneuil synthetics show dichroism through the table, whereas based on the author's experience, 80% or more of natural corundum shows little or none (when viewed with a dichroscope).

These differences are most readily apparent in blue sapphires and are least conspicuous in yellow to

Figure 7. This 15.6 ct zircon displays an obvious pleochroic "bow tie" effect. Photo © Joel Arem, reproduced with permission.

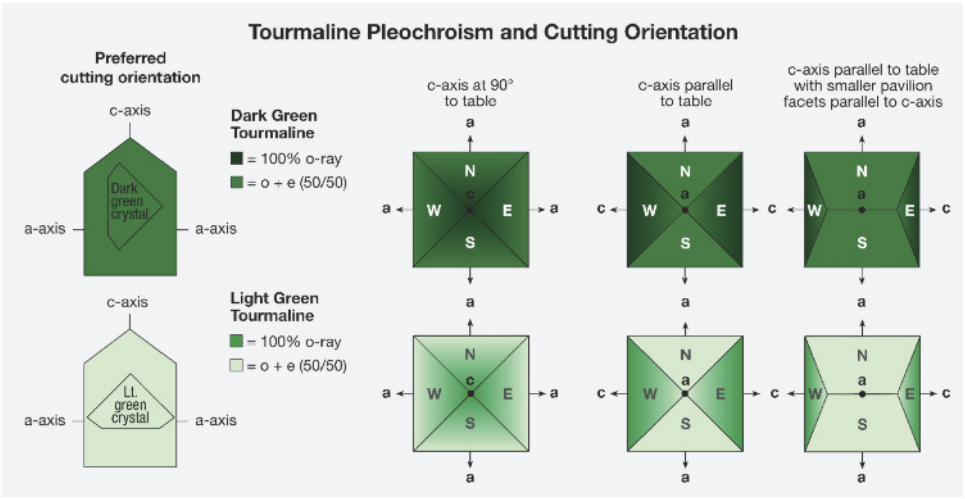

Figure 8. Because of its strong pleochroism, dark green tourmaline (top) must be oriented to minimize the o-ray's effect on face-up appearance. Illustration by Richard W. Hughes.

colorless sapphires. Of course, no pleochroism will be detected in completely colorless stones. The differences in the typical orientation of natural and Verneuil synthetic corundum are shown in figure 10. An example of pleochroism in a Verneuil synthetic sapphire boule is shown in figure 11.

It is important to note that in all strongly pleochroic gems cut with the optic axis or axes at oblique angles to the table, the pleochroism, if visible, will have a symmetrical pattern. The different pleochroic colors will be positioned 90° apart from one another, while identical pleochroic colors will lie exactly opposite each other. This is true for both uniaxial and biaxial stones, even if they are cut in a less-symmetrical (e.g., pear or heart) shape. The pleochroism will always be displayed symmetrically because the important optical directions are always arranged symmetrically within the crystal.

PLEOCHROISM IN BIAXIAL GEMS

In biaxial gems, pleochroism is displayed in a manner similar to that of uniaxial gems, except that there are three different pleochroic directions (X, Y, and Z) instead of just two.

Figure 12 shows how the pleochroism of a faceted biaxial gem might vary. Suppose that the color of the X (alpha) vibration direction (not the direction of travel) is cyan, Y (beta) is blue, and Z (gamma) is brown. The gem has been cut with Z perpendicular to the table, X running east-west, and Y running north-south.

- Ray A travels 4 mm parallel to Z, where it vibrates along X and Y, giving 20% X and 20% Y colors. It travels 6 mm parallel to X (vibrating along Y and Z), giving 30% Y and 30% Z. The total of Ray A will consist of 20% X (cyan), 50% Y (blue), and 30% Z (brown).
- Ray B travels 8 mm parallel to Z, where it vibrates along X and Y, giving 40% X and 40% Y colors. It travels 2 mm parallel to X (vibrating along Y and Z), giving 10% Y and 10% Z. The total of Ray B will consist of 40% X (cyan), 50% Y (blue), and 10% Z (brown).
- Ray C travels 4 mm parallel to Z, where it vibrates along X and Y, giving 20% X and 20% Y colors. It travels 6 mm parallel to Y (vibrating along X and Z), giving 30% X and 30% Z. The total of Ray C will consist of 50% X (cyan), 20% Y (blue), and 30% Z (brown).

Figure 9. Pleochroism in a tourmaline cut with the c-axis parallel to the table, as seen with the unaided eye through the side (left), crown (center), and end (right). Photos by Wimon Manorotkul and Mia Dixon.

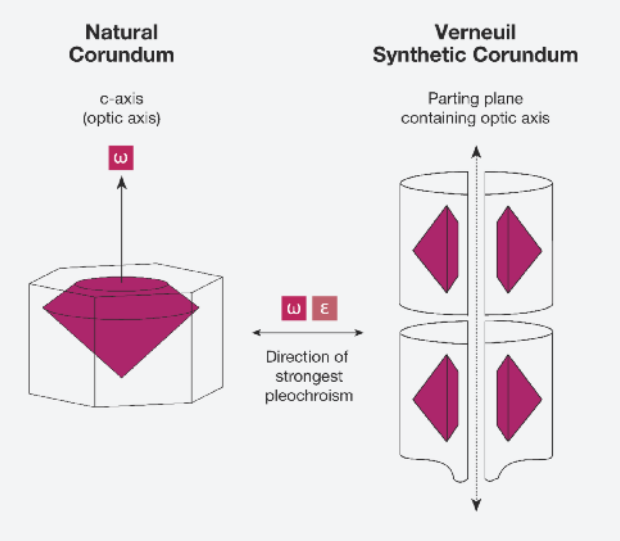

Figure 10. Orientation differences between natural and Verneuil synthetic corundum produce characteristic differences in pleochroism. Natural ruby and sapphire tend to be cut with the table facet perpendicular to the c-axis. As a result, no pleochroism is visible through the table with the dichroscope. The opposite holds true for Verneuil synthetic corundum.

- Ray D travels 8 mm parallel to Z, where it vibrates along X and Y, giving 40% X and 40% Y colors. It travels 2 mm parallel to Y (vibrating along X and Z), giving 10% X and 10% Z. The total of Ray B will consist of 50% X (cyan), 40% Y (blue), and 10% Z (brown).

Figure 11. Pleochroism in a Verneuil-grown half-boule of synthetic sapphire, as viewed with a polaroid-plate dichroscope. In Verneuil-grown synthetic corundum, the optic axis always lies in the plane of the split. Photo by Wimon Manorotkul.

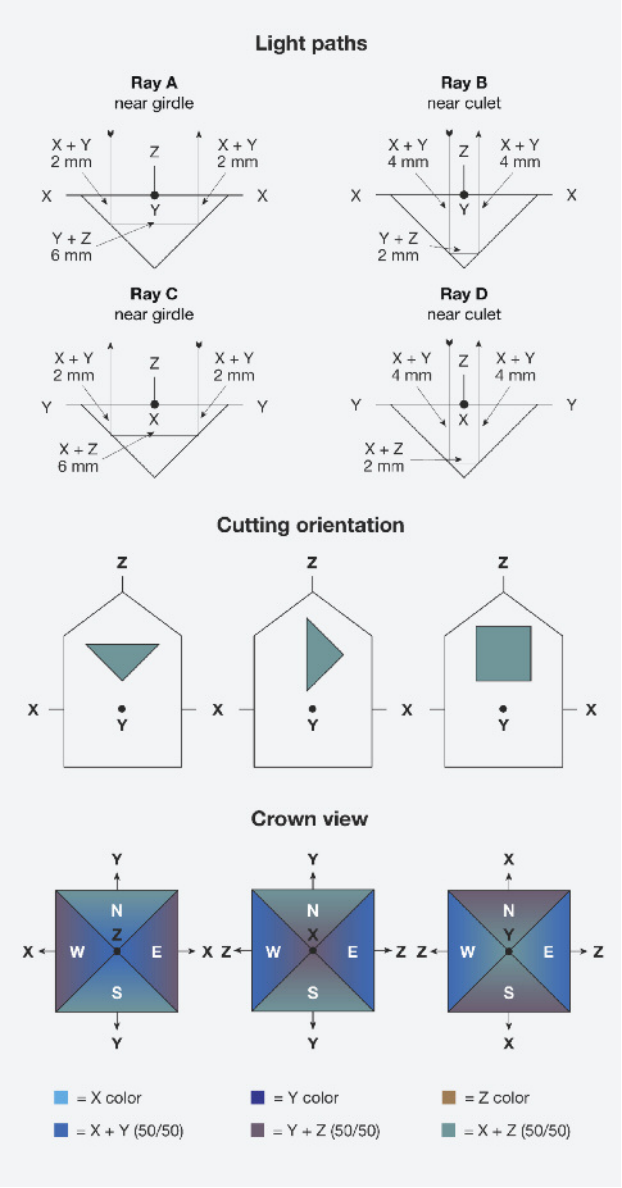

Figure 12. Pleochroism in biaxial crystals. Illustration by Richard W. Hughes.

In summary, we can see that biaxial stones have a more complex pleochroism. Facets N and S will show different amounts of the three pleochroic colors compared with facets E and W. As with uniaxial gems, differences in color will be observed not only when comparing facets N and S to facets E and W, but also when comparing areas closer to or farther from the culet on the same facet. These differences are far more complex in biaxial stones, which have three unique vibration directions (compared with only two in uniaxial stones). Keep in mind, however, that differences in color due to pleochroism will

BOX A: ELECTROMAGNETIC RADIATION AND CRYSTALS

Visible light is one form of electromagnetic radiation. Light is sometimes described as behaving like a particle, but when dealing with transmission and reflection, it is more convenient to describe light as a wave (Frye, 1974). This is often referred to as the "dual nature of light." For the purposes of pleochroism, the wave theory is more appropriate.

Electromagnetic waves consist of electric (E) and magnetic (M) portions, each mutually perpendicular. The electric portion of the wave interacts with, and is altered by electrons, and so it is only the E portion of the wave that will be considered when referring to refraction and polarization (figure A-1).

The electric vector (vibration) of ordinary light, such as sunlight, may extend in any direction perpendicular to the direction of travel (figure A-2). Such light is said to be *unpolarized*. Should the light wave be forced to vibrate in a single plane, the ray is *polarized*.

When light enters a substance of greater optical density, it is slowed because the electron density is greater and thus there is greater interference with the E portion of the wave. If the electron density of that substance is random, such as in a gas or glass, the polarization is not affected. The same holds true when it enters isometric (cubic) crystals, where the lattice points are arranged identically in each of the three dimensions.

Figure A-1. Electromagnetic waves consist of two mutually perpendicular portions, an electric vector and a magnetic vector. The electric vector interacts with, and is altered by, electrons. This produces effects such as refraction and pleochroism. Illustration by Richard W. Hughes.

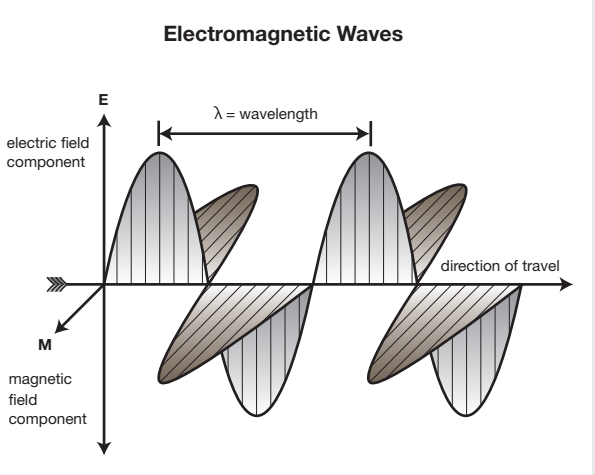

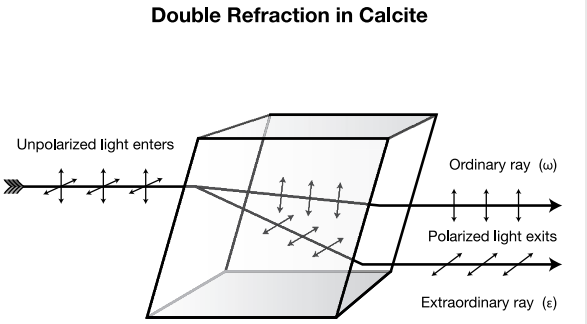

Figure A-2. When light enters a doubly refractive material in directions not along the optic axis, it is split into two portions, each polarized perpendicular to the other. Each ray may also be absorbed differently, resulting in pleochroism. Illustration by Richard W. Hughes.

In all other crystals, the lattice points (and thus the electron clouds) are unevenly spaced. The spacing of lattice points in dimetric crystals varies in two dimensions, while that of trimetric crystals varies in all three dimensions. This affects the manner in which light moves through them. Non-cubic crystals are termed *anisotropic*. They both split and perpendicularly polarize light upon entry, except in directions where the electron clouds are symmetrical. Those directions are termed *optic axes*, and light travels along these directions as it does in isotropic materials.

When light enters an anisotropic substance in a direction not parallel to an optic axis, it splits into two segments, each of which is polarized perpendicular to the other. Polarization can also occur when light strikes a highly reflective surface, such as a lake, producing what our eyes perceive as glare. The direction of polarization is parallel to the reflective surface. If one dons "Polaroid" sunglasses, the glare is eliminated because the lenses contain tiny polarizers oriented perpendicular to the horizon.

occur in a symmetrical pattern, with different pleochroic colors 90° apart from one another, just as in uniaxial gems.

The above descriptions of pleochroism in uniaxial and biaxial gems demonstrate the variation of color on facets of different orientations. But remember that

Figure 13. The color of this 7 ct tsavorite garnet is darker on the ends than in the center, but not due to pleochroism—garnet is singly refractive. Instead, this is an illustration of the Beer-Lambert law, where longer light paths result in greater absorption. Photo by Wimon Manorotkul.

these individual components will mix together to produce the single color seen on any individual point on each facet. A dichroscope can be used to separate that single color into its individual components.

PLEOCHROISM, OR SOMETHING ELSE?

Pleochroism is not the only factor that may cause color variations in faceted gems. Color zoning can result in significant color variations, as can different path lengths of light. Both of these attributes may be present in either singly or doubly refractive gems. Although these should not be confused with pleochroism, they sometimes are.

Consider, for example, an elongated cushion-shaped tsavorite garnet that possesses no visible color zoning (figure 13). With such a stone, the ends of the cushion will appear darker than the sides. This effect could easily be confused with pleochroism, despite the fact that pleochroism cannot occur in singly refractive stones. The actual cause of the darker end facets is the longer light paths.

The Beer-Lambert law states that absorption is directly related to the length of the light path and the concentration of absorbing chromophore. If the path length is doubled while the amount of chromophore remains constant, then the amount of absorption is also doubled. With a 12 mm × 6 mm cushion-cut tsavorite, light internally reflected off the end facets travels down the entire length of the stone, nearly double the path length of light reflected across the side facets. As a result, the end facets are nearly twice as dark as those on the side. If the same piece of rough were cut as a round, however, no variation in color would be seen. Thus, the color variations sometimes seen in singly refractive gems result from variations in light path lengths or color zoning rather than pleochroism.

THE DICHROSCOPE

Not all doubly refractive gems show distinct pleochroism. To determine if color variations across the face of a doubly refractive gem are due to pleochroism or simply variations in path length or color zoning (or even colored inclusions), a dichroscope should be used. Calcite-type dichroscopes (figure 14) are generally preferable to the polarizing types, because calcite is colorless. The polaroid filters used in polarizing dichroscopes generally have a greenish color, which may slightly modify the true pleochroic colors seen, or a grayish color that diminishes the light return.

In using the dichroscope, one must check uniaxial gems at right angles to the c-axis (optic axis) to observe the strongest pleochroism, while biaxial gems should be examined along each of the mutually perpendicular X (alpha), Y (beta), and Z (gamma) directions. But remember that the dichroscope examines transmitted light only. Even if no pleochroism is seen while looking through the table facet, pleochroic

Figure 14. Three tools for observing pleochroism: the calcite dichroscope, the polaroid-plate dichroscope, and polaroid sunglasses. Polaroid sunglasses make an effective field tool, as simply rotating a pleochroic gem in front of them allows one to observe the different colors (albeit one color at a time). A polariscope with the polarizer and analyzer in parallel position can perform the same function. Photo by Wimon Manorotkul.

color variations may still be visible across the face of a faceted gem (closer to or farther from the culet). This is because the facet orientation causes light to be reflected in more than one direction as it traverses the stone, as previously described.

In doubly refractive stones, color zoning, inclusion color, and path length variations (in non-round or non-square cut shapes) must also be taken into account in determining if visible color variations are due to pleochroism or another factor.

When a faceted colored gem is being examined and described, gemologists need to recognize that the overall appearance perceived as "real" is a synthesis of many factors, some related and some not. Pleochroism is but one. The final determination of pleochroism (and all other color attributes) for purposes of color grading should be made with the gem in the face-up position, as the stone was designed to be viewed. Yet this examination should not be restricted to a direction perpendicular to the table facet. Gems are often viewed at oblique angles, so it seems only logical that the grading should be made in an arc ranging anywhere from parallel to the table to perpendicular to the table.

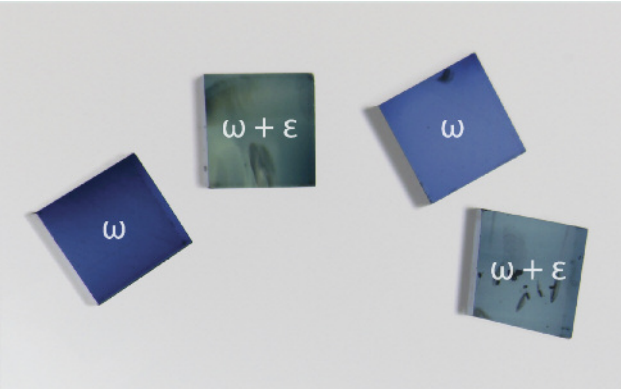

Figure 15. Small cubes of blue sapphire viewed perpendicular to the optic axis through a polarizing filter. Rotating either the gems or the polarizer will reverse the two pleochroic colors of each piece. Photo by Wimon Manorotkul.

CONCLUSION

While gemologists typically observe pleochroism with a dichroscope, or possibly a polarizing filter (figure 15), this attribute's effect on appearance is more complex and generally overlooked. A basic understanding of optical crystallography unlocks the secret of faceted pleochroic gems: When viewing them with the unaided eye, pleochroism is always present, even along an optic axis.

For many gems, pleochroism plays an important role in overall color appearance. It is the wise gemologist and lapidary who understand that this property represents far more than just the twin colors seen in a dichroscope.

ABOUT THE AUTHOR

Mr. Hughes is the cofounder of Lotus Gemology in Bangkok, a laboratory devoted to testing ruby, sapphire, and spinel. He is also the author of Ruby & Sapphire *(1997) and more than 150 articles on various aspects of gemology. Many of his writings can be found at www.lotusgemology.com and www.ruby-sapphire.com. His latest book is* Ruby & Sapphire: A Collector's Guide *(2014).*

ACKNOWLEDGMENTS

The author would like to thank John Emmett for carefully reviewing the manuscript and Joel Arem for allowing the use of his blue zircon photo.

REFERENCES

Arem J. (1977) *Color Encyclopedia of Gemstones*, 1st ed. Van Nostrand Reinhold Co., New York, 147 pp.

Frye K. (1974) *Modern Mineralogy*. Prentice-Hall, Englewood Cliffs, NJ, 325 pp.

Hughes R.W. (1997) *Ruby & Sapphire*. RWH Publishing. Boulder, CO, pp. 80–85.

Hurlbut C.S. (1984) The jeweler's refractometer as a mineralogical tool. *American Mineralogist*, Vol. 69, pp. 391–398.

GEMS & GEMOLOGY 2014

CONGRATULATIONS

This year, hundreds of readers participated in the 2014 *Gems & Gemology* Challenge. Entries arrived from around the world, as readers tested their gemological knowledge by answering questions listed in the Spring 2014 issue. Those who earned a score of 75% or better received a GIA Certificate of Completion recognizing their achievement. The participants who scored a perfect 100% are listed below.

G&G Challenge Winners

Australia
Barbara Wodecki

Belarus
Dmitry Stepanenko

Brazil
Maria Amelia Franco

France
Jurga Lenktaityte

Italy
Chiara Piussi

Switzerland
Julie Chaponnière

United Kingdom
Francesca Lawley
Giulia Nisoli
Ana Lucia Tres

United States
Sakina Bharani
Andrea Blake
John Cason
Elaine Fosmire
Edward "Ned" Goodman
Lois A. Henning
Sarah Horst
Kathryn Howe
Carson Lee
Lisa A. Marsh-Vetter
Paul Mattlin
Daniel Novak
Timothy Schuler
Colleen Walsh
Flora Walters
Thomas Wendt

Answers

See pages 64–65 of the Spring 2014 issue for the questions.

1 (a), 2 (b), 3 (d), 4 (d), 5 (*), 6 (a), 7 (a), 8 (a), 9 (c), 10 (d), 11 (b), 12 (a), 13 (d), 14 (c), 15 (b), 16 (b), 17 (b), 18 (b), 19 (d), 20 (d), 21 (c), 22 (c), 23 (d), 24 (d), 25 (c)

* Question withdrawn

NEPHRITE JADE FROM GUANGXI PROVINCE, CHINA

Zuowei Yin, Cui Jiang, M. Santosh, Yiming Chen, Yi Bao, and Quanli Chen

Nephrite jade with high market value and production potential from the Chinese city of Hechi, in Guangxi Province, was tested by standard gemological methods, polarizing microscopy, scanning electron microscopy (SEM), X-ray diffraction (XRD), Raman spectroscopy, and energy-dispersive spectrometry (EDS). The three samples were mainly white and gray-white (with areas of gray, gray-green, dark green, and black) and had a greasy to waxy luster. Within each of these color varieties, the samples exhibited either "band" or dendritic patterns. The band pattern, composed of tremolite, varied in shape and was either transparent or opaque. Its color, transparency, and distribution were different from the unpatterned areas. The dendritic patterns, which had a brownish yellow and dark brown to black color, were composed of chlorite that formed during metamorphism.

Nephrite is favored by Chinese collectors for its color and luster, as well as its fine texture and outstanding toughness. Primary nephrite deposits are found in more than 20 countries, including China, Russia, Canada, Australia, New Zealand, and South Korea. Chinese deposits are mainly distributed in the areas of Xinjiang, Qinghai, Guizhou, and Liaoning (Liao et al., 2005; Zhang et al., 2011). Research shows that nephrite's excellent toughness is a product of its fine-grained interlocking structure (Bradt et al., 1973; Dorling and Zussman, 1985; Yang, 2011). Its green color is due mainly to the substitution of Cr^{3+} and Fe^{2+} for Mg^{2+} (Flint, 1990). In principle, nephrite can form in two different ways. One is by contact metasomatism between intermediate-acidic intrusive rocks and dolomite and/or limestone. The other is by contact metasomatism between serpentine or serpentinizing peridotite and more silicic rocks (Harlow and Sorensen, 2005; Siqin et al., 2012).

The Chinese nephrite samples in this study were recovered in 2012 from Dahua County, in the city of Hechi. There are several mines in the county, worked by independent miners who also farm the area. One farmer estimated production of more than 1,000 tons per year. The local government controls the mining, and the market for this nephrite is growing in Guangxi and Guangdong. In 2013, the pendant shown in figure 1 sold for US$300, while the bangles in figure 5 brought US$3,000 each.

This paper introduces the mine at Hechi and characterizes the patterns in these nephrites.

GEOLOGIC BACKGROUND AND LOCATION

The nephrite mining area at Hechi, shown in figure 2, belongs to the west wing of the NNE-striking (15°–30°) Yangshan-Damingshan anticline. Regional strata dip steeply, and almost all main structural features strike NNE. The wall rocks are marine carbonate rocks deposited from the Upper Devonian to Lower Permian periods (362–290 Ma). Basic intrusive and volcanic rocks were emplaced during the Permian period (approximately 295–250 Ma). The heat gener-

Figure 1. This nephrite pendant, from a mine at Hechi in China's Guangxi Province, features a dendritic pattern. Photo by Yiming Chen.

See end of article for About the Authors and Acknowledgments.
GEMS & GEMOLOGY, Vol. 50, No. 3, pp. 228–235,
http://dx.doi.org/10.5741/GEMS.50.3.228.

Figure 2. This map shows the main locations of China's nephrite deposits (Zhang et al., 2011) and the working area of this study, in Guangxi Province.

ated by the emplacement caused metasomatism between the igneous rocks and the carbonate rocks. Nephrite is the product of this metasomatism (Bureau of Geology and Mineral Resources of Guangxi Province, 1985).

The mining area has a typical karst landscape. It has been severely weathered by the subtropical climate, and slope sediments, fluvial, and alluvial materials are all visible. The ore-bearing country rocks are limestone, in severely weathered layers of varying thickness. Nephrite occurs as bands and veins in these layers. The width of a single vein ranges from tens of centimeters to several meters. The ore body and wall rock (mainly dolomite marble) are alternately distributed, and the boundary between them is sharp.

The nephrites from these primary and secondary mines are mainly white, gray-white, gray-green, dark green, and black, with a greasy to waxy luster (figure 3). All of these color varieties display either band or dendritic patterns. The band patterns are white and opaque, and their color, transparency, and distribution are different from those of the unpatterned areas. The dendritic patterns are brownish yellow and dark brown to black (figure 4). At Hechi, the dendritic patterns only occur in the nephrites from secondary deposits in river or soil.

Figure 3. The dark green nephrite on the left shows a beautiful green color when illuminated. Black nephrite carvings of the Buddhist goddess Guanyin (center) and necklaces of nephrite beads with various colors (right) are displayed at the local market near the mine. All material shown was mined in Hechi. Photos by Yiming Chen and Zuowei Yin.

Figure 4. A: In the hills near Hechi, nephrite is found in shallow ground, about one meter underground, and belongs to secondary deposits. B: Grayish green rough with a thick weathered surface. C: Nephrites with dendritic patterns and country rock. The country rock is dolomitic marble that has undergone metasomatism. The boundary between marble and nephrite is sharp. D: In the primary deposit, nephrite occurs as bands of dark green, white, and gray. Photos by Yiming Chen.

MATERIALS AND METHODS

Three white and gray-white nephrite samples were examined for this study: the two bangles with dendritic patterns (figure 5, left and center) and a slab with a band pattern (figure 5, right). The dendritic patterns in the two bangles ranged from brownish yellow to black. In the slab, the banded area showed lower transparency than the rest of the sample. The samples were tested by standard gemological methods, polarizing microscopy, scanning electron microscopy (SEM), X-ray diffraction (XRD), Raman spectroscopy, and energy-dispersive spectrometry (EDS). We conducted the tests at the National Key Lab of the China University of Geosciences in Wuhan.

For SEM analysis, the authors fractured the specimens and coated the fracture surfaces with carbon powders using an SCD-005 ion sputter coater. The specimens were then fastened to a round metal disk for observation. An FEI Quanta 200 scanning electron microscope was used to observe the nephrites' microstructure, especially their dendritic and band patterns. The SEM images are from secondary electrons.

The instrument used for XRD analysis was an X'Pert PRO DY 2198 with Cu Kα radiation operating at 40 kV and 40 mA. The instrument was equipped with a small platform and a monocapillary lens with a 100 μm diameter micro-zone. Dendritic patterns were tested by the micro-area method, since it is difficult to detect very small particles through normal analysis.

To detect the mineral composition of the patterns, we used a Bruker Senterra scanning Raman microscope in the 40–3650 cm^{-1} region. The instrument, which features a 785 nm light source and 50 mW laser energy, was set to approximately 3.5 cm^{-1}

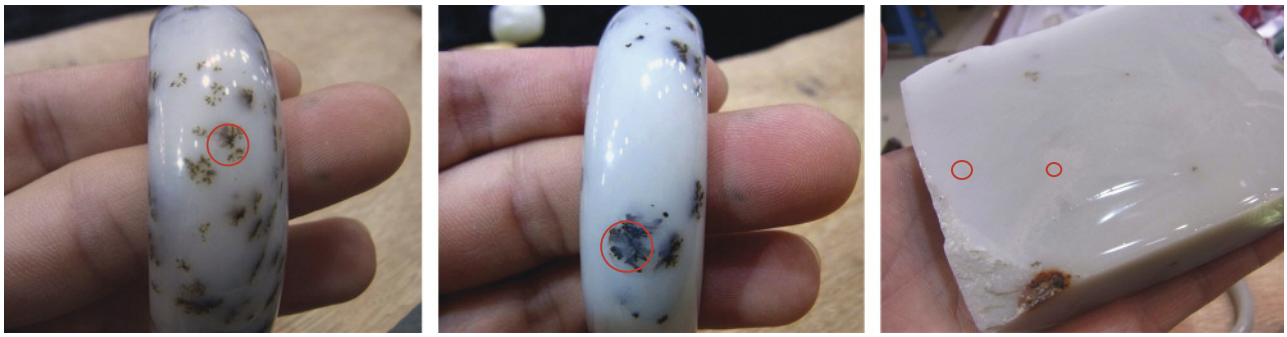

Figure 5. In these photos of the three nephrite samples, the red circles represent the testing points. The two bangles display a dendritic pattern, while the slab contains a band pattern. Photos by Yiming Chen.

resolution and 10 seconds per scan. Dendritic, band, and unpatterned areas were all tested.

For EDS analysis of the dendritic and band patterns, we used an EDAX Genesis 2000. This element-testing method employs back-scattered electrons to obtain chemical composition. Measurement error with the EDS data is 0.1–0.5%.

RESULTS AND DISCUSSION

Gemological Features and Petrographic Study. The samples showed a spot RI of 1.61–1.62 and a hydrostatic SG of 2.88–2.90. The unpatterned and band areas of the nephrite slab were sliced into thin sections. Under polarized light, they displayed different microstructures. The tremolites of the band area (figure 6, left) were fibrous, columnar, of various grain size, and poorly oriented. The individual tremolite crystals ranged from less than 0.05 to 0.2 mm long, occurring in radial beam and fan shapes. The band had a coarser texture than the unpatterned area. The interwoven tremolites of the unpatterned area (figure 6, right) were fine, with a homogeneous grain size. Most of the tremolites were less than 0.05 mm long.

SEM. We performed SEM testing of the dendritic areas in the two bangles, and the band and unpatterned areas of the slab. The tremolites with a dendritic pattern were magnified 1514× and 2840× (figure 7). The tremolite grains occurred as long strips, the dendritic pattern grains as tiny dots. At 2840× magnification, the tremolite grains were clearly visible, while the grain shape of the dendritic pattern was not.

In Brief

- Nephrite jade in China's Guangxi Province displays different colors and dendritic pattern inclusions.
- Dendritic pattern inclusions composed of chlorite in brownish yellow and dark brown to black color only occur in secondary nephrites found in rivers or soil.
- Since these dendritic patterns have not been found in other Chinese nephrite mines, the pattern may be used in origin determination studies.

The grains in the band areas were unevenly distributed, while those in the unpatterned areas were uniformly distributed at 500× magnification. At 2000× magnification, the grains in the band were poorly oriented, while those in the unpatterned areas were better oriented (figure 8). Those distinctions led to different appearances between these two areas of the sample.

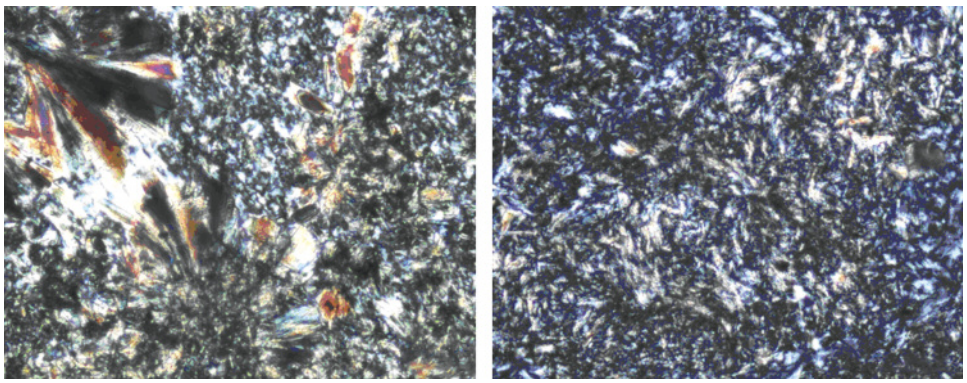

Figure 6. The nephrite slab displays band (left) and unpatterned areas (right). The band's tremolites are fibrous, columnar, of varying particle size, and poorly oriented. The interwoven tremolites of the unpatterned area are fine, with homogeneous particle size. Photomicrographs by Zuowei Yin; image widths 0.57 mm.

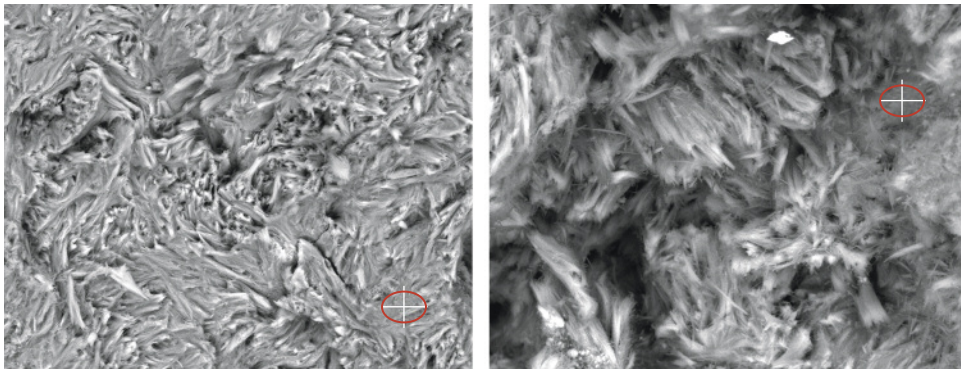

Figure 7. These SEM photos of tremolites with dendritic patterns are magnified 1514× (left) and 2840× (right). The red circles represent the EDS testing points. Photo by Yi Bao.

Raman Spectroscopy. The grains of the dendritic patterns were too small to detect by Raman, even though the dendritic patterns themselves appeared quite large. Only the spectra of the band and unpatterned areas are provided.

According to the Raman spectra of the slab (figure 9), the mineral constituents of the band and unpatterned portions were all tremolites. Among the nephrite peaks, the 3600–3700 cm^{-1} features represent O-H stretching vibration, and the 900–1150 cm^{-1} features represent the stretching vibration and antisymmetric stretching vibration of the Si-O bond. The 677 cm^{-1} band designates the symmetric stretching vibration of Si-O-Si. The 100–400 cm^{-1} features may be caused by the deformation vibration induced by the distortion vibration of the silicon oxygen tetrahedron (Zhao and Gan, 2009; Qiu et al., 2010; Yang et al., 2012).

To verify the dendritic patterns by means of their crystal structure and chemical composition, we turned to XRD and EDS.

XRD. To identify the mineral crystal structure of the dendritic pattern, we used the micro-area XRD

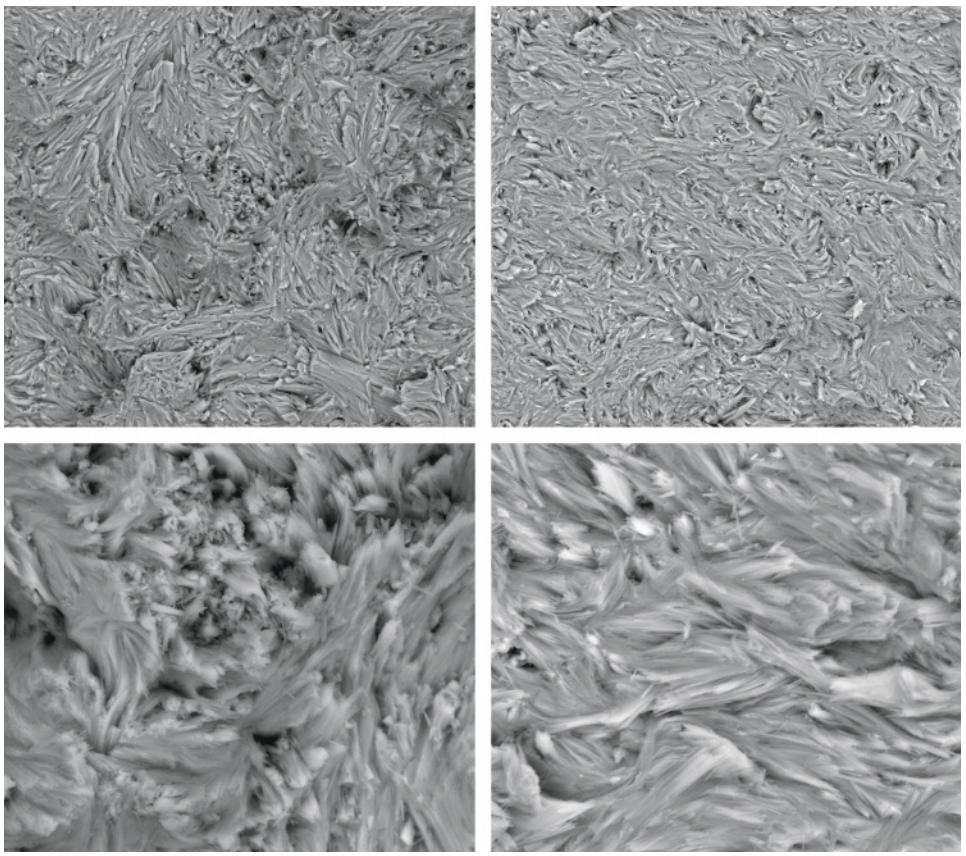

Figure 8. SEM photos of the band (top left) and unpatterned areas (top right) of the nephrite slab are shown at 500× magnification. Note the uneven distribution of the grains in the band area. At 2000× magnification (bottom left and bottom right), the grains are poorly oriented in the band and better oriented in the unpatterned area. Photomicrographs by Yi Bao.

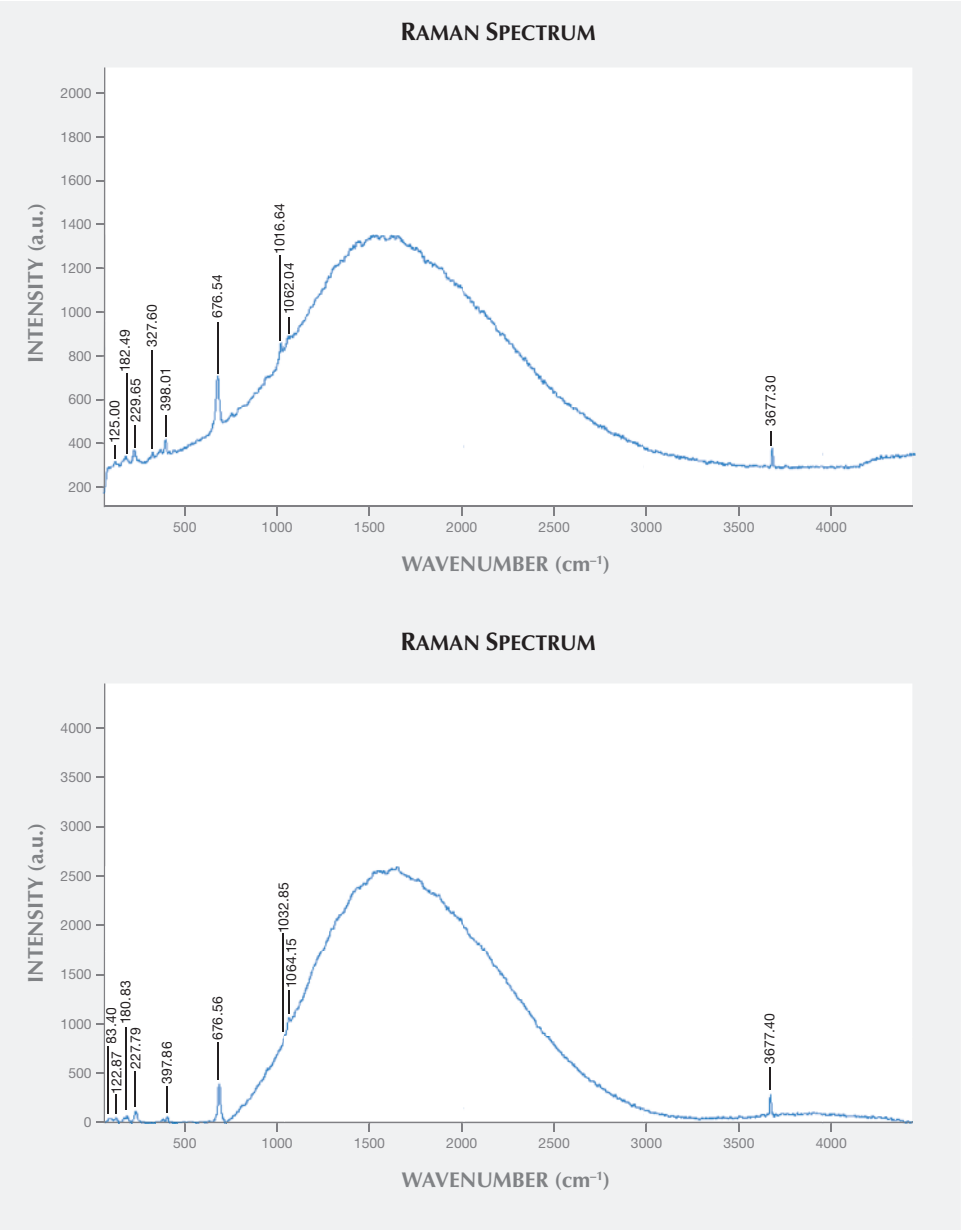

Figure 9. The Raman spectra of the band (top) and unpatterned area (bottom) of the nephrite slab identified them as tremolite.

method, the results of which are shown in figure 10. According to Bragg's law, defined as

$$n\lambda = 2d \sin\theta$$

"d" is the crystal lattice spacing in a certain direction. The dendritic pattern gave d values of 14.4, 7.1, 4.7, 3.5, and 2.8 Å, confirming that the mineral belonged to the chlorite group (Bailey and Lister, 1989; Zhao et al., 2006).

Chemical Composition. The dendritic, band, and unpatterned areas were all tested by EDS. The main composition of the dendritic pattern (table 1) was consistent with chlorite, which has a general chemical formula of $Y_3[Z_4O_{10}](OH)_2 \cdot Y_3(OH)_6$, where Y can represent Ca, Mg, Fe^{2+}, Al, Fe^{3+}, Cr, Ni, Mn, V, Cu, or Li, and Z is mainly Si and Al. According to table 1, the formula of chlorite here is (Ca, Mg, Mn, Fe)$[Si_4O_{10}](OH)_2$(Ca, Mg, Mn, Fe)$(OH)_6$. The band (table 2) and unpatterned areas (table 3) were both consistent with tremolite.

CONCLUSION

Nephrite jade from primary and secondary deposits at Hechi in China's Guangxi Province displays white, gray-white, gray, gray-green, dark green, and black colors, with a greasy to waxy luster. The white and gray-white samples from this study

TABLE 1. EDS chemical composition of dendritic patterns in nephrite from Guangxi Province, China.

Element	Wt.%	At.%
O	39.16	42.23
Si	14.52	8.92
Mg	9.48	6.73
Ca	7.20	3.10
Fe	1.88	0.58
Mn	1.27	0.40
C	26.49[a]	38.05[a]

[a] *C content is from the carbon-coated surface.*

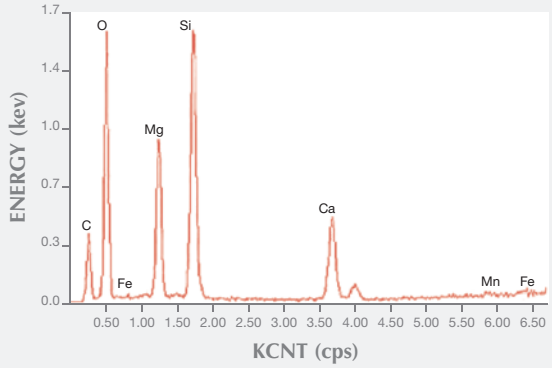

TABLE 2. EDS chemical composition of band patterns in nephrite from Guangxi Province, China.

Element	Wt.%	At.%
O	33.29	39.19
Si	25.88	17.36
Mg	13.26	10.27
Ca	9.16	4.31
C	18.41[a]	28.88[a]

[a] *C content is from the carbon-coated surface.*

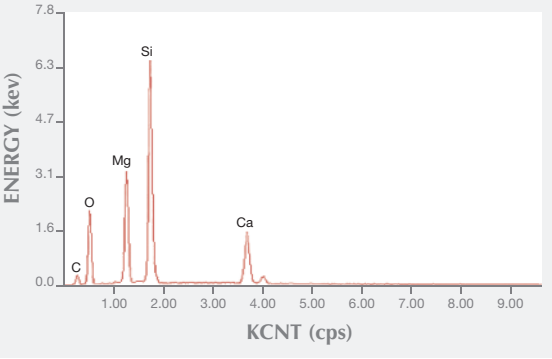

TABLE 3. EDS chemical composition of unpatterned areas in nephrite from Guangxi Province, China.

Element	Wt.%	At.%
O	30.27	37.67
Si	29.91	21.20
Mg	14.05	11.51
Ca	11.28	5.61
C	14.49[a]	24.02[a]

[a] *C content is from the carbon-coated surface.*

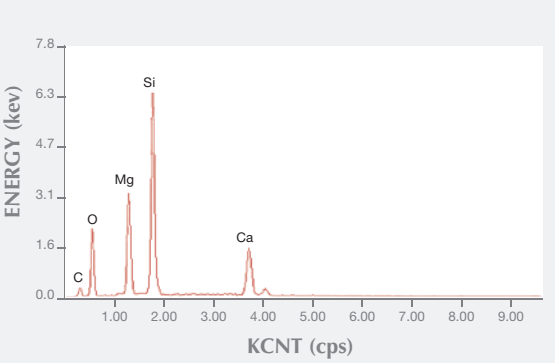

showed band or dendritic patterns. The transparent or opaque bands contained an irregular arrangement of tremolite, and their color, transparency, and distribution of grains were different from the rest of the nephrite. The dendritic pattern only occurred in the secondary nephrites found in river or soil. There were also some dendritic patterns with brownish yellow and dark brown to black color. They con-

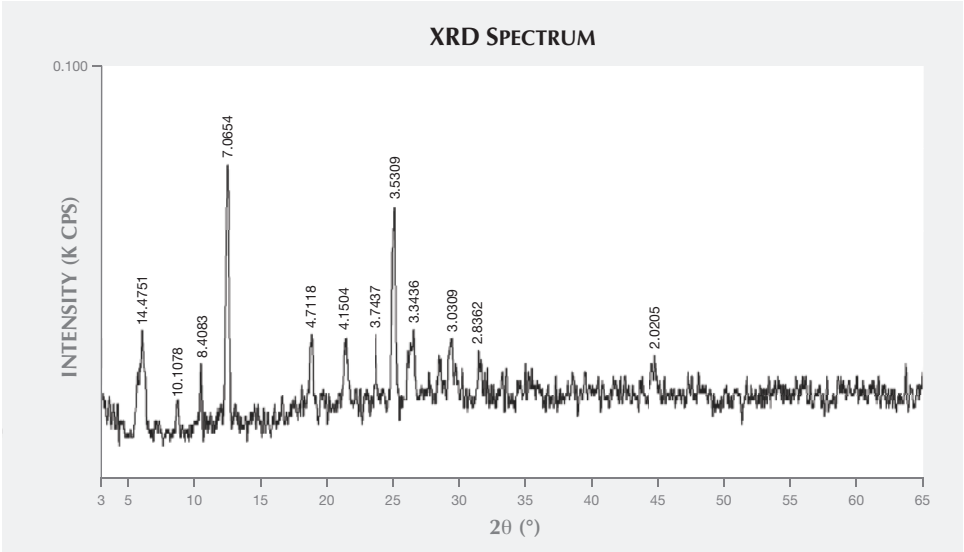

Figure 10. XRD testing of the dendritic patterns gave d values (crystal lattice spacing) characteristic of the chlorite group.

tained very small particles composed of chlorite that occurred during metamorphism. These kinds of dendritic patterns have not been found in other Chinese nephrite mines, making them useful features for identifying the locality. The pattern also proves that these nephrites are from secondary deposits, which have a higher value in the Chinese market.

ABOUT THE AUTHORS

Dr. Yin (yinzuowei1025@163.com) is a professor at the Gemological Institute, China University of Geosciences in Wuhan, where Mr. Chen and Ms. Bao are students and Dr. Chen is a lecturer. Ms. Jiang (jiangcuijane@163.com, corresponding author) is a lecturer at the Foreign Language School, China University of Geosciences in Wuhan. Dr. Santosh is a professor at the School of Earth Sciences and Resources, China University of Geosciences in Beijing.

ACKNOWLEDGMENTS

This research is supported by the National Natural Science Foundation of China (40272021) and the Research Foundation for Experimental Study of CUG (2013 key project). This study also contributed to the Global 1000 Talents award to M. Santosh from the Chinese government.

REFERENCES

Bailey S.W., Lister J.S. (1989) Structures, compositions, and X-ray diffraction identification of dioctahedral chlorites. *Clays and Clay Minerals*, Vol. 37, No. 3, 193–202, http://dx.doi.org/10.1346/ccmn.1989.0370301.

Bradt R.B., Newnham R.E., Biggers J.V. (1973) The toughness of jade. *American Mineralogist*, Vol. 58, pp. 727–732.

Bureau of Geology and Mineral Resources of Guangxi Province (1985) Regional geological documental record of Guangxi province. Geological Publishing House, Beijing, pp. 186–191.

Dorling M., Zussman J. (1985) An investigation of nephrite jade by electron microscope. *Mineralogical Magazine*, Vol. 49, No. 350, pp. 31–36, http://dx.doi.org/10.1180/minmag.1985.049.350.04.

Flint D. (1990) The nephrite of Australia. *China Gems and Jades*, No. 2, pp. 40–42.

Harlow G.E., Sorensen S.S. (2005) Jade (nephrite and jadeitite) and serpentinite: Metasomatic connections. *International Geological Review*, Vol. 47, No. 2, pp. 113–146, http://dx.doi.org/10.2747/0020-6814.47.2.113.

Liao R.Q., Zhu Q.W. (2005) Chemical composition analyses of nephrite from all Chinese locations. *Journal of Gems & Gemmology*, Vol. 7, No. 1, pp. 25–30.

Qiu Z.L., Jiang Q.Y., Luo H., Qin S.C., Li L.F. (2010) Raman spectra and its application of graphite enclaves in nephrite jades in Xiuyan, Liaoning. *Spectroscopy and Spectral Analysis*, Vol. 30, No.11, pp. 2985–2988.

Siqin B., Qian R., Zhuo S. J., Gan F. X., Dong M., Hua Y. F. (2012) Glow discharge mass spectrometry studies on nephrite minerals formed by different metallogenic mechanisms and geological environments. *International Journal of Mass Spectrometry*, Vol. 309, pp. 206–211, http://dx.doi.org/10.1016/j.ijms.2011.10.003.

Yang L. (2011) The preliminary research of Luodian jade of Guizhou. *Guizhou Geology*, Vol. 28, No. 4, pp. 244–246.

Yang X.D., Shi G.H., Liu Y. (2012) Vibrational spectra of black species of Hetian nephrite (tremolite jade) and its color genesis. *Spectroscopy and Spectral Analysis*, Vol. 32, No. 3, pp. 681–685.

Zhang Z.W., Gan F.X., Cheng H.S. (2011) PIXE analysis of nephrite minerals from different deposits. *Nuclear Instruments and Methods in Physics Research B*, Vol. 269, No. 4, pp. 460–465, http://dx.doi.org/10.1016/j.nimb.2010.12.038.

Zhao H.X., Gan F.X. (2009) The Raman spectroscopic analysis on several nephrite jades from different provenances and the application in non-destructive study of ancient jade artifacts. *The Journal of Light Scattering*, Vol. 21, No. 14, pp. 345–354.

Zhao M.Q., Lan Y., Yu N., Zhang T.Y. (2006) Study on mineralogical characteristics of chlorite jade from Russia. *Journal of Gems and Gemmology*, Vol. 8, No. 2, pp. 14–16.

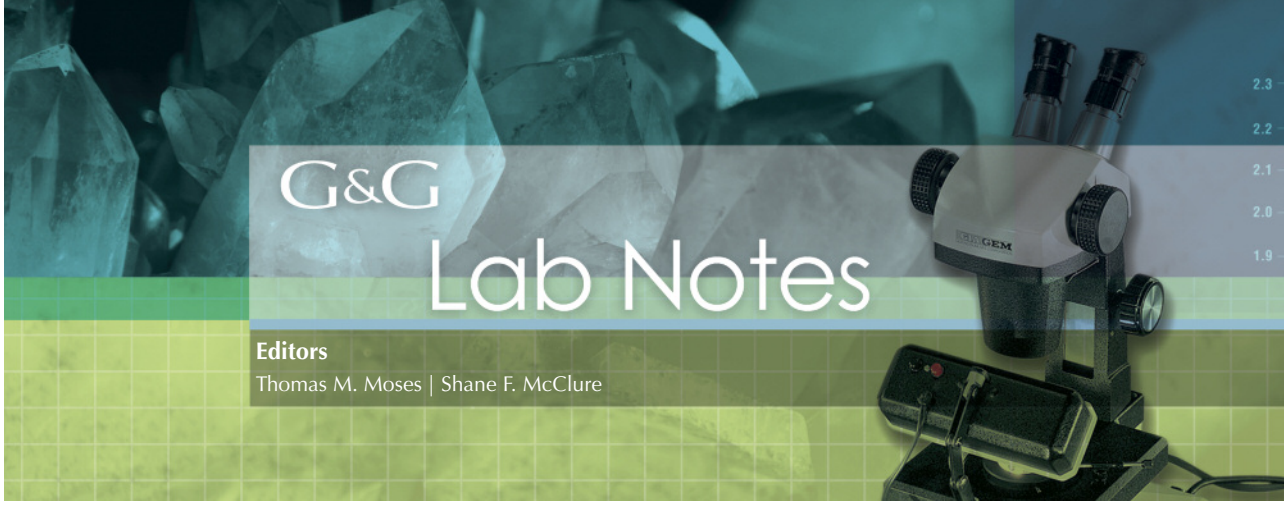

DIAMOND

Artificially Irradiated and Coated Brown

Red is arguably the rarest and most valued color in diamond. It is known to bring record-breaking prices at auction, as in the case of the 0.95 ct Hancock Red, which sold for nearly $1 million per carat in 1987. Some will go to great lengths to achieve this color, even resorting to unusual multiple treatments.

The New York laboratory recently examined a Fancy reddish brown 0.28 ct round brilliant diamond submitted for color origin identification (figure 1). Spectroscopic analysis immediately revealed that it had been artificially irradiated to create the reddish brown color. The presence of an amber center, identified by infrared spectra, indicated that this diamond was likely brown prior to treatment. Further investigation using the DiamondView determined that the stone's pavilion facets had also been coated, a feature not apparent with microscopic observation. DiamondView images displayed weak luminescence, with more intense luminescence concentrated at facet edges, junctions, and where the stone had been scratched. Boiling removed the coating, eradicating the red component and changing the color grade to Fancy Dark orangy brown.

Figure 1. The diamond with a Fancy reddish brown color (left) was revealed to be Fancy Dark orangy brown once the coating and red hue were removed (right).

Removing the coating also produced a much more luminescent DiamondView image (figure 2).

This stone indicates an attempt to induce red color in diamond, presumably to increase the value. Although

Figure 2. DiamondView images of the diamond with the coating (top row) and after the coating's removal (bottom row). The dark spots in the bottom left image are remnants of the coating substance.

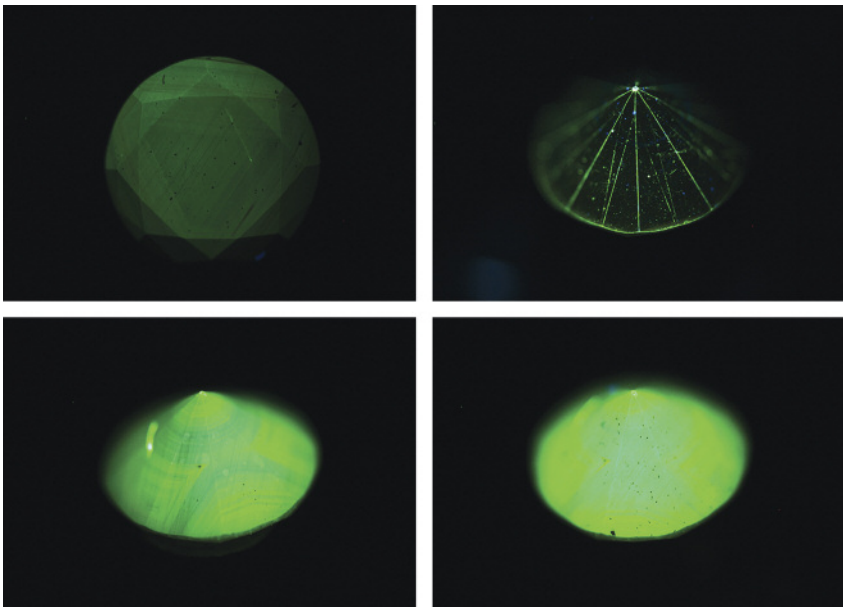

Editors' note: All items were written by staff members of GIA laboratories.

Gems & Gemology, Vol. 50, No. 3, pp. 236–243.

this effort proved unsuccessful, it emphasizes the need for vigilance when analyzing diamonds with rare color. Their appeal, and the number of treatment techniques to create these colors, is sure to grow.

Martha Altobelli, Paul Johnson, and Jason Darley

Mixed-Type Cape Diamond

Natural yellow type Ia or "cape" diamonds, the most common of all colored diamonds, are identified by the N3 (415 nm) and N2 (478 nm) absorption lines in the UV-visible range. These defects produce the characteristic yellow hue, and the N3 line produces the blue luminescence, so often observed in these stones. Weaker bands at 452 and 465 nm may also be visible (C.M. Breeding and J.E. Shigley, "The 'type' classification system of diamonds and its importance in gemology," Summer 2009 *G&G*, pp. 96–111).

The New York laboratory recently examined a 2.16 ct Fancy orangy yellow diamond (figure 3) with unusual features for a cape stone. When analyzed with a UV-Vis spectrometer, it exhibited a cape spectrum and an unexpected 480 nm band, a defect usually associated with orange color (figure 4). Infrared spectrometry revealed a well-defined IaA>B diamond, as opposed to the saturated Ia spectrum typically associated with cape diamonds. These abnormal features prompted further testing, and the DiamondView revealed zoned blue and yellow fluorescence (figure 5). Raman spectroscopy of the transparent, elongated crystal within the diamond, visible in the DiamondView, identified it as a colorless garnet, a common inclusion in cape diamonds.

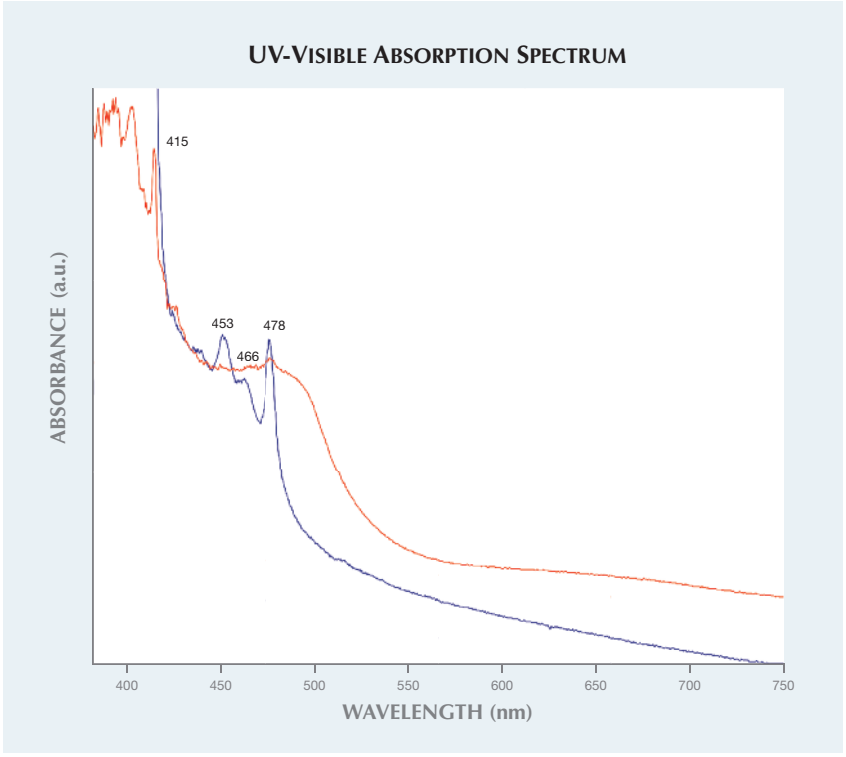

Figure 4. The Fancy orangy yellow diamond's "mixed" cape spectrum (red) is shown along with an overlay of a normal cape spectrum (blue).

Figure 3. This 2.16 ct Fancy orangy yellow diamond is a mixed-type IaA>B.

Figure 5. The cape diamond's DiamondView image displays blue and yellow fluorescence, along with an elongated crystal.

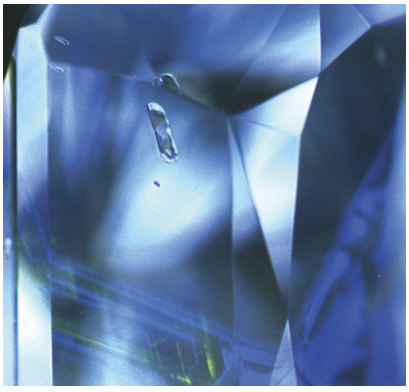

While the specific structure of the 480 nm optical defect is not yet understood, it is known to be associated with yellow fluorescence (Y. Luo and C.M. Breeding, "Fluorescence produced by optical defects in diamond: Measurement, characterization, and challenges," Summer 2013 *G&G*, pp. 82–97). The defect is also sometimes attributed to substitutional oxygen in type I diamonds. From our data and test results showing no evidence of laboratory-produced alteration, we can conclude that this stone is a natural and very rare example of a cape diamond mixed with a 480 nm band causing the orange component.

Martha Altobelli and Paul Johnson

Xenotime Inclusion in Yellow Diamond

Diamond inclusions can be analyzed using Raman spectroscopy, ideally when they are close to or breaking the surface. The New York lab recently

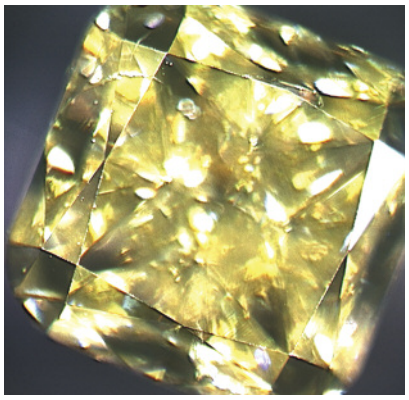

Figure 6. This 0.55 ct yellow diamond contained a rare mineral inclusion of xenotime.

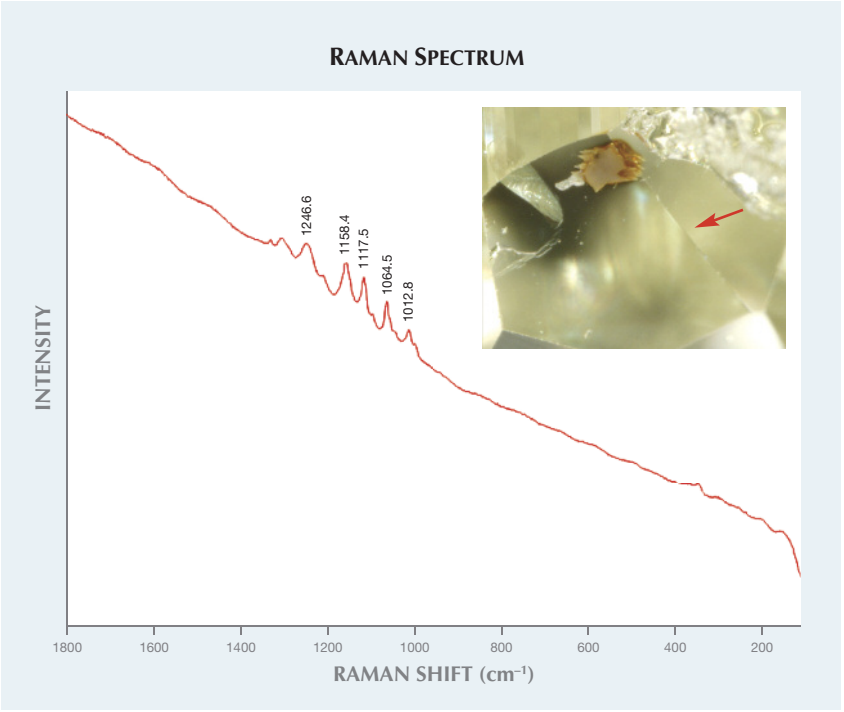

Figure 7. The xenotime inclusion broke through the pavilion surface (inset; magnified 80×). Radiation stains were also observed at the contact with the host diamond (see arrow). The Raman spectrum, using a 514 nm laser, shows xenotime peaks at 1012.8, 1064.5, 1117.5, 1158.4, and 1246.6 cm^{-1}.

had the opportunity to study a rare inclusion of xenotime protruding from the surface of a 0.55 ct Fancy Intense yellow diamond (figure 6).

The yellowish brown inclusion was located in the pavilion near the girdle; radiation stains were observed at the contact area with the host diamond (figure 7, inset). Radiation stains and the nature of the surface penetration suggested that it formed inside an etch channel as an epigenetic inclusion. Raman spectroscopy showed peaks consistent with xenotime at 1012.8, 1064.5, 1117.5, 1158.4, and 1246.6 cm^{-1} as seen in the figure 7 spectrum.

Minerals that formed outside of the diamond stability field can be found inside a diamond (see Spring 2009 Lab Notes, pp. 54–55). Xenotime (yttrium orthophosphate, YPO_4) occurs mainly in granitic pegmatite and also in metamorphic rocks such as biotite gneiss (E.J. Young and P.K. Sims, *Petrography and Origin of Xenotime and Monazite Concentrations, Central City District, Colorado*, Geological Survey Bulletin 1032-F, 1961, pp. 273–297). Young and Sims proposed that granitic fluids such as granodiorite mobilized rare earth elements (REE) and phosphates from biotite gneiss in Colorado. Later, these ions crystallized to form unusually high concentrations of xenotime and monazite in migmatized parts of gneiss. The granitic fluids may have percolated within diamond deposits in continental crust, and REE ions could have been deposited and crystallized inside etch channels, as observed in this yellow diamond. Radiation stains associated with xenotime, which is one of the few naturally occurring yttrium minerals, may contain trace amounts of uranium and be slightly radioactive.

Associations of xenotime with diamond have been previously reported. E. Hussak described intergrowths of monazite and xenotime in diamond-bearing sands in Brazil ("Mineralogische Notizen aus Brasilien," *Tschermaks Mineralogische und Petrographische Mitteilungen*, Vol. 18, 1899, p. 346). More recently, xenotime inclusions have been reported in carbonado from the Macaubas River in Minas Gerais (M. De Souza Martins, *Geologia dos Diamantes e Carbonados Aluvionares da Bacia do Rio Macaubas (MG)*, Ph.D. thesis, Universidade Federal de Minas Gerais, Instituto de Geociencias, Belo Horizonte, Brazil, 2006). To the best of our knowledge, xenotime inclusions in gem-quality diamond have never been reported.

Kyaw Soe Moe, Martha Altobelli, and Paul Johnson

CVD SYNTHETIC DIAMOND with Unusual Inclusions

A 0.34 ct square modified brilliant was submitted to GIA's Carlsbad lab as a synthetic diamond. The specimen, which exhibited good polish and symmetry, received a color grade of K and a clarity grade of SI_2. During advanced testing, the photoluminescence spectra displayed a large 737 nm doublet, a silicon vacancy peak seen in CVD synthetic diamonds. A DiamondView image showed subtle growth dislocations on the pavilion and almost no growth layer structure on the crown (figure 8). A mid-IR spectrum did not show the 3123 cm^{-1} peak, once considered characteristic of CVD synthetics (P.M. Martineau et al., "Identification of synthetic diamond grown using chemical vapor

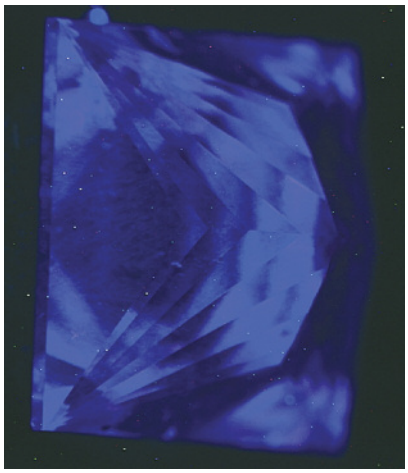

Figure 8. This DiamondView image of the 0.34 ct CVD synthetic shows a pattern of growth dislocations.

deposition [CVD]," Spring 2004 *G&G*, pp. 2–25).

The most unusual features were the inclusions. As seen in figure 9, this item is deserving of its SI_2 clarity grade. In addition to several fractures, there were numerous indented crystal surfaces and included growth remnants. A close-up of the indented crystal surfaces revealed an irregular shape and surface texture (figure 10). The fully included growth remnants lacked any discernible pattern or regularity. Inclusions have been reported in CVD synthetic diamonds, but they have been confined to growth planes (Spring 2013 Lab Notes, pp. 47–49). This specimen's inclusions, which were scattered in a random way,

Figure 9. The pavilion displayed a wide variety of inclusions. Field of view 3.6 mm.

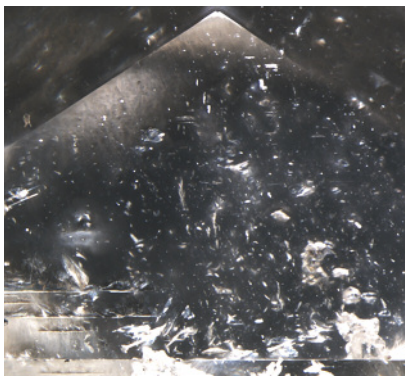

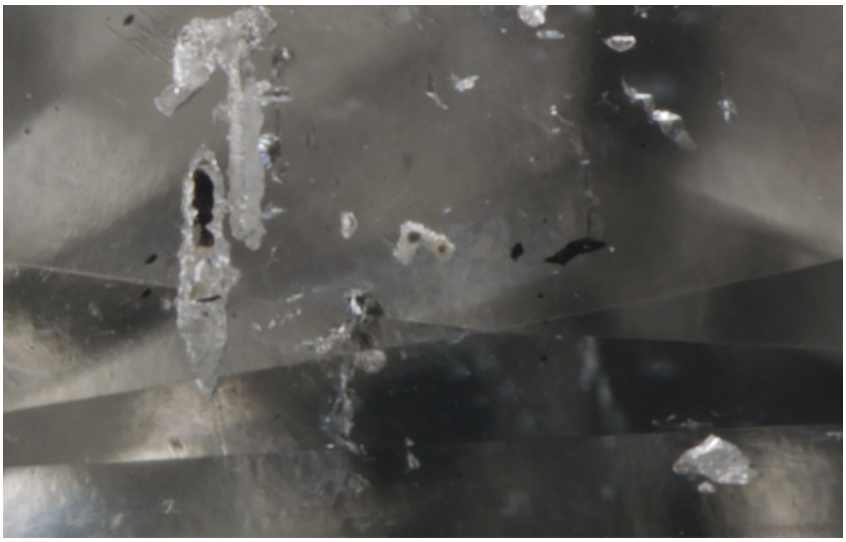

Figure 10. A close-up of some of the indented crystal structures showed etch-like patterns. Field of view approximately 1.4 mm.

showed no uniformity in size, shape, color, or placement. They were whitish or black, pinpoint-sized and larger structures (as seen in figure 10, lower right). Some were flat and pointed, while others were more rounded in shape. Furthermore, some were grouped together, similar to cloud-like inclusions, while others were freestanding, mimicking the inclusion distribution in natural diamond. The strain was mottled around the inclusions and crosshatched in cleaner areas.

The chemical structure and composition of these inclusions is unknown, and why they formed this way is a mystery. It is possible that this material is from a new growth method that yields heavily included product. Synthetic diamond research is a rapidly growing field; as it expands, many new and different types of samples find their way into the trade. The inclusions in this specimen could pass for natural inclusions if observed with a standard 10× loupe or a quick glance in the microscope. The DiamondView image is also difficult to interpret if one is not accustomed to the many fluorescent patterns CVD synthetic diamonds can display. This case is an important reminder to exercise caution when determining natural or synthetic origin, because some synthetic diamonds in the market look very natural.

Troy Ardon

Two Fancy Dark Gray CVD Synthetic Diamonds

Recently, two colored synthetic diamonds examined in the Carlsbad laboratory were determined to have been grown by the chemical vapor deposition (CVD) method. Both received an unusual color grade of Fancy Dark gray. GIA has graded other gray CVD synthetics before, but within the Fancy Light to Fancy range; it is rare for a synthetic to receive a Fancy Dark color grade. The few Fancy Dark synthetic diamonds submitted in the past have all been HPHT synthetics (most of them Fancy Dark reddish brown) with post-growth treatment that created NV centers. The two gray CVD specimens were also noted for their size—0.80 and 1.50 ct. The latter is shown in figure 11.

In addition to their color grade, both showed similar spectra. Neither sample's UV-visible-NIR spectrum displayed any distinct absorption peaks. The mid-IR spectra identified them as type IIa diamond but did not contain

Figure 11. This 1.50 ct Fancy Dark gray CVD synthetic diamond was unusual for its combination of color grade and large size.

features that confirmed synthetic origin. Their photoluminescence (PL) spectra had nearly identical features, suggesting that they originated from similar manufacturing processes. Both PL spectra featured a large silicon-vacancy doublet at 737 nm, a strong indicator of CVD growth (though natural diamonds will occasionally show a weak silicon peak along with other natural features); this was confirmed by the DiamondView images. The 1.50 ct specimen showed light blue fluorescence and striations commonly observed in CVD synthetics (figure 12, left) (P. Martineau et al., "Identification of synthetic diamond grown using chemical vapor deposition (CVD)," Spring 2004 *G&G*, pp. 1–25). The 0.80 ct sample offered a more unusual DiamondView image, with yellow fluorescence interspersed with regions of purple mottling. The purple mottling is seen occasionally in CVD synthetics, but usually combined with a background of pink fluorescence (W. Wang et al., "Latest-generation CVD-grown synthetic diamonds from Apollo Diamond Inc.," Winter 2007 *G&G*, pp. 294–312) instead of the yellow fluorescence seen here. Some regions of the 0.80 ct synthetic had natural-looking fluorescence features (figure 12, right), but a thorough examination of the DiamondView fluorescence in conjunction with the silicon peak unambiguously identified it as CVD.

The DiamondView images of both synthetics also demonstrated blue phosphorescence, which is often associated with boron impurities. No known boron-related peaks were detected in the PL or mid-IR spectra, so the boron concentration would be below the level of detection by FTIR spectroscopy. Boron-related peaks seen in natural and treated type IIb diamonds often are not detected in known IIb HPHT- and CVD-grown synthetics. It is unclear whether the low boron concentration was deliberately introduced to improve growth rate and quality (S. Eaton et al., "Diamond growth in the presence of boron and sulfur," *Diamond and Related Materials*, Vol. 12, 2003, pp. 1627–1632). Boron-containing diamonds with low color saturation often appear gray, making this element the likely cause of color in both of these CVD synthetic diamonds.

Figure 12. Left: In the DiamondView, the 1.50 ct sample showed the familiar color and striations of CVD synthetics. Right: The 0.80 ct specimen displayed a combination of natural-appearing features in some regions (as shown) and CVD-related striations and purple mottling in others.

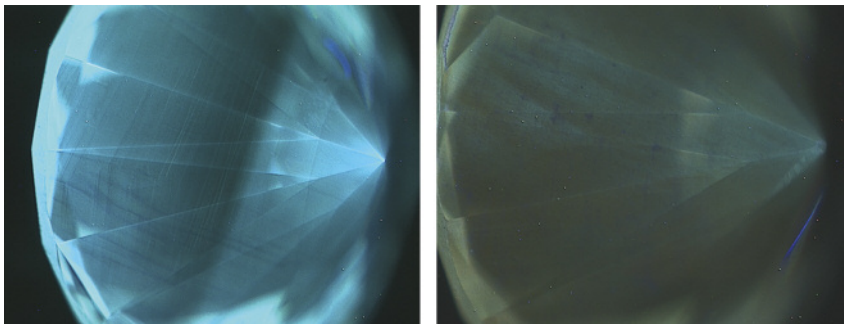

Troy Ardon and
Sally Eaton-Magaña

Heavily Irradiated CVD Synthetic Diamond

A Fancy Deep gray-blue diamond weighing 0.46 ct was submitted to the Carlsbad lab for an identification and origin report. Its UV-Vis-NIR spectrum showed a large GR1 center, indicating artificial irradiation. Furthermore, a small 737 nm silicon doublet was seen and later confirmed with photoluminescence (PL) spectroscopy (figure 13). The silicon doublet is a feature in CVD synthetic diamonds, and only very rarely in natural diamonds.

To confirm the synthetic origin of the material, DiamondView images were collected. This required setting the DiamondView at the highest exposure time, because heavily irradiated diamonds tend to show very weak fluorescence, making the image difficult to resolve. The DiamondView image showed a pattern of growth dislocations, which is characteristic of CVD synthetics (figure 14). The infrared spectrum showed some unknown features in the nitrogen region at 1250 and 1116 cm^{-1}. The infrared spectrum lacked the 3123 cm^{-1} hydrogen-related defect diagnostic of CVD growth (P.M. Martineau et al., "Identification of synthetic diamond grown using chemical vapor deposition [CVD]," Spring 2004 *G&G*, pp. 2–25), or the 3107 cm^{-1} peak sometimes created in synthetic diamonds containing hydrogen by HPHT treatment (I. Kiflawi et al., "The creation of the 3107 cm^{-1} hydrogen absorption peak in synthetic diamond single crystals," *Diamond and Related Materials*, Vol. 5, 1996, pp. 1516–1518).

CVD synthetic diamonds are known to be treated post-growth to improve color, but this has been seen as HPHT treatment or a combination of irradiation and annealing. HPHT treatment of a CVD synthetic diamond can partially or completely re-

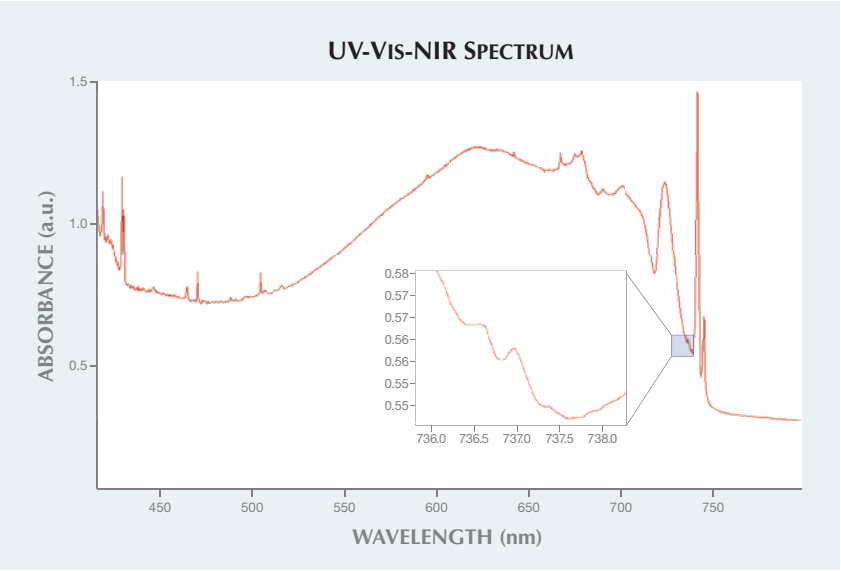

Figure 13. The visible-NIR spectrum of the 0.46 ct irradiated synthetic diamond showed a clear Si-doublet at 737 nm.

move a brownish color created during the growth process. If a CVD synthetic is grown with nitrogen impurities, irradiation and annealing will create nitrogen-vacancy centers, producing a pink to red color (J. Shigley et al., "Lab-grown colored diamonds from Chatham Created Gems," Summer 2004 *G&G*, pp. 128–145).

This is the first CVD synthetic examined at GIA that has been irradiated to a blue color. The fact that the diamond is synthetic automatically means that the irradiation was done in a laboratory; however, the material displayed color zoning near the culet in a manner identical to natural diamonds that have been irradiated artificially. Electron paramagnetic resonance determined a 20 (+/- 5) ppb concentration of isolated nitrogen. If the specimen were to be annealed, the vacancies would combine with the nitrogen to form NV^- centers, as mentioned above. It is possible that the diamond was submitted in an intermediate phase before the final treatment, or that the owner believed it to be a natural but treated stone. Indeed, in the absence of PL spectroscopy and DiamondView images, this specimen could easily be mistaken for an irradiated natural diamond.

As CVD synthetics become more prevalent and subject to a wider variety of treatments, it will only reinforce the role of the gemological laboratory as the most reliable way to separate synthetic from natural diamonds.

Troy Ardon and Wuyi Wang

Figure 14. With DiamondView imaging, the growth dislocations in the irradiated CVD synthetic diamond can be clearly seen as the blue sections among the green fluorescence.

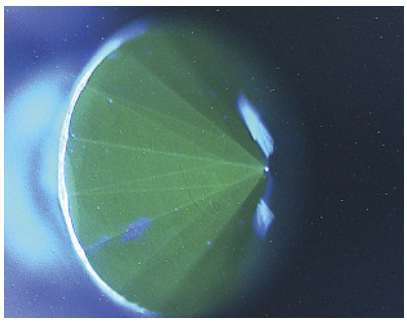

Natural PEARLS Reportedly from a *Spondylus* Species ("Thorny" Oyster)

Non-nacreous conch, clam, *Melo melo*, *Cassis*, and scallop pearls are often submitted to GIA for identification. Four non-nacreous pearls, weighing 5.72 to 12.40 ct and measuring from 9.55 × 8.60 mm to 16.35 × 9.36 mm, were recently submitted to GIA's New York laboratory for identification. These examples caught our attention because of their unusual appearance (figure 15).

Their bodycolors and shapes varied. Each exhibited some degree of pink and orange hues, and either elongated or button shapes. The porcelaneous surfaces also exhibited areas with clear flame structures. Under fiber-optic light, fine flame structures resembling those seen in other porcelaneous pearls such as *Tridacna gigas* and *Strombus gigas* (conch) pearls were observed. While the typical whitish flame structure was readily

Figure 15. Four non-nacreous pearls, weighing 12.40, 11.55, 8.22, and 5.72 ct (left to right), were submitted for identification.

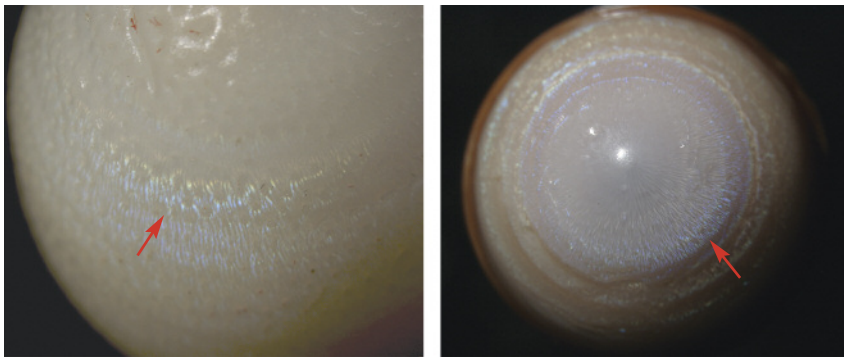

Figure 16. The porcelaneous surface appearances of two of the pearls, weighing 12.40 ct (left, magnified 20×) and 8.22 ct (right, magnified 10×) show their characteristic blue flames, indicated by the arrows.

apparent, the more notable observation was that some of the flames had a distinct blue coloration (figure 16). Other types of pearls usually do not show blue flames. Microradiography was of little diagnostic assistance, as only tight structures were observed; this is not unusual for porcelaneous pearls. Raman spectroscopy detected both aragonite and calcite separately on different parts of the samples. In the authors' experience, this differs from conch or clam pearls, which are usually composed of aragonite only.

Due to their unique shapes, colors, surface, and flame structures, we suspected these pearls were from one of the many *Spondylus* species (figure 17), commonly called "thorny" or "spiny" oysters. Although rarely encountered in GIA laboratories, *Spondylus* pearls have been documented in the past (Winter 1987 Lab Notes, p. 235; E. Strack, *Pearls*, Ruhle-Diebener-Verlag GmbH & Co., Stuttgart, 2006, p. 255), and some samples have been collected by the Qatar Museums Authority (H. Bari and D. Lam, *Pearls*, Skira Editore S.p.A, 2009, pp. 88–89). Our client later informed us that these specimens were found by a fisherman in shells of *Spondylus princeps* off the coast of Baja California, Mexico.

This was a rare opportunity to see natural pearls from a known *Spondylus* species, and to document their unique gemological characteristics as references for mollusk identification in the future.

Figure 17. These shells are from various Spondylus *species. Courtesy of GIA's Bangkok laboratory.*

Joyce WingYan Ho and Chunhui Zhou

Flame-Fusion SYNTHETIC RUBY Boule with Flux Synthetic Ruby Overgrowth

Synthetic rubies with both curved growth and flux-type inclusions in a single stone occasionally appear in the trade. Often these are flame-fusion synthetics that have been quench-crackled and flux-healed to produce a more "natural" appearance. In other instances, flame-fusion material may be used as a seed for flux corundum overgrowth. If the seed crystal is not removed during cutting, it becomes part of the faceted synthetic gemstone (R.E. Kane, "A preliminary report on the new Lechleitner synthetic ruby and synthetic blue sapphire," Spring 1985 *G&G*, pp. 35–39).

The Carlsbad laboratory recently examined a 249.78 ct transparent to semi-transparent rough red crystal (figure 18). Standard gemological testing using a handheld spectroscope revealed a typical ruby spectrum. Observed with a dichroscope, the rough crystal displayed medium orange red to purplish red pleochroism and fluoresced strong red to long-wave UV and medium red to short-wave UV. All of these properties were consistent with ruby.

Microscopic examination using brightfield illumination revealed both curved striae and flux fingerprint patterns (figure 19). Careful examination of one end of the rough crystal showed a noticeable boundary between a flame-fusion core and a flux-grown overgrowth. Part of the core had not been covered by the flux overgrowth (again, see figure 18). The flux fingerprint inclusion penetrated just a few millimeters into the crystal and was only visible in the flux overgrowth (again, see figure 19). What appears to be a pronounced dark grayish reaction zone at the interface of flame-fusion and flux growth was observed (figure 20). The reaction zone

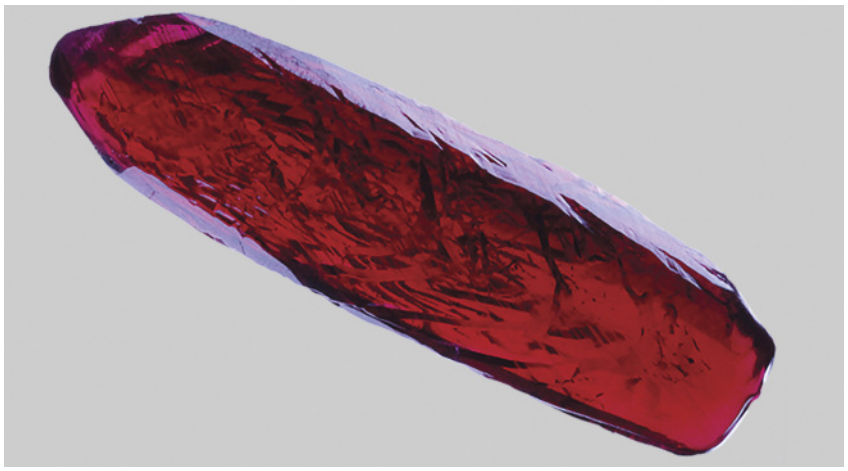

Figure 18. This 73.69-mm-long synthetic ruby crystal is composed of a flame-fusion synthetic ruby boule core with a flux synthetic ruby overgrowth.

likely indicates slight structural and chemical variations between the flame-fusion core and the flux overgrowth. When a new crystal is grown on top of an old crystal, the new growth starts on an irregular surface that was created when the old surface was melted back slightly at the melt temperature. When growth starts on an irregular surface, it creates a nonperfect crystal lattice match between the original seed and new overgrowth. This growth boundary face will disrupt the regularity of the structure of the growth crystal and contribute to the presence of the reaction zone (Schmetzer et al., "Flux-grown synthetic alexandrites from Creative Crystals Inc.," 2012, *Journal of Gemmology*, Vol. 33, No. 1–4, pp. 49–81). In areas where the structural and chemical difference was not very distinct, the reaction zone was partially visible as dark grayish color patches (figure 21). The reaction zone looked grayish because the red bodycolor of the ruby masked what is probably a blue color zone caused by Ti-Fe pairs, a well-known defect that causes blue color in corundum (Summer 1991 Lab Notes, p. 112). The blue zone is along the interface of the flame-fusion core and flux overgrowth.

Advanced testing on the rough crystal using energy-dispersive X-ray fluorescence (EDXRF) analysis revealed traces of Ca, Ti, and Cr in the areas both with and without flux overgrowth; Mo was only detected in areas with the flux overgrowth. The concentration of Fe was below the detection limit of EDXRF. This result is consistent with the chemical element differences between flame-fusion and flux synthetics (S. Muhlmeister et al., "Separating natural and synthetic rubies on the basis of trace-element chemistry," Summer 1998 *G&G*, pp. 80–101).

This synthetic ruby specimen is unusual in that regions originating from the two growth methods occur in the same crystal, with the half of the split boule seed crystal composing the bulk of the entire specimen. While flux overgrowth on flame-fusion seed crystals has been previously reported (E.J. Gübelin and J.I. Koivula, *Photoatlas of Inclusions in Gemstones, Volume 2*, Opinion Verlag, Basel, Switzerland, 2005, p. 352), this type of material is rarely seen in GIA's laboratory, and this example was particularly unusual due to its large size.

Ziyin Sun and Heidi Breitzmann

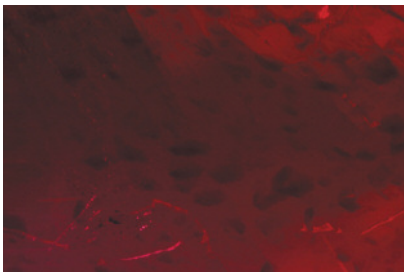

Figure 21. Also observed was a partial reaction zone between the flame-fusion core and the flux overgrowth. Image width 5.85 mm.

Figure 19. Subtle curved striae (right arrow) and fingerprint-like flux residue (left arrow) are indicative of both flame-fusion and flux growth. Image width 6.94 mm.

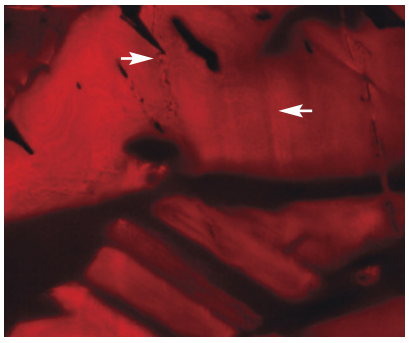

Figure 20. A dark grayish reaction zone was observed between the flame-fusion core and the flux overgrowth. Image width 15.67 mm.

PHOTO CREDITS:
Jian Xin (Jae) Liao—1, 3, and 11; Paul Johnson—2 and 5; Kyaw Soe Moe—6 and 7; Troy Ardon—8, 9 and 10; Sally Magaña—12; Wuyi Wang—14; Sood Oil (Judy) Chia—15; Joyce WingYan Ho—16; Nuttapol Kitdee —17; Nathan Renfro—18, 19, 20, and 21.

G&G

Gem News International

Contributing Editors
Emmanuel Fritsch, *CNRS, Team 6502, Institut des Matériaux Jean Rouxel (IMN), University of Nantes, France* (fritsch@cnrs-imn.fr)
Kenneth Scarratt, *GIA, Bangkok* (ken.scarratt@gia.edu)

COLORED STONES AND ORGANIC MATERIALS

Aquamarine with unusually strong dichroism. Recently, a transparent grayish blue oval mixed cut (figure 1) was submitted for identification at the Gem Testing Laboratory in Jaipur. The 4.49 ct stone (12.04 × 8.88 × 7.53 mm) was relatively clean to the unaided eye. Its RI of 1.582–1.590, birefringence of 0.008 with a uniaxial negative optic sign, and hydrostatic SG of 2.71 suggested a beryl, which we later confirmed with FTIR and Raman spectroscopy. The specimen's natural origin was established by planes of dendritic platelets (usually ilmenite) oriented along the basal plane and liquid fingerprints.

The stone's most striking feature was its unusually strong dichroism, displaying deep blue and pale bluish green colors (figure 2). The deep saturated blue resembled that of a top-quality sapphire. Such strong dichroism was reminiscent of Maxixe-type (irradiated) beryls, although their dichroic colors are usually deep blue and colorless. The deep saturated blue was seen along the e-ray, the pale bluish green along the o-ray. Such a pattern of color absorption is associated with aquamarine; the opposite effect occurs in Maxixe-type beryl, which appears colorless along the e-ray and deep blue along the o-ray (R. Webster, *Gems*, 5th ed., Butterworth-Heinemann, London, 1994, pp. 124–127).

Further analysis was performed with UV-Vis-NIR spectroscopy to confirm the cause of color and differentiate between aquamarine and Maxixe-type beryl. Polarized spectra (figure 3) revealed an absorption peak at approximately 427 nm along the o- and e-rays, a typical feature in aquamarine due to the presence of ferric iron (see I. Adamo et al., "Aquamarine, Maxixe-type beryl, and hydrothermal synthetic blue beryl: Analysis and identification," Fall 2008 *G&G*,

Figure 1. This 4.49 ct grayish blue aquamarine was unusual for its strikingly intense dichroism. Photo by Gagan Choudhary.

Figure 2. The dichroic aquamarine displayed unusually intense dichroism, with a deep saturated blue along the e-ray (left) and a pale bluish green along the o-ray (right). The images were taken by fixing the polarizing filter on the camera lens and rotating the polarizer 90 degrees to separate out the two directions. Photos by Gagan Choudhary.

Editors' note: Interested contributors should send information and illustrations to Justin Hunter at justin.hunter@gia.edu or GIA, The Robert Mouawad Campus, 5345 Armada Drive, Carlsbad, CA 92008.

Gems & Gemology, Vol. 50, No. 3, pp. 244–249.

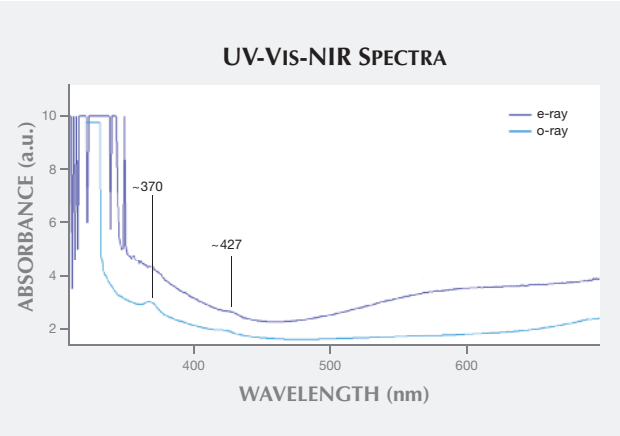

Figure 3. The aquamarine's polarized UV-Vis-NIR spectra displayed Fe^{3+}-related bands at approximately 370 and 427 nm.

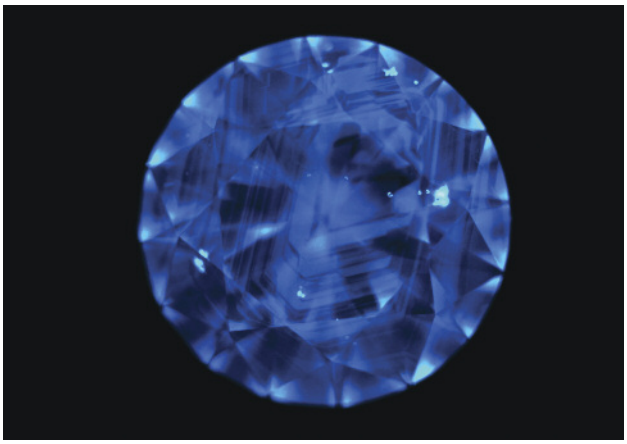

Figure 5. This DiamondView image of the host diamond shows octahedral growth zones (notice the crystal inclusions). Image by Meenakshi Chauhan.

pp. 214–226); an additional peak at about 370 nm also occurred along the o-ray. No features associated with radiation-induced color centers were present between 500 and 700 nm; these are typically observed in Maxixe-type beryls.

Standard gemological properties along with absorption spectra and the pleochroic color directions were sufficient to identify this stone as aquamarine. It displayed the most intense dichroism we have seen in an aquamarine. While there are deep sea-blue aquamarines (see O. Segura and E. Fritsch, "The Santa Maria variety of aquamarine: Never heated," *InColor*, No. 23, 2013, pp. 34–35) as well as deep blue Maxixe-type beryls, this was the deepest blue we have observed in an aquamarine with a grayish blue hue.

Gagan Choudhary (gagan@gjepcindia.com)
Gem Testing Laboratory, Jaipur, India

Color-change garnet in diamond. The Indian Gemological Institute's Gem Testing Laboratory recently examined a 0.30 ct colorless round brilliant-cut diamond containing an interesting inclusion. Infrared spectroscopy revealed features found in type IaA diamond, with a slight absorption peak due to hydrogen impurities. With a clarity grade of SI_2, the diamond contained several colorless crystals and one surface-breaking grayish green crystal (figure 4, left). Under incandescent light, the grayish green crystal appeared purplish red (figure 4, right), displaying a strong color-change phenomenon.

Under the Chelsea filter the inclusion showed a bright red reaction, suggesting the presence of chromium. There was a polished area of the included crystal on the surface, but it was too small for us to measure the refractive index.

The included crystal did not display pleochroism under microscopic observation with crossed polarizers. Viewed in immersion, it appeared to be singly refractive. DiamondView imaging showed the fluorescence pattern of growth planes found in natural diamond (figure 5). Typical octahedral growth zones of blue N3 fluorescence were evident, with no disturbance in the zones around the color-change crystal.

For conclusive identification of the inclusion, we sent the diamond to the Gem Testing Laboratory in Jaipur for laser Raman spectroscopy. As the color-change crystal

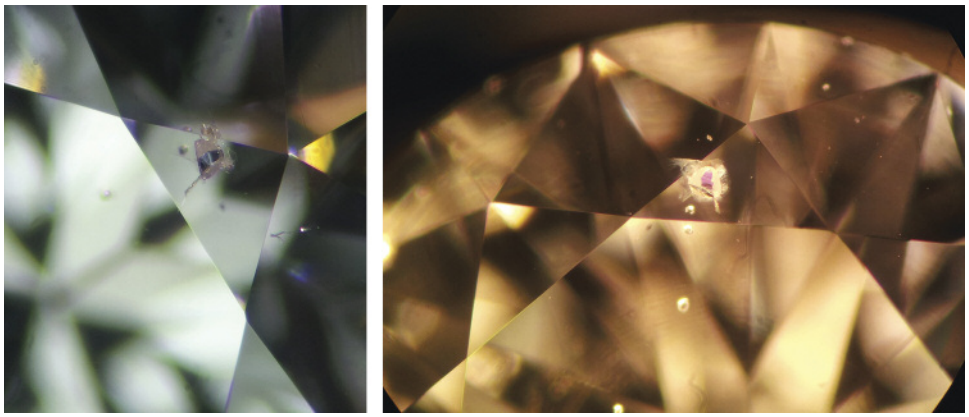

Figure 4. This inclusion, a color-change pyrope-spessartine garnet crystal in diamond, appeared grayish green in fluorescent light (left) and purplish red in incandescent light (right). Photomicrographs by Meenakshi Chauhan; field of view 2 mm (left) and 3 mm (right).

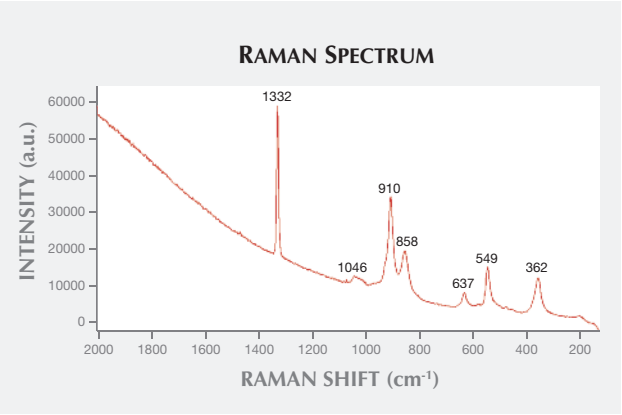

Figure 6. The Raman spectrum of the color-change pyrope-spessartine garnet inclusion showed the 1046, 910, 858, 637, 549, and 362 cm^{-1} peaks assigned to garnet. The 1332 cm^{-1} peak is assigned to diamond.

broke through the diamond's surface, a clear Raman spectrum could be obtained (figure 6). The peak at approximately 1332 cm^{-1} is assigned to diamond, and the peaks at approximately 1046, 910, 858, 637, 549, and 362 cm^{-1} are assigned to garnet. The 910 cm^{-1} peak is associated with the pyralspite isomorphous series, which is comprised of pyrope, almandine, and spessartine garnet. The inclusion was therefore identified as garnet belonging to the pyralspite series.

Meenakshi Chauhan
Indian Gemological Institute
Gem Testing Laboratory, GJEPC, New Delhi

First discovery of topazolite in Mexico. Garnet occurs in a wide variety of colors according to composition: pyrope and almandine (typically red), spessartite (brownish to orange), grossular (brown, yellow, and green), andradite (brown to black), and uvarovite (bright green). The three varieties of andradite are melanite, topazolite, and demantoid. *Topazolite*, a name that has been criticized as too similar to that of the gem species topaz, is a greenish yellow to yellow-brown andradite. According to some studies (e.g., C.M. Stockton and D.V. Manson "Gem andradite garnets," Winter 1983 *G&G*, pp. 202–208), it rarely occurs in crystals large enough to be faceted.

In January 2014, during mineralogical investigations of Mexican garnet, we made the first reported discovery of fine topazolite crystals in Mexico. These yellow to yellow-brown crystals, measuring 1.5–2.5 cm, are hosted by the Las Vigas skarn deposits (the Cerro de la Concordia mine in Las Vigas de Ramirez municipality and the Piedra Parada mine in Tatatila municipality). The deposits are located in Veracruz State, about 50 km southeast of the town of Valle de Veracruz.

The garnet composition was determined by electron microprobe, using a 41-point analysis and standard conditions of 20 kV, 20 mA, and 1 µm beam size on a JEOL JSM-35c microprobe. We chose a euhedral, relatively homogeneous crystal about 1 cm in diameter from the specimen shown in figure 7. Measurement time was 30 seconds on the peak center. The standards used were MgO for Mg, Al_2O_3 for Al, jadeite for Si, wollastonite for Ca, and elemental Fe and Mn. The electron microprobe analyses showed little compositional variation or zoning. We calculated the structural formula on the basis of 12 oxygen atoms, with the assumption of all iron as ferric. The approximate composition averaged $(Ca_{2.86}Mg_{0.06}Mn_{0.02})_{2.94}(Al_{1.20}Fe^{3+}_{0.72})_{1.92}Si_{3.03}Ti_{0.05}O_{12}$, which may be expressed as $Gr_{60.50}And_{36.70}Py_{2.80}$.

UV-visible spectroscopy showed absorption bands at 375, 416, 442, 497, and 584 nm, which can be assigned to the spin-forbidden crystal-field transition of Fe^{3+} substituted on the octahedral Al^{3+} site of the garnet structure. The correlated set of these bands also show a pattern close to that characteristic of a d^5 trivalent ion in octahedral oxygen coordination. The Mössbauer spectra were characterized by a sharp, slightly asymmetric ferrous doublet. The UV-visible and Mössbauer spectra are comparable to those reported for some garnets in previous reports (A.S. Marfunin, Ed., *Advanced Mineralogy*, Vol. 2, Springer-Verlag, Berlin, 1995, pp. 74–75, 114).

The three samples of rough topazolite (measuring 1.0–1.5 cm in longest dimension) gave the following properties: yellow-brown color; isotropic and weakly anisotropic; weak strain birefringence; RI—n_α = 1.84–1.89; hydrostatic SG—3.75–3.85; and fluorescence—inert to both long- and short-wave UV radiation.

This Mexican topazolite deposit has not been mined, and in the absence of detailed geological, mineralogical, and gemological study, no estimate of the reserves is avail-

Figure 7. This topazolite specimen is from a recent discovery in the Mexican state of Veracruz. Photo by Cristobal Castillo.

Figure 8. This giant clam pearl was recovered from a Tridacna gigas *mollusk in Papua New Guinea. Photo by Lai Tai-An Gem Lab.*

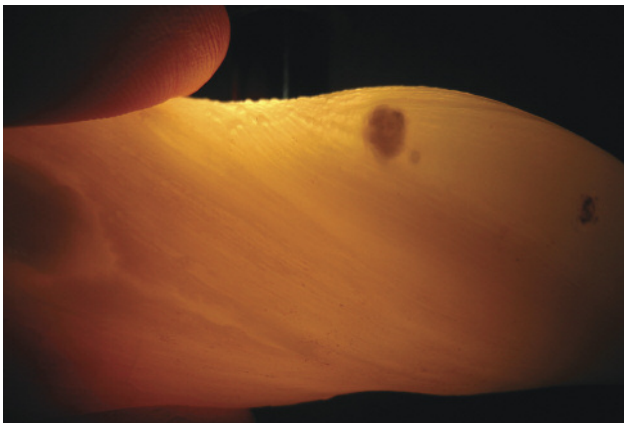

Figure 10. The Tridacna *pearl exhibited pronounced banding when viewed with transmitted light. Photo by Lai Tai-An Gem Lab.*

able. For now, there are no specimens or fashioned material from Las Vigas in the Mexican lapidary market.

Mikhail Ostrooumov (ostroum@umich.mx)
Institute of Earth Sciences (INICIT)
University of Michoacan, Morelia, Mexico

A large baroque *Tridacna gigas* (giant clam) pearl. Natural pearls from various clam species are not as rare as many believe, and plenty of samples are available in the market. But with the exception of a few very large specimens, they tend to occur in sizes under 20 carats. A client of the Lai Tai-An Gem Lab in Taipei recently requested a report on what he claimed was a natural clam pearl (figure 8) recovered from a huge *Tridacna gigas* mollusk from a fishery in Papua New Guinea in 1981.

The pearl exhibited an elongated baroque shape with uneven brown and white coloration, lacking the lustrous and shimmering iridescent colors of a nacreous pearl. It weighed 360.59 ct and measured 76.7 × 28.0 × 25.8 mm. We also recorded an SG of 2.88, which fell within the range of other *Tridacna* pearls examined in our laboratory. Long-wave UV produced a moderate chalky blue reaction. FTIR, Raman, and UV-visible spectra were collected. The Raman spectrum clearly showed that the pearl was composed of aragonite, given the peaks at approximately 142, 199, 701, and 1082 cm^{-1}. FTIR reflectance spectra also revealed calcium carbonate in the form of aragonite, with peaks at approximately 873 and 1483 cm^{-1}.

Figure 9. The natural Tridacna *pearl showed a characteristic sugary surface texture. Photo by Lai Tai-An Gem Lab; magnified 60×.*

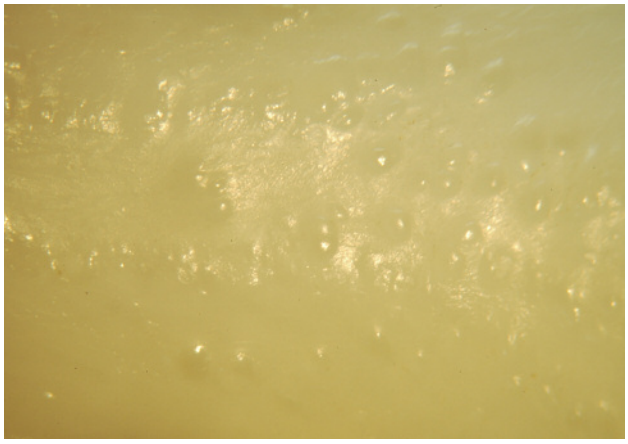

While microradiography is usually applied to the identification of pearls, it is considered especially beneficial when various types of nacreous pearls need to be separated from one another. It is usually less helpful with non-nacreous or non-porcelaneous pearls such as this one, since many reveal little in the way of helpful structure. Observed through the loupe and microscope, the pearl showed the grainy or sugary surface texture (figure 9) typical of some natural *Tridacna* pearls. This example was noteworthy for its size and interesting coloration, and its pronounced banding when viewed with transmitted light (figure 10), a feature that is often considered indicative of shell fashioned into imitation pearls. This *Tridacna* pearl was clearly no imitation.

Larry Tai-An Lai (service@laitaian.com.tw)
Lai Tai-An Gem Laboratory, Taipei

TREATMENTS

Coated fire opal in the Chinese market. Fire opal is an attractive variety of gem opal characterized by its red-orange-yellow bodycolor, with or without play-of-color. Since about 2013, the Chinese market has seen an increase in natural, synthetic (sold as Mexifire), and treated fire opals, posing identification challenges for the gemologist.

At the July 2014 Beijing Jewelry Fair, a fire opal with a rather unusual orange bodycolor (figure 11) attracted our

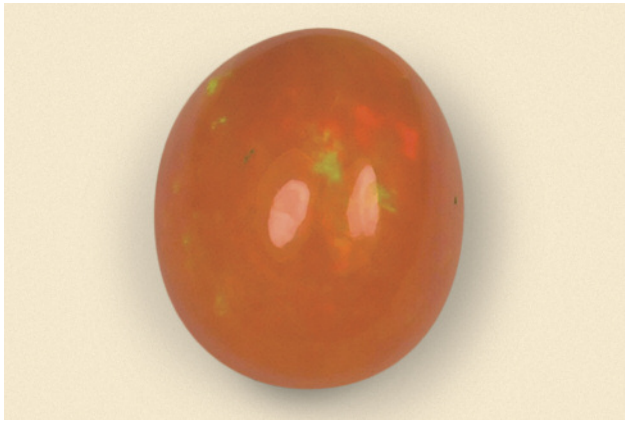

Figure 11. This 3.87 ct translucent orange fire opal with play-of-color was identified as a coated stone. Photo by Wen Han.

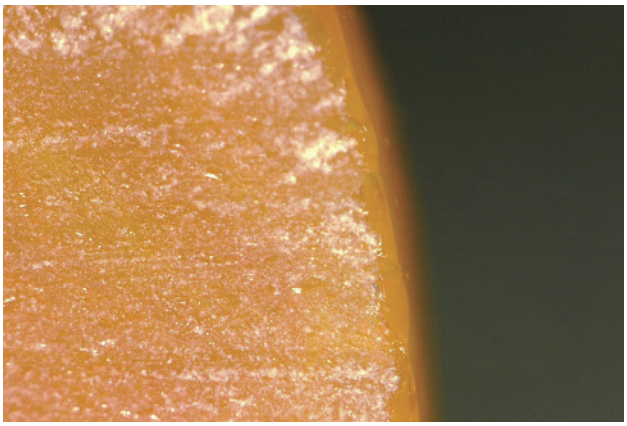

Figure 13. A cross-section image of the fire opal shows a coated surface layer about 60–90 µm thick. Photo by Wen Han; magnified 100×.

interest. It was a 3.87 ct oval cabochon with fair play-of-color, measuring approximately 14 × 10 × 6 mm. Its spot RI of about 1.39 and hydrostatic SG of 1.85 were both lower than the values for most natural fire opal. It was inert to both long- and short-wave UV radiation; untreated fire opal may also be inert to UV radiation or show green and blue fluorescence. Magnification revealed obvious scratching and small pits on the surface (figure 12), suggesting a lower hardness and the presence of a coating. We cut the sample in half for further examination. High magnification clearly showed the boundary between the orange layer and the substrate, which was also orange opal. The coated layer was about 60–90 µm thick (figure 13).

EDXRF chemical analysis detected mainly Si and minor amounts of Ca, Na, and K. Fourier-transform infrared (FTIR) and Raman spectroscopy were used to identify the coating. Infrared reflectance spectroscopy revealed three strong bands at 1099, 789, and 474 cm^{-1} that are related to the fundamental Si-O vibrations, as expected for natural fire opal. Then we scraped off the coating with a razor blade to obtain its infrared transmittance spectrum. The peaks, specifically those at 2926, 1729, 1451, and 1159 cm^{-1}, indicated the presence of organic matter consistent with acrylic polymer (figure 14). The Raman scattering spectra of the fire opal revealed several peaks attributed to both the substrate opal and the coating (figure 15). The Raman bands at about 350, 785, and 1080 cm^{-1}, due to different stretching and bending vibration modes of the Si-O system, are typical for opal-CT. Other peaks, including 1320 and 1610 cm^{-1}, are attributed to the acrylic coating material. Acrylic coatings are applied to various gem materials, such as lapis lazuli and jadeite (Summer 1992 Gem News, p. 135). This coating of acrylic polymer was used to enhance the fire opal's color and seal its fissures. The coating also lowered the stone's RI and SG values.

Our investigation, believed to be the first report of coated fire opal in the Chinese market, reinforces the need

Figure 12. Surface scratches and small pits were visible on the coated fire opal. Photo by Wen Han.

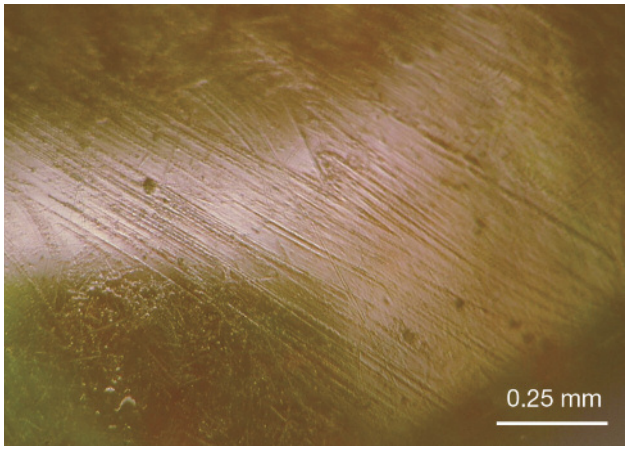

Figure 14. The FTIR spectrum of the coating scraped from the surface of the fire opal exhibits characteristic peaks at 2926, 1729, 1451, and 1159 cm^{-1} consistent with acrylic polymer.

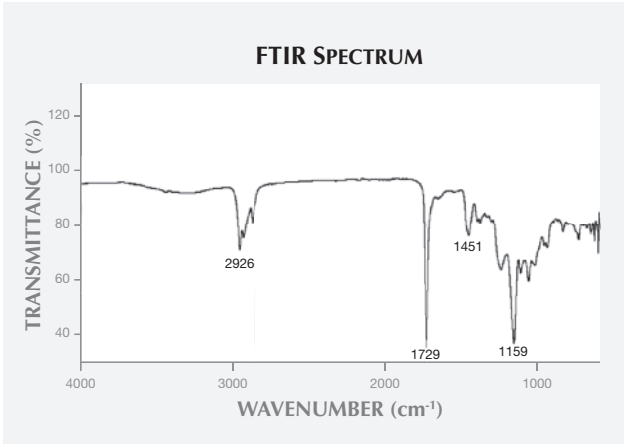

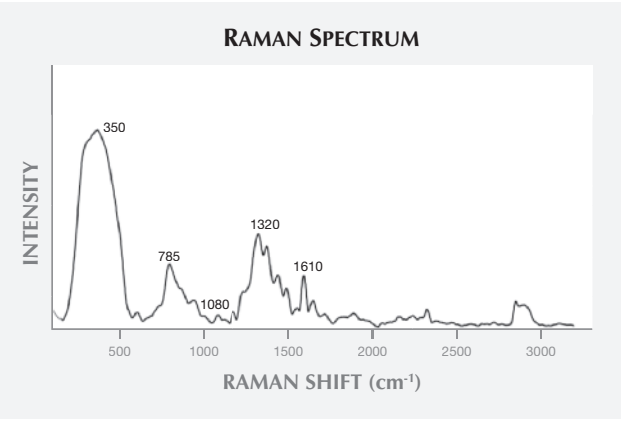

Figure 15. Raman bands at approximately 350, 785, and 1080 cm^{-1} are typical for opal-CT; the other peaks, including those at 1320 and 1610 cm^{-1}, are attributed to the acrylic coating.

for caution when buying these products. This coated fire opal's lower RI and SG values, combined with magnification and Raman spectroscopy, are effective and nondestructive means of identification.

Wen Han (winnerzx@126.com), Taijin Lu, Hua Chen, and Jian Zhang
National Gems & Jewelry Technology Administrative Center (NGTC) BeijingT

CONFERENCE REPORTS

IMA General Meeting. The 21st General Meeting of the International Mineralogical Association (IMA) was held September 1–5 in Johannesburg, South Africa. Several oral and poster presentations were presented in a session on gem materials.

Giovanna Agnosi (University of Bari, Italy) discussed preliminary results of an X-ray diffraction topography study of Colombian trapiche emeralds, which revealed a consistent crystallinity between the arms and the hexagonal core. She presented a model of trapiche formation in which the growth of the hexagonal core occurred first, followed by the six arm sections. **Ulrika D'Haenens-Johansson** (GIA, New York) outlined the status of synthetic diamond production. She reviewed the means of identification based on visual observations, structure-related ultraviolet fluorescence reactions, and distinctive spectroscopic features. In concluding, she noted that synthetic diamonds can be unequivocally recognized by major gem laboratories.

Andrew Fagan (University of British Columbia, Vancouver) presented the geologic setting and a model of formation of the Fiskenæsset corundum district in southwest Greenland. Estimates of ore reserves suggest that this could become a commercial ruby deposit. **Gaston Giuliani** (Centre de Recherches Pétrographiques et Géochimiques, Nancy, France) studied the oxygen isotope and trace-element chemistry of sapphire xenocrysts in basalts from Changle, China, and of corundum from the Mbuyi-Mayi kimberlite in the Democratic Republic of Congo, to trace their primary sources. In both cases, the host basalt and kimberlite transported the corundum crystals from the lower crust and upper mantle.

Daniel Ichang'i (University of Nairobi) described efforts by the Kenyan government to document and better understand the geologic setting of the country's numerous gem deposits. He discussed two main occurrence lithologies: the metamorphic rocks of the Neoproterozoic Mozambique orogenic belt, and the Paleogene-Neogene basaltic volcanics in the Northern and Central Kenya rift regions.

Stefanos Karampelas (Gübelin Gem Lab, Lucerne, Switzerland) detailed the gemological characteristics of emeralds from Itatitia in Minas Gerais, Brazil. The emeralds formed along the contact between phlogopite schists and highly evolved granitic pegmatites. Based on minor and trace-element chemistry, they can be distinguished from emeralds from other Brazilian and world deposits. **Vincent Pardieu** (GIA, Bangkok) gave a talk about Montepuez in northern Mozambique, which is currently the world's largest source of rubies. He also presented a short film about GIA expeditions he has led to gem deposits in eastern Africa. **Wuyi Wang** (GIA, New York) presented a study of carbon isotopes of synthetic and natural diamonds. The latter displayed $\delta^{13}C$ values from 0 to –20‰, while the former ranged from –25 to –75‰.

Christopher M. Breeding (GIA, Carlsbad, California) described the interesting features of alluvial diamonds from the Marange deposit in eastern Zimbabwe. These type Ia diamonds display surface radiation staining, aggregated nitrogen impurities, and elevated hydrogen impurity contents, but these features do not provide a reliable indicator of geographic origin. **Julien Feneyrol** (Centre de Recherches Pétrographiques et Géochimiques, Nancy, France) presented a model of the metamorphic formation of tsavorite nodules in primary deposits. The tsavorite nodules are always contained within graphitic gneiss and calc-silicates with intercalations of marble. **Elena Sorokina** (Fersman Mineralogical Museum, Moscow) described a model of ruby and sapphire formation in marbles at Snezhnoe in Tajikistan.

James E. Shigley
GIA, Carlsbad, California

ERRATA

1. The S. Saeseaw et al. emerald inclusions article in the Summer 2014 issue (pp. 114–132) listed the photomicrograph image widths ten times larger than their actual width.

2. The Summer 2014 Gem News International section (pp. 158–159) erroneously cited "absorption peaks" in the Raman spectrum of a jadeite bangle. We thank Thierry Cathelineau for bringing this to our attention.